Functional consequences of Cross-Linked Actin Networks in bovine trabecular meshwork cells

Thesis submitted in accordance with the requirements of the University of Liverpool for the degree of Doctor in Philosophy

by Steven Christopher O'Reilly

November 2010

Eye and Vision Sciences, Institute of Ageing and Chronic disease, Faculty of Health and Life Sciences.

Abstract

The trabecular meshwork (TM) is the tissue responsible for outflow resistance and hence intraocular pressure. TM cells contain a contractile apparatus that is composed of actin stress fibres that run parallel to the axis of the cell and are responsible for facilitating contraction. Cross-Linked Actin Networks (CLANs) are polygonal arrangements of actin that form a geodesic network found predominantly in TM cells both in situ and in vitro. Bovine TM cells appear to display an increased sensitivity to induction of these CLANs in vitro. Therefore giving an excellent model for further work. The aim of this work was to determine the functional significance of CLANs in bovine TM cells and to determine other CLAN inducing agents and inhibitors.

Studies in this thesis have shown for the first time that CLANs may inhibit the contractile function of TM cells using an established model of contraction. CLANs are not associated with apoptosis. Aqueous humour stimulates CLAN formation and at least one component facilitating this is TGF-β2. The pleotropic cytokine induced CLANs are coupled to the canonical Smad pathway and the endogenous inhibitor decorin induces CLANs more robustly. Studies have also shown that cyclic mechanical stretch induces CLANs similar to in vivo levels and that this mechanical stimulation is accompanied by an activation of NF-κB and subsequent inflammatory and stress related protein response. Further I have shown that CLAN containing cells have a polarised cell phenotype that is easily discernable and will facilitate identification of CLAN containing cells for further study.

It is important to identify signalling components in CLANs in TM cells as if CLANs are pathogenic in POAG targeting their formation will open a new therapeutic paradigm.

List of Contents

List of Figures

Chapter 1

Chapter 2

Chapter 3

List of Tables

Chapter 4

Acknowldegments

I must acknowledge that figure 3.21 is Natalie Pollack's image and figure 3.20 was generated together by me and Natalie Pollack. I also acknowledge help compiling figure 3.32. I am grateful to Prof. Grierson and Dr Williams for help, supervision and advice throughout the project and also to everyone in the Unit of Ophthalmology who helped along the way. Thanks also to Vikki Kearns for keeping me motivated.

Publications

O'Reilly S., Pollack, N., Paroan, L., Grierson, I et al Inducers of Cross-Linked Actin Networks (CLANs) include TGF-β2 and decorin *Invest Ophthalm. Vis Sci* Under Review

Job, R., Raja, V., Grierson, I., **O'Reilly, S** et al Cross-linked Actin Networks are present in lamina cribrosa cells *B J Ophthalmol* 2010: 1388-1392

Wade, NC., Grierson, I., **O'Reilly, S.**, Hoare, MJ et al Cross-Linked Actin Networks in Bovine trabecular meshwork cells *Exp Eye Res* 2009 89: 648-659

Abstracts

Modulation of contraction of bovine trabecular meshwork cells by Cross-Linked Actin Networks (CLANs) ARVO meeting abstract April 11 2009 Fort Lauderdale

Modulation of contraction of bovine trabecular meshwork cells by Cross-Linked Actin Networks (CLANs) The Physiological Society meeting Abstract June 2009 Dublin, Ireland

Abbreviations

2D	2 Dimensional
3D	3 Dimensional
ADP	Adenosine diphosphate
ATP	Adenosine triphosphate
AMH	Anti-muellarian hormone
BMPs	Bone morphogenetic proteins
BSA	Bovine Serum Albumin
BTM	Bovine Trabecular Meshwork
Ca(2+)	Calcium
CD	Cluster of differentiation
Cdc42	Cell division cycle 42
CLANs	Cross-Linked Actin Networks
CO_2	Carbon dioxide
CMV	CytoMegalovirus
CTGF	Connective tissue growth factor
Cx43	Connexin43
DEX	Dexamethasone
DNA	Deoxyribonucleic acid
DMEM	Dulbecco's Modified Eagles Medium
Drebrin	Developmentally-regulated brain protein
DPBS	Dulbecco's Phosphate Buffered Saline
DMSO	Dimethyl Sulfoxide
ECM	Extracellular matrix
ELAM-1	Endothelium leukocyte adhesion molecule-1
ER	Endoplasmic reticulum
F-actin	Filamentous actin

FCS	Fetal calf serum
GAP	GTPase activating proteins
GDP	Gaunasine diphosphate
GEF	Guanine nucleotide-exchange factors
GFP	Green-fluorescent protein
GRP78	Glucose related protein 78
GTPase	Guanasine triphosphatase
Gly	Glycine
HEK293	Human embryonic Kidney cells 293
Hsp70	Heat shock protein70
IL	Interleukin
IL-1ra	Interleukin-1 receptor antagonist
IOP	Intraocular pressure
LAP	Latency associated peptide
LTBP	Latent TGF-β-binding protein
MgATP	Magnesium Adenosine triphosphate
MMPs	Matrix metalloproteases
MT-MMPs	Membrane-type metalloproteinases
MTT	(3-(4,5-Dimethylthialthiazol-2-yl)-2,5-diphenlytetrazolium
mRNA	messengerRibonucleic acid
NaOH	Sodium hydroxide
NaCl	Sodium chloride
NADPH	Nicotinamide adenine dinucleotide phosphate
NBF	Neutral buffered formalin
NIH	National Institutes of Health
NO	Nitric oxide
Nf-κB	Nuclear factor κB

p38	p38 Mitogen-activated protein kinase
PAAs	Polygonal Actin Arrangements
PA	Plasminogen activator
PAI-1	Plasminogen activator inhibitor-1
PAK	p21-activated kinase
PBS	Phosphate buffered saline
POAG	Primary Open Angle Glaucoma
PS	Phosphatidylserine
RGD	Arginine-Glycine-Aspartate
ROS	Reactive oxygen species
RPE	Retinal pigment epithelium
sFRPs	secreted Frizzeled Related Proteins
siRNA	small interfering Ribonucleic acid
Smad	S-Mothers against decapentaplegic
TEMED	N,N,N'N-Tetramethylethylenediamine
TGF-β	Transforming growth factor-β
TIMPs	Tissue inhibitors of matrix metalloproteases
TM	Trabecular meshwork
TBS	Tris-Buffered Saline
TBS-T	Tris-Buffered Saline + Tween
Tris	Tris(hydroxymethyl)aminomethane
Triton X-100	t-Octylphenoxypolyethoxyethanol
TSP-1	Thrombospondin-1
UV	Ultraviolet
vol/vol	Volume/Volume
wt/vol	Weight/Volume
Wnt	Wingless in *Drosophila* int

ZO-1	Zonula occluding-1

1. Introduction

1.0 Cross-Linked Actin Networks (CLANs)

The actin cytoskeleton is essential in mediating many functions of the cell including locomotion, division, contraction and phagocytosis. The common patterns of actin microfilament arrangement within cells are diffuse F-actin arrangements and bundles of parallel microfilaments tightly bundled together to form stress fibres (Pellegrin and Mellor, 2007). However, there is another type of actin arrangement of F-actin found within cells. This is a dome like arrangement of F-actin microfilaments made up of units of polygonal actin networks (Lazarides, 1976). Lazarides first described these polygonal actin structures in culture and found that these appear after freshly plated out from trypsinisation and then disappeared as the cultures became established (Lazarides, 1976). CLANs appear very similar to these actin structures, they contain polygonal actin arrangements, with a central hub and radiating vertices, often in patterns of five or six and are found in confluent cultures of trabecular meshwork cells (TM) (Clark et al., 1994, Clark et al., 2005, Clark et al., 1995) (figure 1.1). These CLANs appear to have architectural similarities to the transient structures seen in other cells (Lazarides, 1976, Ireland and Voon, 1981, Mochizuki et al., 1988), however CLANs appear to be only expressed in confluent monolayers of TM cells (Clark et al., 1994) (figure 1.2).

Another important feature of CLANs is that they are induced upon exposure to various steroids and not induced in a variety of other cell types tested (Clark et al., 1994). The functional significance of CLANs are unknown however, atomic force microscopy of these structures appears to suggest they impart a structural rigidity to the cells (Meller and Theiss, 2006) and Ingber has suggested that such geodesic actin arrangements impart structural rigidity in line with his 'tensegrity' theory (Ingber,

2006). Such structural rigidity may impact on the vital functions of the cells and hence play a role in disease, their study is therefore important.

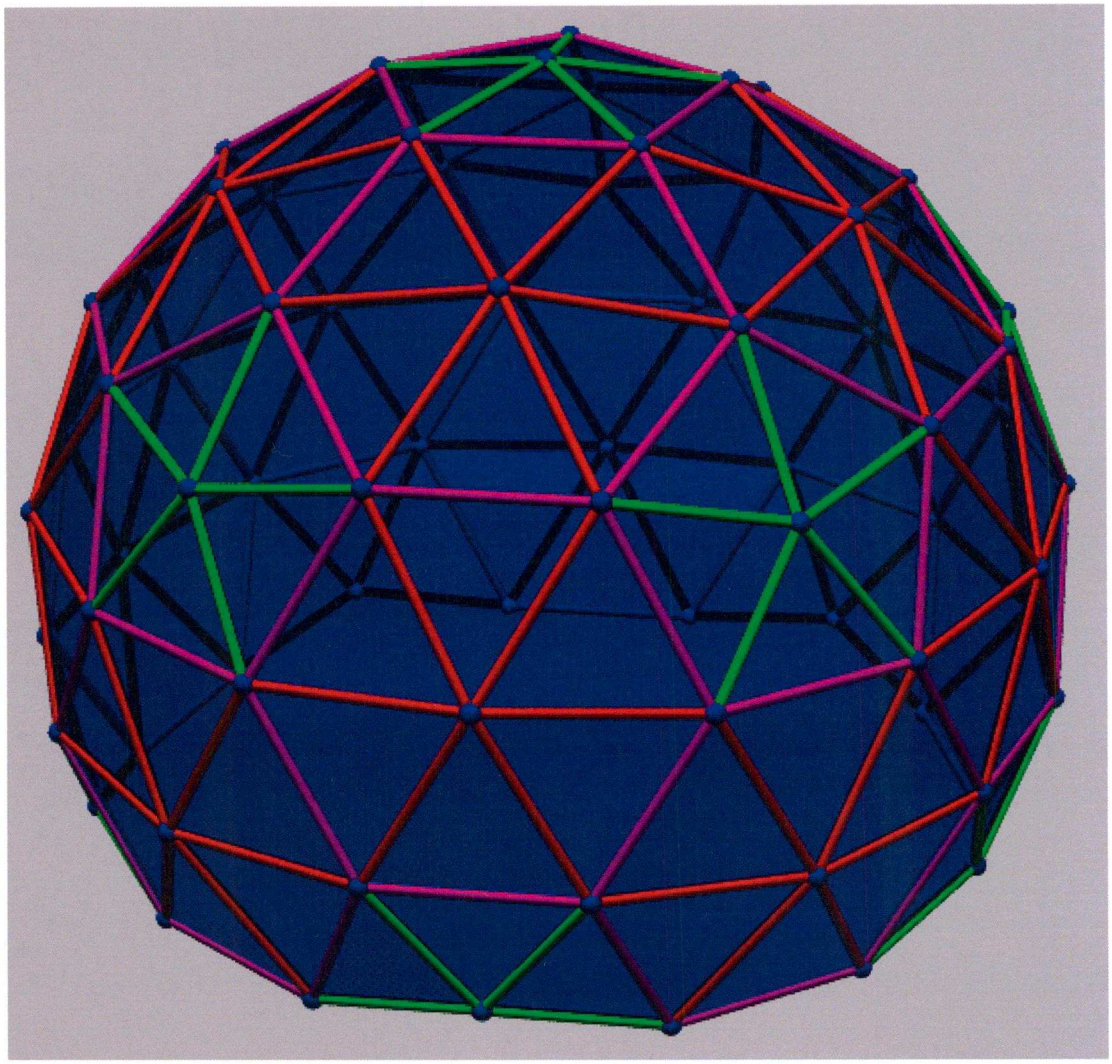

Figure 1.1 Schematic diagram of a geodesic dome comprised of polygons with a central 'hub' and spokes radiating outwards from the hubs. The polygons are often in units of five (green) or six (red). Image taken from: http://userwww.sfsu.edu/

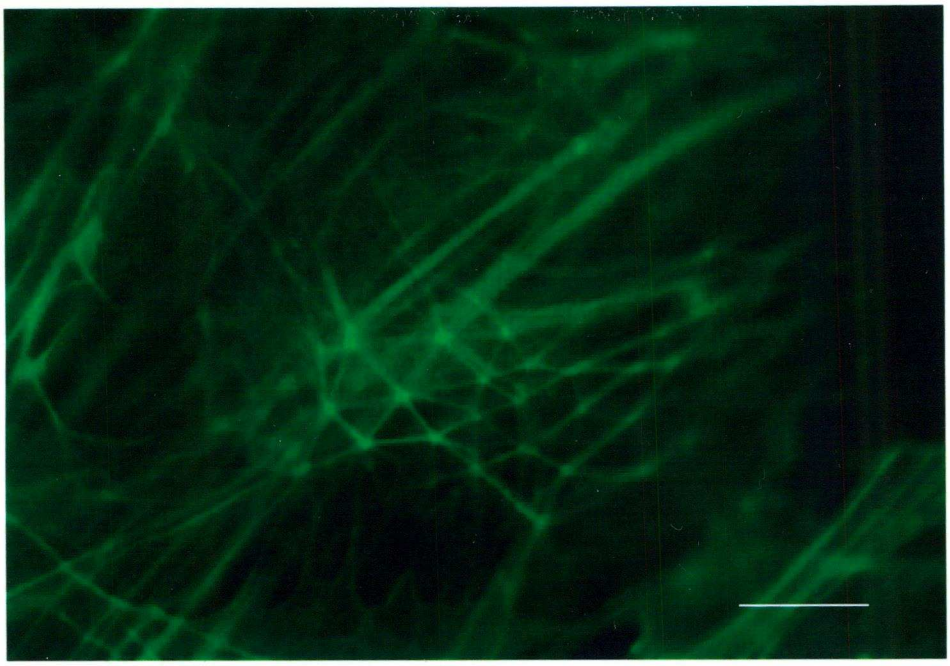

Figure 1.2 CLAN in TM cell. The F-actin arrangement is ordered into areas of 'hubs' and 'spokes' of five and six polygons. Scale bar = 10μm

1.1 The Eye

The eye is the organ that gives us the sense of sight, thus allowing us to observe the world around us. The eye is a roughly spherical tissue that is divided into three layers: the external layer, formed by the sclera and cornea, the intermediate layer, including the anterior and posterior chamber and the interior layer, the sensory part of the eye the retina (figure 1.3).

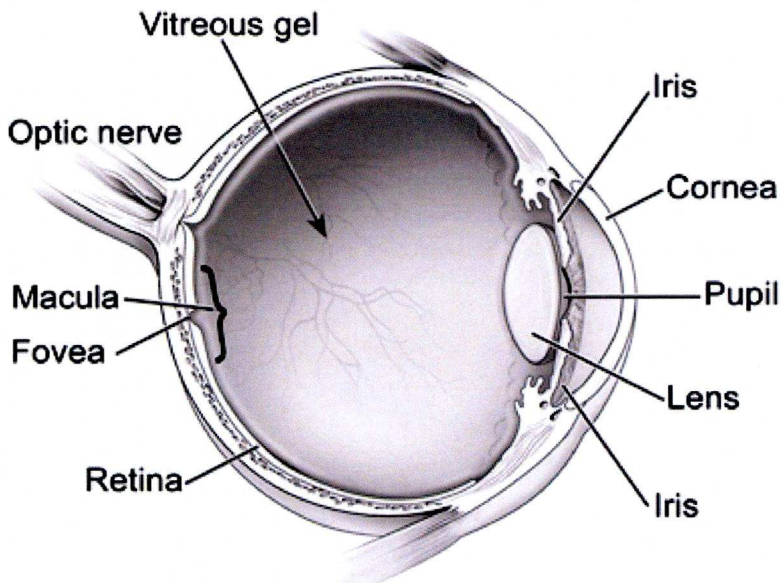

Figure 1.3 Schematic representation of the whole eye globe highlighting the major structures of the globe.

National Eye Institute (National Institutes of Health)

1.1.1 Sclera and cornea

The Sclera makes up most of the fibrous tunic of the eye and extends from the edges of the clear cornea at the front of the eye to the optic nerve at the back of the eye (Riordan-Eva et al., 2008). The sclera is a thick, opaque, white tissue that covers 95% of the surface area of the eye. It is thickest posteriorly around the optic nerve and is thinnest at the equator. The sclera serves as an attachment for the extraocular muscles that help move the eye and helps protect the intraocular components from injury. A large proportion of the outer layer of the eye bulges forward as the cornea. The cornea is a unique biological tissue that is transparent to light and contains no blood vessels. Centrally the cornea is around 500μm and peripherally is around 650μm thick. The cornea is the primary structure focussing light entering the eye.

The cornea is composed of five layers: The corneal epithelium, Bowman's membrane, the stroma, Descemet's membrane and the corneal endothelium. The corneal epithelium is the outermost layer of the cornea and is comprised of 5/6 layers of cells of stratified squamous epithelium with a total thickness of around 50μm. These are constantly regenerating to replace any damaged epithelium to avoid microbial infection. Bowman's membrane is an acellular matrix which lies between the epithelium basal lamina and the corneal stroma. It is comprised mainly of small collagen fibrils and is approximately 10μm thick (Riordan-Eva et al., 2008). The corneal stroma comprises 90% of the corneal thickness. The stroma is comprised of regularly arranged collagen fibers interspersed with keratocytes which allows the light to pass without being diffracted or reflected. It consists of approximately 200 layers (lamellae) of collagen fibers. The collagens unique shape, arrangement and spacing are essential in producing the cornea's light-conducting transparency. Descemet's membrane is a basement membrane that lies between the corneal stroma and the endothelium and is composed of collagen. The innermost layer of the cornea is the corneal endothelium lies directly below Descemet's membrane. It is a monolayer of squamous epithelial cells lining the posterior corneal surface and is responsible for regulating fluid and solute transport between the aqueous and corneal stromal compartments. Thus endothelial transport of water and electrolytes is governed by solute transporters.

1.1.2 Anterior chamber

Below the cornea is a fluid filled space termed the anterior chamber. The aqueous humour is secreted by the epithelium of the ciliary processes; tight junctions between cells form the blood-aqueous barrier. This is not merely a passive process and is actually an active transport system; chiefly ionic transport. Aqueous humour forms at

a rate of about 2-3ul/min with the fluid volume of the anterior chamber being completely changed over a period of one hundred minutes. The aqueous humour passes through the posterior chamber through the narrow space between lens and iris and passes through the pupillary opening into the anterior chamber. The two main functions of the aqueous humour are to transport nutrients to the avascular cornea and lens, and to maintain correct intraocular pressure (IOP); both of which are critical for vision.

1.1.3 Posterior chamber

The posterior chamber is a small area posterior to the iris and anterior to the lens and in front of the suspensory ligament of the lens (Riordan-Eva et al., 2008).

1.1.4 Retina

The retina is the innermost layer of the eye. The human retina is around 200μm thick and is composed of ten different layers (Yamada, 1969). The layers are the inner limiting membrane, the nerve fiber layer, the ganglion cell layer, the inner plexiform layer, the inner nuclear layer, the outer plexiform layer, the outer nuclear layer, the outer limiting membrane, the photoreceptor layer contains rods and cones and finally the retinal pigment epithelium (figure 1.4). The nerve fiber layer contains the retinal ganglion cell axons that lead to the optic nerve. The ganglion cell layer is the ganglion cell bodies, the inner plexiform layer is a network of axons and dendrites from ganglion cells and amacrine cells (Riordan-Eva et al., 2008). Next the outer plexiform layer composed of the nerve endings of bipolar cells, horizontal cells and photoreceptor cells; here cone pedicules and rod spherules are synaptic upon various bipolar cell and horizontal cell types. The outer nuclear layer is the layer that contains the nuclei and cell bodies of the rod and cone cells. Next the outer limiting

membrane is not really a membrane; instead it is the site of numerous occluding junctions, these seal off the base of the rods and cones. The next layer is the photoreceptor layer composed of rods and cones. The photoreceptor layer is responsible for converting light into electrical signals. Electrical signal integration is what the brain performs. The rods are more numerous, some 120 million, and are more sensitive than the cones. However, they are not sensitive to colour. The 6 to 7 million cones provide the eye's colour sensitivity and they are much more concentrated in the macula. In the centre of the macula is the fovea centralis, a 300μm diameter rod free area with densely packed cones. The cones are thinner and more rod-like in appearance to cones elsewhere in the retina. Compared to the rest of the retina the cones have a smaller diameter and can be more densely packed in a hexagonal pattern. The high spatial density of cones accounts for the high visual acuity capability at the fovea.

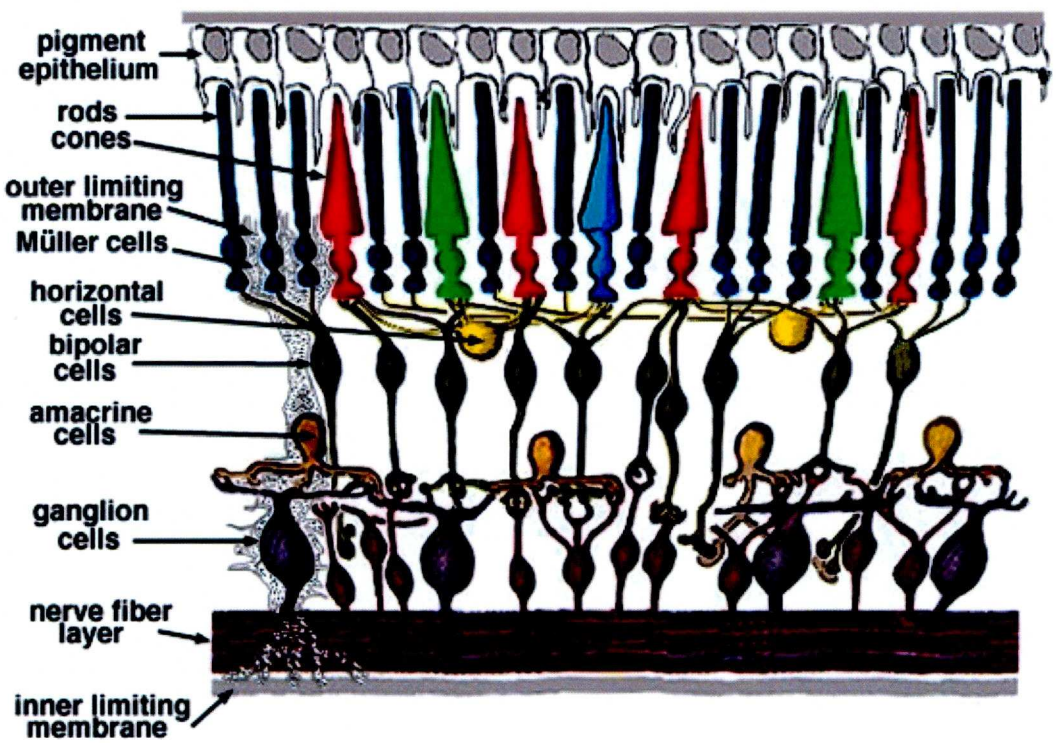

Figure 1.4 Simple diagram of the retina. Highlighting the major areas. Taken from: http://www.personadigital.net/Persona/neuroscience/Vision.htm

Retinal ganglion cells are the final output neurons of the retina and are responsible for sending the signal to the brain via the optic nerve.

1.2. The trabecular meshwork

The anterior and posterior chambers of the eye are filled with aqueous humour and functions to supply nutrients to the avascular sections of the eye, cornea and lens, and to maintain the correct IOP (figure 1.5). IOP is caused by the flow of aqueous humour against resistance in the outflow pathway. There are two different pathways of aqueous humor outflow: the conventional outflow pathway and the uveoscleral or non-conventional pathway.

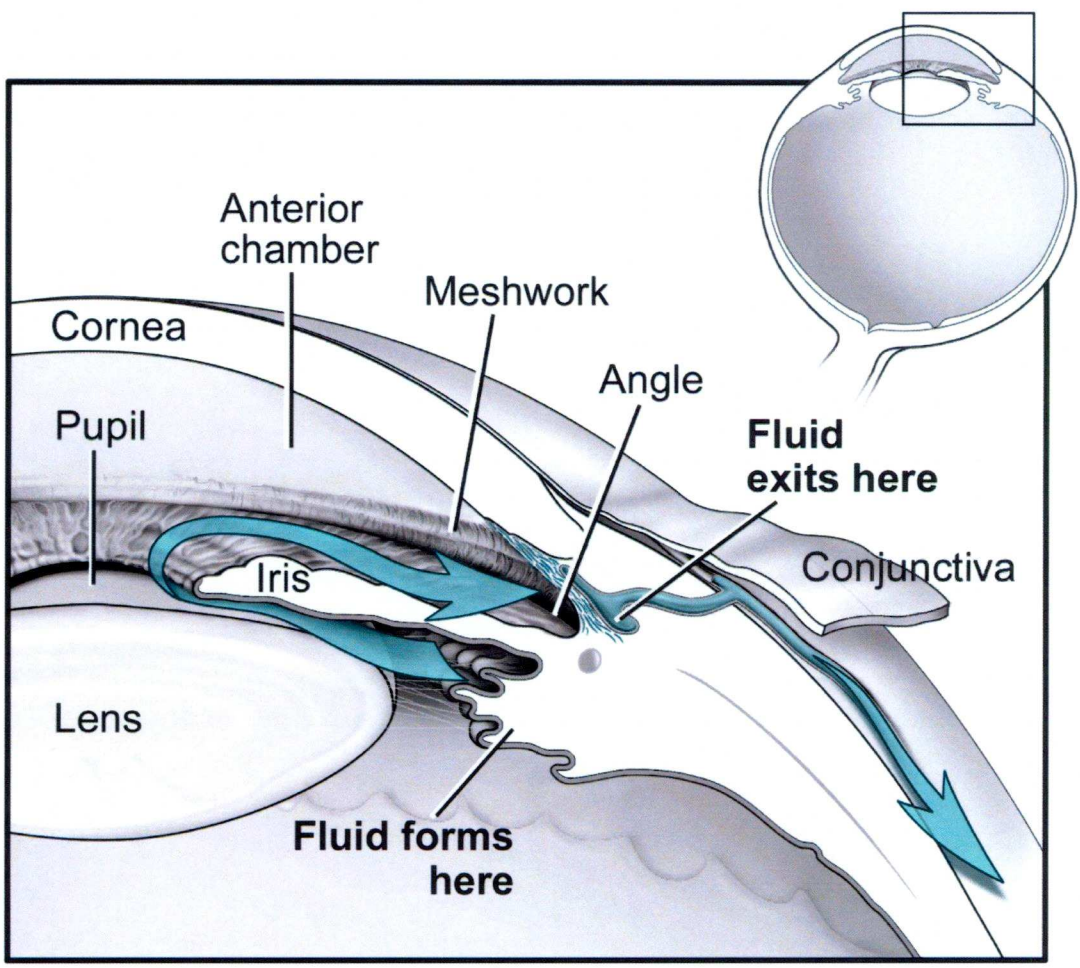

Figure 1.5 Schematic representation of the major areas of the eye involved in the creation and flow of aqueous humour. The aqueous humour is produced by the non-pigmented epithelium and passes through the small space between the lens and iris before passing through the pupillary opening and passes through the trabecular meshwork to exit via Schlemm's canal and aqueous veins and to a lesser degree through the unconventional outflow pathway.

National Eye Institute (National Institutes of Health)

1.2.1 The uveoscleral pathway

The uveoscleral pathway for aqueous humor outflow consists of the interstitial spaces between the ciliary muscle bundles, into the superchoroidal space, where it is absorbed into the venous system. Anders Bill first described the uveoscleral pathway and that in the cynomolgus monkey that about 50% of the aqueous humor exits through the ciliary muscle. This unconventional outflow was then observed in human eyes and found that the total percentage outflow attributed to the uveoscleral pathway was approximately 10-20% (Bill and Phillips, 1971). Although indirect calculations in human eyes via non-invasive methods have suggested values of around 35% (0.8µl/min flow) (Townsend and Brubaker, 1980). The rate is difficult to measure in humans as it requires injection of high molecular weight tracers into the anterior chamber. Cyclodialysis was also shown to increase uveoscleral outflow and hence intraocular pressure (Suguro et al., 1985). However, the normal ageing eye results in a decrease in uveoscleral outflow facility (Carol et al., 1999). Indeed the current therapeutic drugs used in the treatment of POAG, such as latanoprost, lower intraocular pressure by increasing outflow through the uveoscleral pathway. Most drugs are based on prostaglandin-F2α and have little if any effect on the conventional outflow system. The mechanism of action of increasing uveoscleral outflow is still debated but likely includes relaxation of the ciliary muscle and an increase in matrix metalloproteases leading to extracellular matrix breakdown (Lindsey et al., 1997, Sagara et al., 1999). Also a role of increased connective tissue-filled spaces among

the ciliary muscle bundles has been suggested as a possible mechanism of action (Tamm et al., 1990). Although much research is underway to determine the effects of the prostaglandins on TM cells in vitro and in vivo.

1.3 The TM is a multi-layered tissue

The TM is located at the iridocorneal angle of the eye and is the main route through which outflow of aqueous humor occurs (figure 1.5). The TM is a filter made up of extracellular matrix (eg. collagens), most of which is organised into a network of beams covered by endothelial like trabecular cells. These endothelial-like cells cover the collagenous beams and are the main cell in the TM. As the aqueous humour travels from the interior part of the meshwork to the middle and to the exterior side of the TM, the porosity of the tissue decreases. This tissue contains three differentiated layers: the uveal meshwork, the corneoscleral meshwork and the third layer which is in direct contact with the endothelial cells from Schlemm's canal is the juxtacanalicular meshwork (sometimes called the cribiform region) (Ashton et al., 1956). The aqueous humor passes through the TM and to Schlemm's canal, and from there to episcleral veins via collector channels that traverse the limbal sclera. The TM is a porous structure that spans the opening of the internal scleral sulcus and overlies Schlemm's canal. It is through these pores the aqueous humor travels to the episcleral veins into the circulation (Alvarado et al., 2005).

The inner uveal meshwork lies most internal forming the lateral border of the anterior chamber (Ashton et al., 1956). This is arranged in bands or trabeculae that extend from the iris root to the peripheral cornea. They have larger intervening spaces that measure 25-75μm (figure 1.6). The extracellular matrix of the uveoscleral beams includes interstitial collagen with intermixed elastin fibrils and proteoglycans

(Gong et al., 1989, Umihira et al., 1994). The uveal meshwork is thought not to offer much resistance to aqueous humor outflow because intercellular spaces are large.

The corneoscleral meshwork makes up the inner portion and most extensive part of the TM. It consists of connective tissue plates with a complex extracellular matrix environment. The trabeculae of the corneoscleral meshwork have fewer, smaller openings that give them the appearance more like that of perforated sheets. The connective tissue plates arise primarily from the scleral spur and extend over the internal scleral sulcus. These corneoscleral meshwork perforated sheets contain round or oval pores that gradually decrease from around 50μm down to 5μm in diameter as they approach Schlemm's canal. The TM cells lining these structures sit upon a basement membrane and are interconnected by desmosomes and gap junctions (Raviola and Raviola, 1981). The gap junctions facilitate intercellular communication between cells by the passage of small molecules. These TM endothelial cells are not simply passive structural cells but active participants in outflow resistance by altering the pore size.

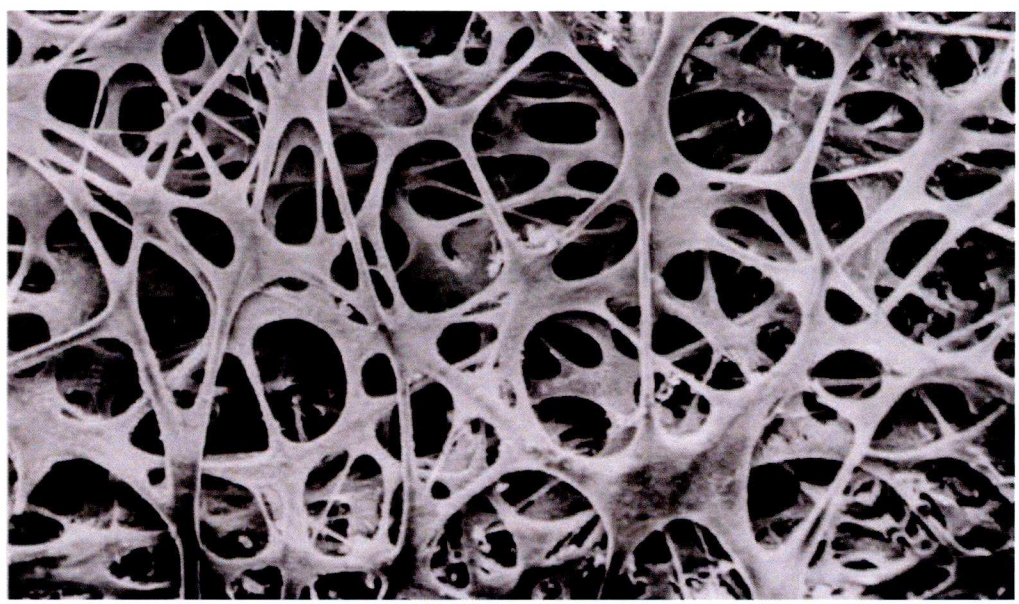

Figure 1.6 Scanning electron micrograph of uveal TM. Scanning electron micrograph showing the appearance of the uveal trabecular meshwork and the clear trabecular beams (x500 magnification); the intratrabecular spaces are evident. There are no endothelial cells present in this image and is just the decellularised tissue with collagenous beams present. Reproduced from (Freddo et al., 1984).

The juxtacanalicular region of the TM is the outermost part and it is thought that here much of the resistance to outflow resistance takes place (Grant, 1963). This structure is composed of a single layer of layer of tissue that borders Schlemm's canal (Rohen et al., 1981). This meshwork contains very narrow and small irregular openings. The outermost portion of the juxtacanilicular meshwork consists of a layer of endothelial cells that form the inner wall of Schlemm's canal (Rohen et al., 1981, Lutjen-Drecoll et al., 1981, Grierson and Lee, 1975). In Schlemm's canal giant vacuoles are responsible for drainage of the aqueous humour to the episcleral veins and into the circulation (Grierson and Lee, 1975).

The ligamentous insertions of the ciliary muscle into the TM mediate the permeability of the tissue to aqueous humor (Rohen et al., 1981). After the ciliary muscle contracts, its insertions extend the intercellular spaces and pores in the TM leading to increased egression of aqueous humor. At the same time uveoslceral outflow decreases. When the ciliary muscle relaxes the intertrabecular spaces become narrower and outflow facility is reduced. Thus the tone of the ciliary muscle modulates TM outflow facility. This can be used to great effect with muscarinic drugs such as pilocarpine. Pilocarpine, working through contraction of the ciliary muscle, is a very effective IOP lowering compound.

1.3.1 BTM

The bovine (*Bos Taurus*) TM (BTM) is anatomically similar to the human TM. However the BTM is more "reticular" rather than the human "trabecular"

organisation (Flügel et al., 1991) and there is no clear connection between the ciliary muscle and the outflow tissue. Moreover, the BTM contains an aqueous plexus which is the functional equivalent of the human Schlemm's canal and as such is analogous (Wade et al., 2009). The tissue is larger that of the human TM and has been used since Barany used this species to investigate the influence of hyaluronidase on outflow resistance (Barany and Scotchbrook, 1954). Since then BTM tissue has been used to determine and characterise the activities of catalase and superoxide dismutase (Freedman et al., 1985) and glutathione peroxidase (Scott et al., 1984). Indeed this model has been used to evaluate the effect of steroids on extracellular matrix deposition by prednisolone (Tektas et al., 2010). Intraocular administration of steroid leads to an increase in collagen type VI in the outflow loops from cattle (Tektas et al., 2010).

1.3.2 The constituent cells of the TM

The cells that reside upon the basement membranes of the trabecular beams in the TM are endothelial like cells, broad and flattened. These are the only cells in the TM and derive their nutrition from the aqueous humour. Their isolation and characterisation in culture began a new era of outflow biology giving a tractable model with which to investigate the cells (Grierson et al., 1983, Polansky et al., 1979a, Polansky et al., 1981). The establishment of in vitro tissue cultures of human TM endothelial cells demonstrated that they are similar to those in vivo in terms of characteristics and have synthetic properties (Grierson et al., 1983), thus giving a model to investigate the TM further. It has been shown that they possess prominent intracellular lysosomes, golgi apparatus and endoplasmic reticulum and therefore can secrete proteins. Grierson then established BTM cell cultures (Grierson et al., 1985a) derived from cattle as an easier tissue procurement. These BTM cells were found to

be very similar to human TM cells and were rich in extracellular collagen and other extracellular matrix macromolecules such a type I collagen (Grierson et al., 1985a). Moreover, the BTM cells had the functional ability to phagocytose latex microspheres in vitro (Day et al., 1986) and could migrate in vitro an actin-dependant process (Hogg et al., 1995a). Subsequently it was shown that BTM cells lose cell-matrix cohesion after phagocytosis in vitro (Zhou et al., 1995). This loss of cell-matrix cohesion may underlie the migration of TM cells subsequent to phagocytosis in situ (Grierson and Lee, 1973). BTM cells were then investigated for cytoskeleton filaments and found to exhibit strong actin stress fibres (Grierson et al., 1986). Indeed it was demonstrated that they contained an extensive cytoskeleton network and a prominent stress fibre pattern and that these cells contracted when exposed to magnesium adenosine triphosphate (MgATP) (Grierson et al., 1986). Many authors now use the BTM as a model system to study the TM due to its large size and relative ease of dissection and procurement and similarities to human tissue (Grierson et al., 1985a, Flügel et al., 1991).

1.3.3 The TM is an active and not passive tissue

The dogma that the TM was a passive tissue that was merely distended by the ciliary muscle to mediate outflow of aqueous humor is now outdated. It is now established that TM cells serve an active role in governing outflow resistance and intraocular pressure. Grierson et al. initially showed that TM cells respond to MgATP application with a contractile response (Grierson et al., 1986). Subsequently it was demonstrated that TM cells are highly contractile displaying smooth muscle like properties and contract robustly to acetylcholine and pilocarpine (Lepple-Wienhues et al., 1991). This has been demonstrated both in in vitro cell preparations and whole tissue ex vivo (Lepple-Wienhues et al., 1991). Further research has shown that the

TM cells display electrophysiological properties and calcium (Ca(2+)) is the main compound mediating this (Steinhausen et al., 2000). Thus free intracellular Ca(2+) mobilisation serves to facilitate TM cell contraction. TM cells are also known to express muscarinic receptors and respond to agonist-mediated receptor activation with intracellular calcium rises (Thieme et al., 2001). The TM cells themselves may synthesis and secrete proteins in a paracrine manner that regulate contraction and hence modulate outflow resistance and IOP. Endothelin antagonists are currently pursued as a drug target in POAG (Rosenthal and Fromm, 2011).

1.3.4 Contractile nature of TM cells

A growing body of evidence shows that the TM cells are themselves contractile (Grierson et al., 1986, Lepple-Wienhues et al., 1991) and have similar properties to smooth muscle cells. It has been demonstrated that endothelin-1, a potent vasocontractile protein, is expressed by TM cells and pharmacological inhibition of the endothelin receptor subtypes supresses endothelin-induced contraction in a dose dependant manner (Choritz et al., 2005). Evidence also points to a role of the cytoskeleton in contraction as incubation with RhoA kinase inhibitor attenuates agonist-induced contraction (Rosenthal et al., 2005b). Inhibition of RhoA kinase also results in an alteration of actin architecture and a significant increased outflow facility (Rao et al., 2001) and blockade of contraction in collagen gel contraction matrices therefore indicating that actin plays a role in contraction of TM cells (Koga et al., 2006). Nitric Oxide (NO) is an important signalling molecule in many tissues and cells. It is biosynthesised from L-arginine, oxygen and NADPH by nitric oxide synthase and is highly reactive. NO may serve to relax smooth muscle cells after contraction serving as a homeostatic mechanism. NO has been shown to regulate TM cell contraction-relaxation (Wiederholt et al., 1994). Thus the contractile nature of

TM cells is without doubt and is mediated by the cytoskeleton and helps regulate outflow physiology.

1.4 TM extracellular matrix

The extracellular matrix of the TM is rich in many compounds. The extracellular matrix is comprised of various collagens, laminin, fibronectin, proteoglycans and glycosaminoglycans which interact with the TM cells that reside upon the collagenous beams (Tamm, 2009). The small leucine-rich proteoglycans decorin and biglycan are constitutively expressed and bind collagen and may help stabilise the collagen in the meshwork. Collagens are one of the most abundant proteins found in the TM and in the animal kingdom. They consist of three polypeptide α-chains, each containing a characteristic repeating tripeptide sequence of Gly-Xaa-Yaa, in which proline and hydroxyproline are often in the Xaa and Yaa positions, respectively. The primary sequence of each chain results in the formation of a left-handed helical secondary structure. Triple helix formation occurs first by selection of the α-chains, followed by nucleation at the C-terminus, and finally propagation of the triple helix from C-to N-terminus (Beck and Brodsky, 1998). Different types of collagen are present in the TM and include collagen type I, III and IV (Lutjen-Drecoll et al., 1981, Rehnberg et al., 1987). Collagen fibrils impart tensile strength to the tissue.

Deposition of excessive extracellular material in the TM has been proposed as the pathogenic mechanism leading to increased outflow resistance and development of POAG (Lutjen-Drecoll et al., 1981). Previous ultrastructural and histochemical investigations have demonstrated an increase in the amount and location of extracellular material (Lutjen-Drecoll et al., 1981, Lutjen-Drecoll et al., 1986) suggesting that the increased outflow resistance observed in POAG is due to the

abnormal accumulation of extracellular matrix material. Some authors called areas of trabecular thickening of elastic fibres from the sheaths 'sheath derived plaques' and that these sheath derived plaques increase with increasing age and POAG (Lutjen-Drecoll et al., 1986). This was further confirmed in untreated cases of POAG tissue with no prior medical therapy; the increased deposition of collagen was clearly apparent within the TM. Additionally a conspicuous deposition of fibrillar material was observed under the inner wall of Schlemm's canal (Tektas and Lutjen-Drecoll, 2009).The extracellular matrix is not static and is a fine balance between the synthesis of matrix and the proteolytic breakdown of the matrix. This is mediated mainly my matrix metalloproteases (MMPs) and their inhibitors: tissue inhibitors of matrix metalloproteases (TIMPs) (Cawston, 1996). TIMPs bind non-covalently to MMPs forming a 1:1 stoichiometry that is essentially irreversible. Mutations have been found in TIMP-3 leading to an accumulation of matrix in the inherited macular degenerative disease Sorsby's fundus dystrophy (Weber et al., 1994).

1.4.1 MMPs

The first vertebrate MMP was identified in 1962 by Gross from tadpole tissue, by the collagenolytic activity of this tissue on collagen gels. Tadpole collagenase was shown to cleave collagen at a specific site at neutral pH and physiologic temperatures and was subsequently purified in 1966 (Nagai et al., 1966). Since then many MMPs have been identified in many tissues including the TM (Alexander et al., 1998).

In mammals the MMP family consists of 23 neutral enzymes, traditionally subdivided according to their substrate specificity, primary structure and cellular location. The four main groups are the collagenases, stromelysins, gelatinases and membrane-type metalloproteinases (MT-MMPs). MMPs expression and activation

can be modulated by various growth factors and cytokines and these help facilitate the breakdown of the extracellular matrix. MMPs have several common properties: they contain common amino acid sequences; contain zinc at the active site and also require $Ca(2^{+})$ and are secreted as inactive proenzymes that require activation. Activation is accompanied with a fall in molecular weight. Their pre-domain encodes a hydrophobic leader sequence that targets them for secretion into the extracellular space. These mediate the constant flux between synthesis and breakdown of matrix and a modulation of either can lead to increased deposition of matrix (Cawston, 1995). Although there is an increase in extracellular matrix material in POAG and also ageing, the exact contribution to POAG remains unresolved. As does the question of whether the matrix deposition is a consequence rather than a cause of the disease.

1.5 The cytoskeleton

Eukaryotic cells have distinct shapes and a high degree of organisation that is highly dependent on complex networks of protein filaments in the cellular cytoplasm that mediate such shape and shape changes; this is called the cytoskeleton. Indeed recently it has been found that bacteria contain a homologue of actin: MreB and share high structural similarity and form filaments (Figge et al., 2004). The cytoskeleton, in association with many other proteins, mediates a diverse range of functions including locomotion and contraction (Pellegrin and Mellor, 2007). The three main types of filaments of the cytoskeleton are actin filaments or microfilaments, microtubules and intermediate filaments. All three types are made from globular protein subunits and are in constant dynamic flux.

1.5.1 Microfilaments

The microfilament network is a network of filaments 6-7nm in diameter composed entirely of actin. There are a least six different types of actin synthesised by vertebrate cells; however, their amino acid sequences are conserved and have similar properties (Vandekerckhove and Weber, 1978). Actin is found in all vertebrate cells and is one of the most conserved genes. Its conservation and ubiquitous nature argue for an indispensible role. Globular actin known as G-actin is composed of a single polypeptide of molecular weight ~42000. Each molecule of G-actin is associated with one tightly bound Ca^{2+} , which stabilises its globular conformation, and one molecule of non-covalently bound adenosine triphosphate (ATP) (figure 1.7).

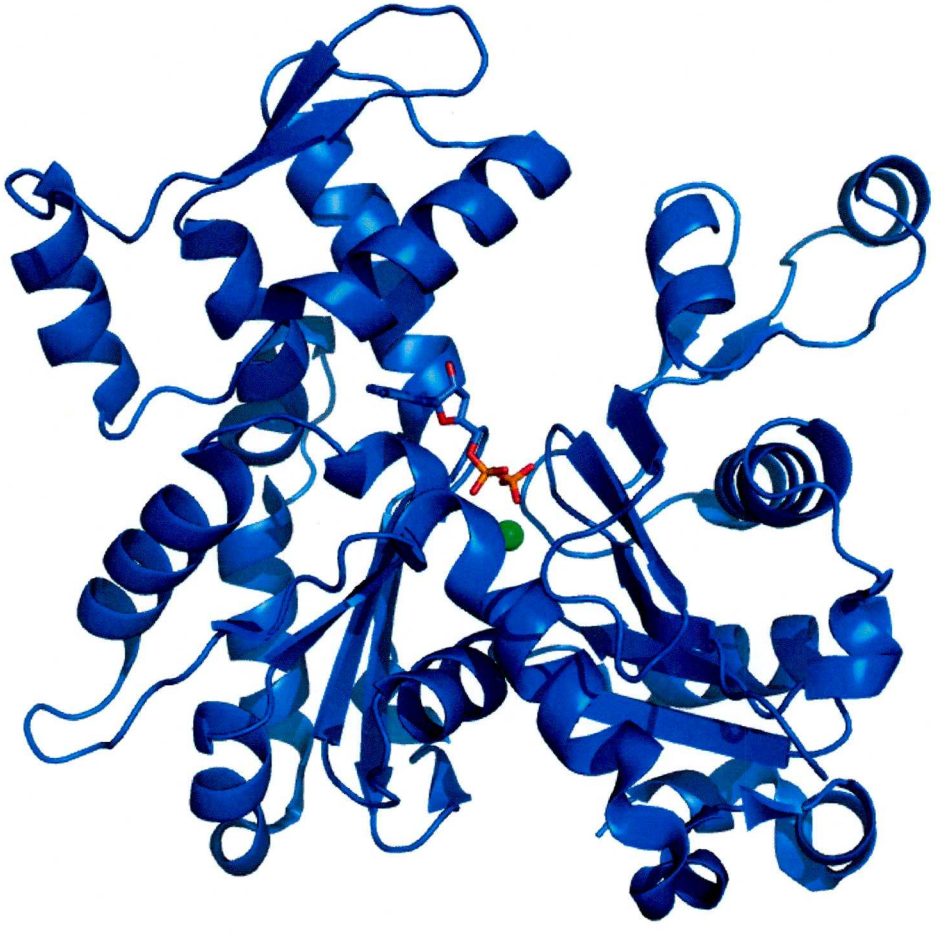

Figure 1.7 Ribbon cartoon of G-actin monomer with a bound ATP molecule in the central groove (green dot). This is the building block of F-actin. Taken from: www.websters-online-dictionary.com

Actin filaments as seen in electron micrographs consist of two strands of globular molecules about 4nm in diameter twisted into a helix with 13.5 molecules per turn.

Actin filaments have polarity. The polarity of an actin filament can be determined by decorating the microfilament with myosin "S1" fragments, visualising so called barbed (+) and pointed (-) ends on the filament. Once formed many arrangements of F-actin are formed into bundles that run parallel to the axis of the cell and are termed stress fibres. These are contractile actin-myosin arrangements mediate contraction and migration reminiscent of the structures in muscle cells.

1.5.2 Microtubules and intermediate filaments

Microtubules are rigid, hollow rods approximately 25nm in diameter. Like microfilaments, microtubules are dynamic structures that undergo constant assembly and disassembly. They function in intracellular movement of intracellular cargo and cell division in all eukaryotic cells. Intermediate filaments are so called because their size is in between that of microfilaments and that of microtubules. They have an average diameter of around 10nm. There are five different types of intermediate filaments.

1.5.3 Cytoskeleton architecture

The cytoskeleton of many cell types is in a constant flux between polymerisation of F-actin and depolymerisation to G-actin. The F-actin arrangement of many cells underlies many cellular processes. Indeed migrating fibroblasts or most vertebrate cells but not all, in tissue culture show a unique polarised morphology; a broad flat lamella extending in the direction of migration that terminates in a ruffling lamellipodium and a retracting tail at the rear of the cell (Abercrombie et al., 1970). The lamellipodium requires the polymerisation of F-actin to mediate cell movement

and gain traction. However the exact actin arrangement is dependent on the exact function required to carry out by the cell. Migrating cells use actin filaments to push at the front, by polymerisation and to pull at the rear, by forming contractile assemblies with myosin.

It has been demonstrated in certain cells that there is a unique actin arrangement of F-actin that displays characteristics of geodesic domes in culture (Lazarides, 1975, Lazarides, 1976). These geodesic F-actin arrangements were first described in non-muscle cells by Lazarides after plating out in culture conditions and were suggested to be a precursor to the stress fibre formation found in well spread cells (Lazarides, 1976).

1.5.4 Stress Fibres

Stress fibres are arrangements of bundles of actin-myosin that are contractile and are composed of approximately 10-30 actin filaments (Cramer et al., 1997). Such bundles are tied together by the actin crosslinking protein α-actinin (Lazarides and Burridge, 1975). α-actinin is composed of two anti-parallel peptides with four spectrin-like repeats with the actin binding domain at the N-terminus. The staining of α-actinin is very periodic along the fibre and alternates with bands containing non-muscle myosin and tropomyosin (Lazarides and Burridge, 1975, Lazarides, 1976). This is very similar to the sarcomere in muscle in that the z lines slide along the filament, but their arrangement is less uniform. The stress fibre bundles of F-actin are polarised in the cell and terminate at focal adhesion points at the cell-extracellular interface. Figure 1.8 shows a BTM cell with clear stress fibres. By coupling to the extracellular matrix and exerting force they enable cells to mechanically influence their environment and sense the mechanical properties (Askari et al., 2009).

Many cells contain at least three different categories of stress fibers: ventral stress fibers, transverse arcs, and dorsal stress fibers. Ventral stress fibers are contractile actin filament bundles that are typically associated at both their ends to focal adhesions. These molecules are located at the ventral surface of the cell and play an important role is adhesion and contraction. Transverse arcs are curved bundles of actin that are not attached to focal adhesions. Dorsal stress fibres are actin bundles that have an end associated with focal adhesions and are located at the dorsal surface of the cell. The focal adhesions are large macromolecular complexes through which the cytoskeleton connects with the extracellular matrix and are regions of signal transduction. Stress fibres have been shown to shorten and generate tension in intact living cells (Kumar et al., 2006, Kreis and Birchmeier, 1980). These cell-generated tensional forces drive cell shape and contraction and play a fundamental part in the control of many cellular processes.

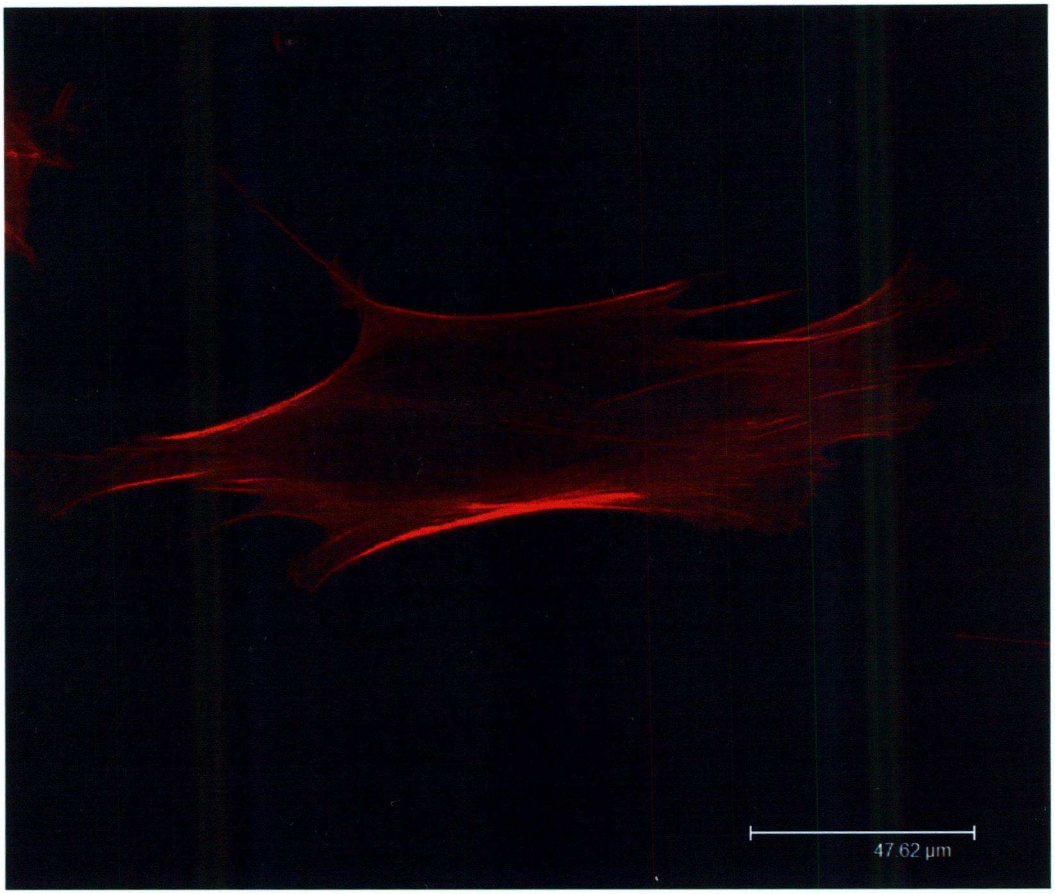

Figure 1.8 BTM cells expressing stress fibres. A BTM cell in pre-confluent culture fixed and stained for phalloidin-rhodamine for F-actin.

1.5.5 Stress fibre assembly regulation

The regulation of stress fibre assembly is mainly through a signalling cascade including RhoA small Guanasine Triphophatase (GTPase) protein (Ridley and Hall, 1992). A small GTPase protein Rac promotes actin polymerisation at the plasma membrane leading to lamellipodia and Cell division cycle 42 (Cdc42) induces the formation of microspikes or filopodia formation (Nobes and Hall, 1995). Microinjection of recombinant RhoA protein into cells results in induction of stress fibres and the concomitant assembly of focal adhesions. In vertebrates, the gene encoding RhoA has undergone duplication yielding two more isoforms: RhoB and RhoC. These protein share high homology with RhoA and themselves induce stress fibre formation (Giry et al., 1995).

Rho GTPases cycle between an active GTP-bound form and inactive GDP-bound form. Their activity is regulated by guanine nucleotide-exchange factors (GEF), which promote the exchange of GDP for GTP, and GTPase activating proteins (GAP), that enhance the GTPase activity of these proteins, thereby controlling cell signalling. In the active GTP-bound conformation, RhoA binds to and regulates a variety of downstream effectors (Ridley, 2001). In the main, RhoA leads to a clear increase in stress fibres and focal adhesion assembly. Indeed migration and malignant transformation is linked to inappropriate RhoA activation. The downstream targets of RhoA are many and varied but include the serine threonine kinase p160ROCK; this interacts with RhoA in a GTP-dependant manner and when overexpressed it mimics the actions of RhoA (Riento and Ridley, 2003). Another effector of RhoA appears to be myosin light chain phosphatase (Kimura et al., 1996). Downstream targets of Rac include p21-activated kinase (PAK) family members (Manser et al., 1994). Rac and Cdc42 bind to the regulatory domain and displace leading to phosphorylation. It appears that RhoA mediated signalling to the cell resulting in an increase in stress fibres is through the bundling of actin filaments (Machesky and Hall, 1997). Signalling through Rho GTPases can be initiated by activation of many different types of plasma membrane receptor including tyrosine kinase, G-protein-coupled and cytokine receptors (Ridley, 2001).

1.5.6 Integrins

Integrins are a large family of cell-surface type 1 transmembrane adhesion receptors that mediate both cell–cell and cell–extracellular matrix (ECM) interactions and are an interface between the ECM and cytoplasmic events (Morgan et al., 2007). Integrins can also support bi-directional signalling. Integrins are heterodimers of α and β subunits, each containing a large extracellular domain (~ 80–150 kDa), a single

transmembrane α-helix and a short, largely unstructured, cytoplasmic domain or tail of 10–70 residues (Askari et al., 2009). Activation of integrins from the inside out is initiated by the separation of the two subunits at their cytoplasmic and transmembrane regions, leading to unbending of the ligand-binding headpiece leading to conformational change that increases ligand-binding affinity (Kim et al., 2003). Binding of integrin β-subunits cytoplasmic domains to the cytoskeletal adaptor protein talin, is a critical point of convergence for integrin activation signals (Tadokoro et al., 2003). Indeed knockdown of talin results in no integrin signalling, thus demonstrating its importance in mediating integrin signalling (Tadokoro et al., 2003). Indeed CLANs have been shown to be induced through activation of integrin mediated signalling by using soluble antibodies against β1 and β3 subunits in human TM cells (Filla et al., 2006). Moreover immobilised substrates for integrins plated onto coverslips mediates an integrin-dependant increase in CLANs (Filla et al., 2006) and the authors suggest an 'inside out signalling' mechanism facilitated by integrins. However these were freshly plated TM cells and not stable cultures and they may not actually be CLANs *per se*. Therefore this suggests that CLANs are mediated by extracellular ligand binding via integrins to compartmentalise cytoplasmic signalling events.

1.6 CLANs in TM cells

As stated in section 1.0 geodesic arrangements of F-actin have been described in numerous cultures of different cell types (Lazarides, 1975, Lazarides, 1976, Ireland and Voon, 1981, Mochizuki et al., 1988). Indeed such polygonal actin structures have been seen in cardiac myocytes where the distal tips of the geodesic structures terminate into adhesion plaques (Lin et al., 1989). These striking polygonal structures in all cells were then shown to disappear after a prolonged time in culture

and the emerging pattern of F-actin was that of stress fibres running parallel to the axis of the cells (Lazarides, 1975). Thus the described 'geodomes' were considered an intermediate step in the formation and stabilisation of stress fibres in culture and not considered a permanent actin structure.

A totally different structure has now emerged that is similar but not a precursor to stress fibres and are called CLANs. These geodesic structures of F-actin were initially discovered in TM cells in confluent monolayer cultures after treatment with the glucocorticoid Dexamethasone (DEX) (Clark et al., 1994) (figure 1.9).

CLANs are polygonal arrangements of actin comprised of a central hub and vertices and often arranged into units of five of six (figure 1.2). These geodesic structures were found to be expressed in a variety of TM cell lines examined but not found in any other ocular tissue tested and while a variety of different steroids were tested for their potency in inducing CLANs in TM cells, DEX was by far the most potent steroid (Clark et al., 1994). It was also shown that a concomitant increase in cell size was apparent (Clark et al., 1994). These CLANs were composed of F-actin and the hubs also contained α-actinin, just as stress fibres have α-actinin attached to the filament. CLANs maybe attached to the apical cell surface via syndecan-4, but this is still debated (Filla et al., 2006). They were of various sizes and could encompass the whole of the cell, however different cell lines displayed large heterogeneity in CLAN incidence.

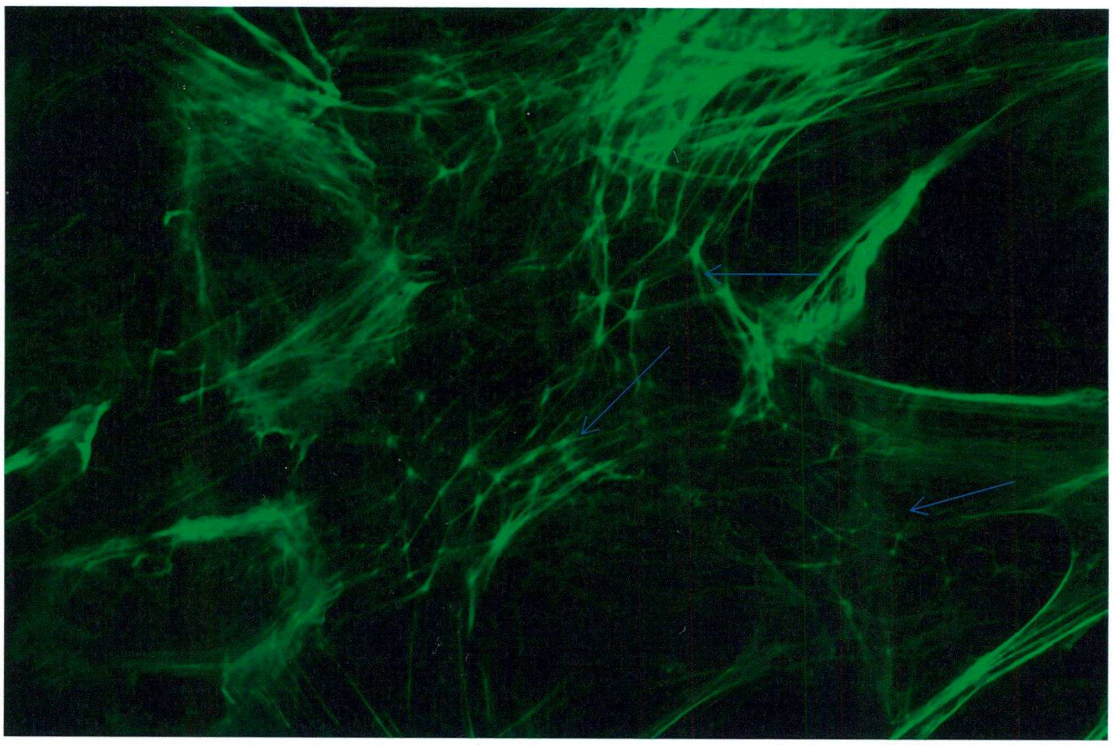

Figure 1.9 CLANs in BTM cells. Image of multiple CLANs in a BTM culture that had not been exposed to any steroid and fixed and stained with phalloidin-Alexa-488. The arrows indicate CLANs.

It was subsequently demonstrated that TM cells derived from glaucomatous donors displayed a significantly higher amount of basal CLANs without the addition of exogenous glucocorticoid (Clark et al., 1995). Moreover these diseased derived TM cells upregulated CLANs more efficiently than 'normal' cell lines (Clark et al., 1995). Using Green-fluorescent Protein (GFP)-tagged actin under a strong CytoMegalovirus (CMV) promoter we have imaged real time CLAN formation in TM cells and this indicated that CLANs can form in a relatively short time frame (unpublished observations).

A possible reason for high CLAN incidence in glaucoma TM cell lines this may be that glaucomatous cells possess low amounts of glucocorticoid receptor-β (Zhang et al., 2005). Glucocorticoid receptor β is a dominant negative regulator of glucocorticoid-α function and act to repress signalling and has been suggested to play

a role in steroid resistance in many steroid resistance diseases such as rheumatoid arthritis; it is a splice variant (Derijk et al., 2001, Chatzikyriakidou et al., 2009). Interestingly forced overexpression of glucocorticoid receptor β in TM cells supressed DEX-induced myocilin expression and fibronectin synthesis and release (Zhang et al., 2005). Myocilin is a gene and protein that is associated with POAG and is a target gene of DEX in TM cells, in other words this protein is hugely induced by exposure to DEX in cell culture (Clark et al., 2001). The first glaucoma gene, *GLC1A*, was mapped to chromosome 1q, and is responsible for autosomal dominant glaucoma, however, mutations in this region can lead to POAG and the gene was mapped to this region is myocilin (*MYOC*) (Stone et al., 1997). Although often different names are used they all refer to the same gene: myocilin. Myocilin is the preferred nomenclature.

CLANs however, had only been shown in vitro and to demonstrate that they are not an artefact of cell culture conditions this group undertook an *in situ* study to determine CLANs in TM tissue. An exhaustive study clearly demonstrated that CLANs are found in TM cells in situ in the outflow pathway and that these CLANs are remarkably similar to CLANs found in cell culture (Clark et al., 2005). This large study using reconstructed confocal 'slice' images showed that the normal non-pathologic TM system contains copious CLANs in situ and that CLANs are found in large numbers in the corneoscleral region of the outflow apparatus. Indeed using an organ culture whole eye perfusion model that was perfused with DEX before fixation it was shown that DEX induced many CLANs in the whole intact tissue compared to non-DEX perfused tissue (Clark et al., 2005). Therefore DEX induced CLANs ex vivo.

CLAN like structures were further found in TM tissue but this study was restricted to the juxtacanilicular region of the TM and Schlemm's canal and no clear definitive quantitative data could be garnered (Read et al., 2007). Due to the limitations of this study the authors may not have been convinced they were seeing true 'CLANs'. The authors also could not rule out the possibility that the structures observed were not secondary effects due to glaucoma medication that the subject was taking (Read et al., 2007). A further quantitative and qualitative study using TM tissue demonstrated that CLANs are numerous in normal TM tissue and are increased in aging and glaucomatous donors (Hoare et al., 2009). CLAN and 'CLAN-like' structures where demonstrated in all regions of the TM. However, CLANs were found to be more prominent in the uveal and corneoscleral regions than in the juxtacanilicular region. This study also showed the complexity of CLANs ranging from small structures to more elaborate 'network CLANs', and we estimated that the CLAN prevalence was 184,000 per eye in the POAG samples (Hoare et al., 2009). We predicted that every cell from glaucomatous trabecular meshwork tissue contained a CLAN (Hoare et al., 2009). However it was not an all or none situation and CLANs are in appreciable numbers in apparently healthy tissue, this was a surprising finding. However there was an increase in CLAN incidence in glaucomatous donors, however, due to the power of the study this was not statistically significant. With more samples this would have reached statistical significance.

Due to the limitations of collecting human tissue for research we then undertook a study for CLANs using BTM tissue. BTM cultures have been established and characterised previously and are easily available (Grierson et al., 1985a). It was found that BTM cultures have an increased number of CLANs without the addition of exogenous steroids (Wade et al., 2009). Moreover, that these cells have a

predisposition for the formation of CLANs. After 14 days in culture with DEX 50% of BTM cells contained CLANs. Some polygonal arrangements were found to be ordered into fives or sixes in a remarkably repetitive way (Wade et al., 2009). Indeed using the whole BTM tissue CLANs were found to be abundant and qualitatively the same as human TM CLANs. Soaking the BTM tissue in DEX for some time also increased the incidence of CLANs. Whilst this is not the same as an organ perfusion chamber model that has full tissue cohesion, nonetheless it is a useful tool. Although BTM has a more reticular nature than the human counterpart it is essentially the same and serves as useful model. It is interesting to note that cows given topical steroids all respond with an increase in intraocular pressure (Gerometta et al., 2004) in every cow treated. Thus the BTM serves as a useful model with which to probe the effect(s) of CLANs. Moreover due to its large size is easier to dissect and plentiful available.

1.7 The role of DEX in pathology of POAG

The use of glucocorticoids, topically or systemically, can lead to the development of corticosteroid-induced ocular hypertension and a clinically similar iatrogenic POAG in susceptible individuals (Armaly, 1966). That it is only induced in certain individuals implies that it has a genetic basis. The exact molecular mechanism that governs steroid-induced glaucoma remains elusive. The fact that glucocorticoids can lead to a clinically similar POAG, presumably through increased outflow resistance, has led a number of investigators to examine the effects of DEX on cultured TM cells in vitro (Clark et al., 1994). It has now been demonstrated that TM cells express glucocorticoid receptors both in cultured cells and whole TM tissue (Weinreb et al., 1981, Hernandez et al., 1983). These membrane bound receptors interact with their

cognate ligand, translocate to the nucleus and alter transcription of target genes mediated by co-activators or co-repressors.

DEX exposure to TM cells results in a variety of morphological and biochemical changes. Of the morphological changes induced by DEX one of the most dramatic is the increase in TM cell size (Wilson et al., 1993, Clark et al., 1996). DEX has also been shown to increase the density of secretory vesicles compared to control suggesting an increased secretion of proteins, possibly extracellular matrix proteins (McCartney et al., 2006) and a decrease in proteolytic enzymes (Snyder et al., 1993). Several studies have shown that DEX increases the secretion of extracellular matrix components including fibronectin (Steely et al., 1992). Fibronectin is a high molecular weight glycoprotein that serves generally as an adhesion molecule. Fibronectin could act as signalling cue for various TM cell functions. Thrombospondin-1 (TSP-1), a putative antiangiogenic factor, is also increased in TM cells after exposure to DEX in vitro (Flügel-Koch et al., 2004). TSP-1 is a large molecular weight glycoprotein that can interact with MMPs, ECM molecules and CD47.

It is known that DEX leads to an increase in CLANs in TM cells from both human and bovine origin (Clark et al., 1994, Wade et al., 2009), however the mechanism(s) that underlie the DEX-induced CLAN formation remain undetermined. Filla et al has shown that integrins may play a role in the formation of CLANs in TM cells (Filla et al., 2006). This demonstrated that immobilised activating antibodies against β3 and β1 integrins induced CLANs and that they have distinct signalling pathways (Filla et al., 2009). Indeed they showed that this integrin-induced CLAN formation was, at least partly dependant on activation of CD47, also called integrin-associated protein. CD47 is a receptor for TSP-1, the expression of which is upregulated by treatment

with DEX (Flügel-Koch et al., 2004), therefore increased TSP-1 would lead to an increased activation of its receptor CD47 leading to increased CLANs via integrin signalling in TM cells. This is a possible mechanism of CLAN formation but this study was using freshly plated TM cells within a few hours of trypsinisation and not confluent stable cultures (Filla et al., 2009). Also the authors did not address activation of CD47 receptor directly via addition of exogenous TSP-1 or the functional peptide of TSP-1 and how this augments integrin signalling. It is possible perturbations in this system may lead to CLANs.

A recent paper has also demonstrated DEX-induced CLANs in human TM cells and elevated the expression of zonula occluding-1 (ZO-1) and connexin43 (Cx43), both junctional proteins (Zhuo et al., 2010). Suggesting aberrations in signal transduction at cell-cell contacts and possible defects in actin signalling. It has been suggested CLANs alter the mechanical properties of the cells and a recent modelling study identified the glaucomatous TM as stiffer compared to normal TM tissue (Last et al., 2011).

1.8 Transforming Growth Factor-β (TGF-β)

TGF-β superfamily consists of a diverse range of proteins that regulate many different physiological processes including embryonic development, wound healing, chemotaxis, inflammatory responses and cell cycle control. Cytokines of the TGF-β superfamily are dimeric proteins with conserved structures and have pleiotropic functions both in vitro and in vivo. The human TGF-β family comprises more than 30 factors that can be divided into two distinct branches. Proteins such as activin, nodal, lefty, myostatin and TGF-β are clustered in one family branch and, bone morphogenetic proteins (BMPs) anti-muellarian hormone (AMH), and various

growth and differentiation factors are grouped into the other branch (Derynck and Akhurst, 2007). Activin, nodals and BMPs are critical regulators of stem cell differentiation and fate, left-right axis symmetry and organ development (Ying et al., 2003). TGF-β branched members of the superfamily function in many different ways and is dependant on cell and tissue context as TGF-β often inhibits but can induce cell proliferation. Thus, elucidating the role of TGF-β signalling complex is difficult. Through activation of TGF-β receptors, TGF-β initiates intracellular signalling cascades involving S-Mothers against decapentaplegic (Smads) leading to gene activation in a cell and tissue-specific context (Massagué and Gomis, 2006).

TGF-β members are in three isoforms termed TGF-β1, TGF-β2 and TGF-β3, each are encoded by different genes and located on different chromosomes. All three isoforms are express in the eye and anterior chamber (Tripathi et al., 1994a). However TGF-β2 isoform predominates in the eye. Physiologically, TGF-β2 is mainly produced by the ciliary epithelium and lens epithelium as a latent inactivate protein complex, consisting of mature TGF-β2, latency associated peptide (LAP), and the latent TGF-β-binding protein (LTBP) and is called the latent TGF-β complex. Latent TGF-β complex is not able to bind its receptor until LAP and LTBP are removed via proteolytic cleavage (Sato and Rifkin, 1989) (Tatti et al., 2008) to yield the active functional cytokine. The whole latent TGF-β complex is associated with the ECM. This helps sequester the TGF-β complex. The secretion of a latent form of TGF-β is a principle regulatory event that restricts its biological availability and hence functional effects.

One of the main potent activators of latent TGF-β is the glycoprotein TSP-1 (Schultz-Cherry and Murphy-Ullrich, 1993, Ribeiro et al., 1999). DEX administration is known to upregulate TSP-1 in TM cells (Flügel-Koch et al., 2004).

Another activator of latent TGF-β to active TGF-β is reactive oxygen species (ROS) (Jobling et al., 2006, Barcellos-Hoff and Dix, 1996). Indeed in an animal model asbestos-derived-ROS mediated activation of TGF-β via oxidation of LAP (Pociask et al., 2004). The integrin αvβ6 has also been demonstrated to activate latent TGF-β through binding of the RGD motif in LAP (Munger et al., 1999). Mice with genetic deletion of αvβ6 integrin develop emphysema and that this is completely abrogated by transgenic expression of the integrin or simultaneous transgenic expression of active TGF-β (Morris et al., 2003).

1.8.1 Effects of TGF-β in the TM

TGF-β2 is the main isoform expressed in the eye and anterior chamber and its expression is elevated in aqueous humour from POAG donors (Tripathi et al., 1994a, Tripathi et al., 1994b, Jampel et al., 1990), however, it is difficult to determine between the active and latent forms of the cytokine and therefore it is difficult to know the actual biologically relevant amount of the cytokine present. Deletion of the gene for TGF-β1 in mice leads to a progressive wasting disease and early death (Kulkarni et al., 1993). TGF-β2 gene ablated mice have a range of developmental defects, and in line with its expression in the TM display an altered anterior chamber and have a thin corneal stroma and absence of corneal endothelium (Sanford et al., 1997) and demonstrated non-redundant functions. Therefore TGF-β2 is necessary in formation of the anterior chamber and post development inhibits TM cell proliferation and is responsible for the immune deviation in the anterior chamber (Wilbanks et al., 1992). Because of the elevated levels of TGF-β2 in aqueous humour in POAG and its association with POAG researchers have focused on the effects of TGF-β2 on TM cells. It has been demonstrated that TGF-β2 leads to an increased expression of tissue transglutaminase, an enzyme that mediate cross-linking of ECM

(Welge-Lüßen et al., 2000) and also found to polymerise fibronectin. Also TGF-β2 has been shown to increase mRNA and protein expression of the ECM component fibronectin (Li et al., 2000) and lead to increased TIMP-1 expression (Alexander et al., 1998). Indeed Fuchshofer demonstrated that TM cells incubated with TGF-β2 led to decreased active MMP2, but not pro-MMP2, expression facilitated by increased Plasminogen activator inhibitor-1 (PAI-1) expression (Fuchshofer et al., 2003). PAI-1 is a serine protease inhibitor that inhibits fibrinolysis through tissue plasminogen activator and urokinase type plasminogen activator. Perfusion of isolated human anterior segments with recombinant TGF-β2 leads to a significantly decreased outflow facility compared to control perfused eyes (Gottanka et al., 2004). Histological analyses showed that TGF-β2 treated anterior sections altered the ECM and increased expression of the small heat shock protein α-B-crystallin (Gottanka et al., 2004).

A large study also confirmed that TGF-β2 in isolated human TM cells leads to an increased gene expression of TSP-1 (a potent activator of latent TGF-β) as well as multiple ECM genes (Fleenor et al., 2006). Indeed as well as an increase in mRNA expression for multiple ECM genes, TGF-β2 exposure leads to a significant and reproducible increased secretion of the ECM component fibronectin and PAI-1 and the addition of PAI-1 to cultures leads to an increased secretion of fibronectin. Moreover the TGF-β2-induced increase in fibronectin and PAI-1 is blocked by incubation with the TGF-β type I receptor inhibitor (ALK-5) (Fleenor et al., 2006). The authors also demonstrated that perfusion of TGF-β2 to isolated ex vivo anterior segments leads to a time-dependant increase in IOP with a concomitant decrease in outflow facility and correlated with fibronectin content in the perfusate (Fleenor et al., 2006). A correlation between TGF-β2 and elevated IOP is an important finding.

It has recently been demonstrated that as well as elevated TSP-1 after TGF-β2 treatment TM cells also upregulate Connective Tissue Growth Factor (CTGF) and identified this as a target gene and these molecules could be inhibited by co-administration of BMP-7, thus suggesting an endogenous regulator of TGF-β2 signalling in the eye (Fuchshofer et al., 2007). Moreover another antagonist of the TGF-β superfamily BMP-4 has been found to counteract the effects of TGF-β2 signalling in the TM (Wordinger et al., 2007). Therefore any alteration in BMP-4 signalling would lead to increased TGF-β2 mediated signalling and effects. Wordinger demonstrated that Gremlin is an antagonist of BMP-4 signalling and therefore blocks the regulatory effect of BMP-4 on TGF-β2 signalling and significantly, showed that Gremlin expression is perturbed in diseased TM cells (Wordinger et al., 2007). Thus suppression of Gremlin signalling would lead to decreased TGF-β2 effects via regulation of BMP-4 signalling. Indeed Gremlin has been demonstrated to be important in mediating TGF-β2 signalling effects in proliferative vitreoretinopathy (Lee et al., 2007). Gremlin has also been demonstrated to be involved in the sustained activation of fibroblasts into myofibroblasts and excessive deposition of ECM components in lung fibrosis (Myllarniemi et al., 2008). Studies using gene expression profiling in TM cells exposed to TGF-β2 and/or its antagonist BMP-7 found Smad-7 to be differentially expressed and subsequent silencing of Smad-7 using small interfering RNA (siRNA) and subsequent treatment of cells with TGF-β2 abrogated CTGF expression; a target gene of TGF-β2 (Fuchshofer et al., 2009). Thus Smad-7 is an inhibitory mechanism to limit local TGF-β signalling.

1.8.2 TGF-β2 and cytoskeletal modification

It is clear that TGF-β2 alters many genes and proteins in the TM and can have a profound effect on ECM deposition but can it effect the TM cytoskeleton? A body of evidence shows that TGF-β of many isoforms affects cell morphology and actin dynamics which will have an impact upon cell function (Boland et al., 1996). It has been shown in fibroblasts that TGF-β exposure leads to reorganisation of the cytoskeleton and in particular alpha actin was induced to form stress fibres (Lee et al., 1999). TGF-β has been shown to induce rapid actin rearrangements with an increase in lamellipodia in cultured astrocytes (Gagelin et al., 1995). Further research has shown that the coordinated cytoskeleton rearrangement requires the GTPase RhoA and Smad signalling to elicit TGF-β effects (Edlund et al., 2002).

In terms of TM cells the only study so far looked at the effect of TGF-β1 on BTM cell mediated collagen gel contraction and demonstrated that TGF-β1 (not TGF-β2) increased contraction and that this increased contraction was dependant on intracellular Ca2+ release and was mediated, at least partly, on RhoA signalling (Nakamura et al., 2002). Given the fact that TGF-β2 is the main isoform in the TM and anterior chamber and that its levels are significantly elevated in aqueous humour from POAG and that it mediates cell morphology via downstream signalling it is likely that it plays a role in promoting CLAN formation in TM cells.

1.8.3 Aqueous humour

The aqueous humour is produced by the non-pigmented ciliary epithelium at a rate of 2-3µl/min and it function is to supply nutrients to the avascular lens and cornea and maintain optimum IOP (Riordan-Eva et al., 2008). The formation of aqueous humour involves three different mechanisms: diffusion, ultrafiltration and active transport. Although the rate of production cannot be measured directly in humans it

can be assumed to be proportional to rate of aqueous humour outflow. Often this is determined by the introduction of a tracer dye such as fluorescein and measuring its clearance (flourophotometry) (Jones and Maurice, 1966). The produced aqueous humour crosses the pupil before reaching the TM and leaving via Schlemm's canal and the episcleral veins. Aqueous humour is a clear fluid that is slightly alkaline pH 7.2 (de Berardinis et al., 1965). Compared to blood plasma it has one ninth of the protein content, this is due to the blood aqueous barrier (de Berardinis et al., 1965) and contains amino acids, ions, pyruvate and glucose. The fluid also has an unusually high concentration of ascorbate relative to plasma (Reiss et al., 1986). The reason for this elevated ascorbic acid is unknown but has been speculated that it is there to quench oxidation induced by constant exposure to UV radiation from the sun (Reddy et al., 1998). The total protein composition of aqueous humour is low compared to serum and mainly contains low molecular weight proteins such as cytokines.

Many studies have investigated the protein content of aqueous humour in both normal and diseased states (Tripathi et al., 1989). Indeed, total protein content has been shown to be higher in POAG samples (Dan et al., 2005). Along with increases in specific proteins including PAI-1 (Dan et al., 2005) (a peptidase inhibitor), hepatocyte growth factor (Hu and Ritch, 2001), vascular endothelial growth factor (Hu et al., 2002) and TIMPs (inhibitors of MMPs) (Schlötzer-Schrehardt et al., 2003) multiple inflammatory cytokines are elevated. A recent study has identified elevated concentrations of myocilin in human aqueous humour in POAG patient samples (Howell et al., 2010). The cytokine milieu in the aqueous humour may be very important in disease pathogenesis. Thus there are multiple specific proteins elevated in aqueous humor along with an increase in total protein in POAG samples when compared to control, however, they may or may not play a role is disease

pathogenesis and may simply be a reflection of the disease or a consequence. Defining individual pathogenic roles for each is difficult and as yet not done. Except for one protein that is consistently elevated: TGF-β2. TGF-β2 has been studied extensively and found to play a role in many TM cell functions in vitro and forced overexpression in mice TM leads to increased IOP. Thus TGF-β2 is a viable CLAN promoting agent whose investigation is warranted.

1.8.4 Inflammatory cytokines in the aqueous humour

Multiple cytokines are found in the aqueous humour. Among these are the interleukins (IL) (Liton et al., 2005b). These are classic pro-inflammatory cytokines secreted by many cells to help orchestrate the immune response. It is known many interleukins can activate MMPs and IL-1 has been shown to activate MMP-3 in TM cells (Kelley et al., 2007). And IL-1-α has been shown to increase outflow facility in rat eyes (Kee and Seo, 1997). Indeed a diagnostic indicator of glaucomatous TM cells was defined in an authoritative *Nature* paper as being Endothelial Leukocyte Adhesion Molecule-1 (ELAM-1) (Wang et al., 2001). ELAM-1 expression is dependent on IL-1 activation through Nuclear factor κB (Nf-kB) transcriptional activation and links a 'stress response' (Wang et al., 2001). This may be beneficial but sustained activation may not.

1.8.5 Apoptosis

There is an appreciable loss of TM cells that occurs with increasing longevity (Grierson and Howes, 1987, Alvarado et al., 1984) and estimates put the reduction of viable TM cells at 6000cells/year (Grierson and Howes, 1987). In addition to the obvious decline in cellularity with age there is also further cell depreciation in glaucoma. Whether the scarcity of cells in the glaucomatous meshwork is due to

accelerated age-associated loss, a side effect of chronic medication or a true pathological apoptotic event is less clear. On the other hand more apoptosis is associated with glaucomatous than the normal meshwork (Baleriola et al., 2008) possibly related to down regulation of glucose related protein 78 (GRP78) (Chai et al., 2010) or to Fas activation (Agarwal et al., 1999a). The appreciable loss of TM cells in both normal ageing and disease may have a functional impact upon outflow facility and hence IOP.

CLANs may impact upon TM cells by inducing apoptosis or by altering pro or anti-apoptotic proteins. It is well established that a direct effect of DEX on TM cells is the production of the glycoprotein myocilin and that myocilin mutation is associated with POAG. One mechanism may be that the mutant myocilin sensitises the TM cells through increased endoplasmic reticulum (ER) stress and oxidative stress-induced apoptosis (Joe and Tomarev, 2010). This gives the rationale for studying CLANs in the context of cell death.

Cell death is often described dichotomously as either necrosis or apoptosis. Necrosis is a form of cell death that is characterised as lacking the usual features of apoptosis and autophagy. Cell necrosis is characterised by cell swelling affecting both cytoplasm and nucleus with subsequent cell lysis-this results in parts of the cell exposed extracellular and only small parts are internalised by macropinocytosis by other cells. Apoptosis on the other hand is a described as an active, programmed process of autonomous cellular destruction that avoids eliciting inflammation (Rich et al., 1999). Morphological examination can distinguish apoptosis from necrosis. Apoptotic cells have a characteristic set of events that initiates with shrinking of the cytoplasm and nuclear condensation (pyknosis), membrane blebbing and formation of apoptotic bodies (Coleman et al., 2001). Over the past twenty years apoptosis

research has exploded due to the fact that alterations in the pathways underpinning the process may underlie many common diseases. Modulation of apoptosis could augment several disease processes, therefore making it an attractive viable drug target.

1.9 The Glaucomas

The glaucomas comprise a group of diseases characterised by progressive optic nerve damage subsequent to retinal ganglion cell loss which may or may not be in association with raised IOP leading to visual loss (Kerrigan et al., 1997, Quigley et al., 1995). However, there are many different types of glaucoma, which can be primary or secondary, but the retinal ganglion cell loss seems to be the final common pathway in possibly diverse etiological pathways. Glaucoma can be classified in many different ways, primary or secondary, by age of onset or by open and closed angles.

1.9.1 Epidemiology of POAG

POAG encompasses a spectrum of disorders characterised by optic nerve cupping and visual field loss in eyes with open drainage angles. Glaucoma is the leading cause of blindness worldwide (Quigley, 1996, Quigley and Broman, 2006) after cataract (figure 1.10). With an estimated 45 million people with POAG (Quigley and Broman, 2006) worldwide in 2010 and by 2020 this is expected to increase to 58.5 million. Almost half of these people will reside in Asia, while 24% will be European. The mean prevalence is estimated to be 1.96%. Women are expected to comprise >55% of those with POAG; presumably due to their increased longevity compared to men. In the United States of America the overall prevalence of POAG in individuals >40 years old is 1.86% equating to around 2.2 million people. However variation

occurs between populations also it has been recognised for some time that 50% or more of POAG cases in any given community are not diagnosed (Hollows and Graham, 1966). From the perspective of the person with the disease the impact of visual loss can be devastating.

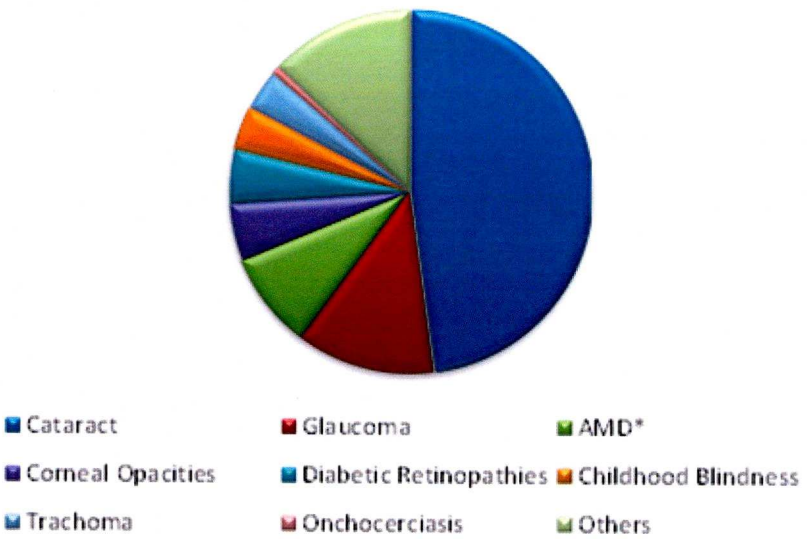

Figure 1.10 Global causes of blindness as a percentage of total blindness in 2002. *AMD: Age Related Macular Degeneration. Adapted from the World Health Organisation Global data on visual impairment document 2002. Glaucoma is the single largest cause of blindness after cataract worldwide.

1.9.2 Risk factors for POAG

There are a number of risk factors for the development and progression of POAG including IOP, age, family history and race. One of the most important is raised IOP. Several studies have confirmed that reduction of IOP at any point along the spectrum of disease severity reduces disease progression (Anderson et al., 2001, Drance et al., 2001, Heijl et al., 2002). The evidence for causal association between IOP and POAG is robust. Indeed the Ocular Hypertensive Treatment study showed that, in patients with no clear optic nerve damage and normal visual fields but an increased intraocular pressure (>24mmHg), progression to POAG was reduced from 9.4 to 4.4 % over five years if the intraocular pressure was reduced by at least 20% (Kass et al.,

2002). Such a small reduction of 20% in eye pressure lead to a decrease in POAG progression, therefore showing the importance of intraocular pressure as a risk factor for POAG. A 'high' intraocular pressure is arbitrary based on the distribution of intraocular pressure in the population. 21mmHg is traditionally used as the cut-off point as this represents the mean (16mmHg), plus two standard deviations. In the Baltimore eye survey, the prevalence of POAG increased with intraocular pressure (Sommer et al., 1991). Indeed those with an intraocular pressure <15mmHg overall compared to those with an intraocular pressure >35mmHg the prevalence of POAG was 30 times higher than of the former (Sommer et al., 1991).

Several studies consistently show that age is a risk factor for POAG. One study showed that in people aged 43-53 the prevalence of POAG was 0.9% and that this prevalence was 4.7% in people aged 75 or older (Klein et al., 1992). Indeed the Blue Mountains eye study determined an exponential increase in POAG prevalence with increasing age (Mitchell et al., 1996). Moreover, the overall prevalence figures for POAG increased from 0.2% (95% CI: 0.16, 0.24) in the age group of 55-59 years of age to 3.3% (95% CI: 2.57, 4.04) in the age group 85-89 years of age (Dielemans et al., 1994). This increased risk factor with increasing age has been demonstrated in other populations including Japan (Aiko et al., 2004).

Family history is another major risk factor for POAG development. In the patterns of POAG in the Barbados eye study, 30% of the probands (the affected person of the family) studied had one relative with POAG and 10% had two or more relatives affected (Leske et al., 2001). The Baltimore eye survey also showed an higher risk of POAG from a positive family history of POAG (Tielsch et al., 1994). The increased risk of developing POAG in family members likely is the result of a genetic abnormality.

Ethnicity has an impact on the development of POAG. The Barbados eye study demonstrated the importance of race on POAG. This large study showed that the prevalence of POAG was 7% in black, mixed-race 3.3% and 0.8% (1/133) in white participants (Leske et al., 1994). Indeed this study also demonstrated that in the 40-49 year POAG group the observed prevalence was similar to that seen in much older white populations (Leske et al., 1994). And in the older age groups there were large increases in prevalence of POAG that reached 25% in the oldest age group 80-86 years old. The racial difference was also demonstrated based on data from the Baltimore eye study they clearly demonstrated that the prevalence among black Americans was four to five times time higher compared to whites (Tielsch et al., 1991). Not only was the overall prevalence higher among blacks compared to whites but they began at an earlier age and affected 1 in 10 of the black population aged 70 or older (Tielsch et al., 1991). Indeed due to the increasing longevity of the human race there is going to be an increased prevalence of POAG. Moreover developing countries seem to be disproportionately affected (He et al., 2005). This will result in a major public health problem. The disease is asymptomatic until its advanced stages when the patient may be aware of the peripheral visual field loss and this adds to the problem.

The public health consequences of POAG are large and significant and whilst it is well established that retinal ganglion cells are the final cell type that ultimately perishes in POAG the lesion likely occurs upstream of this. The pathophysiology of POAG is poorly understood and increased IOP is the most significant risk factor known and death of the retinal ganglion cells is the common end point. Significant research and effort has been focussed on so called ''neuroprotection'' in POAG (as well as other neurological diseases) at the cost of the underlying pathology. This

pathogenic insult may occur in the TM, the site of outflow resistance and offers a new therapeutic option in the armoury. CLANs could, if pathogenic, be targeted and alterations in cytoskeleton dynamics are likely temporal and spacial. CLANs are not an artefact of cell culture and have been found to be expressed in BTM cells and intriguingly by aqueous humour. Thus a factor or factors present induces such cytoskeletal architectural rearrangement.

There are a number of questions still to be answered about CLANs and this research has set out to determine those using an established model of TM cells.

1.9.3 Aims of this thesis

The aims of this thesis are:

To determine a functional consequence of CLANs; specifically contraction.

To determine is CLANs are associated with apoptosis of the BTM cells

To find inducers of CLANs other than DEX

To find any inhibitors of CLANs

To determine if biomechanical stimulation results in CLANs

To determine if CLANs are associated with an adaptive response

To determine if CLAN containing cells are associated with a polarised phenotype

To determine if CLANs and temporary geodesic actin arrangements are one and the same thing

2. Methods

2.1 Isolation of primary cultures

Bovine eyes reached our laboratory on ice from a local abattoir and the globes were washed in Dulbecco's Phosphate Buffered Saline (DPBS) (Sigma) containing antibiotic solution (penicillin and streptomycin) (100U/ml). They were dissected within 24 hours of arrival to provide strips of TM tissue which served as explants for primary culture. Briefly, each globe was cut in half and the lens was removed from the anterior segment in a sterile hood. This segment was further divided into quadrants and each positioned with the cornea facing down. The iris was carefully reflected backwards so that the chamber angle was exposed. The BTM is extensive and usually it is heavily pigmented so that it is easily visualised under a dissecting microscope (Grierson et al., 1985b). The micro-dissection process is far less demanding than for the successful removal of HTM strips (Polansky et al., 1979b). Ultra-fine forceps (Agar Scientific, UK) and razor blade knives (made from Wilkinson Sword razor blades) were used to extract strips of BTM. The strips were placed in tissue culture flasks and evaluated after 24 hours. In all situations the BTM cells were grown in Dulbecco's Modified Eagle Medium (DMEM) (Sigma) containing 10% (vol/vol) heat inactivated Fetal calf Serum (FCS), 2mM L-glutamine, penicillin (100 U/ml), streptomycin (100 µg/ml) and fungizone (amphotericin B - 2.5 µg/ml) (all from Life Technologies, Scotland) at 37°C in a humidified atmosphere of 95% air and 5% CO_2 with change of medium twice per week. Cells were cultured in 75 cm^2 vented cell culture flasks to allow diffusion of air and CO_2 (Corning, UK). The cells were regularly checked for dead floating, nonadherant cells. BTM cells were trypsinized (0.25% trypsin and 0.02% EDTA)

(Gibco), passaged at split levels of either 1:3 or 1:5 and established cultures at 3rd to 8th passage were used routinely throughout (Grierson et al., 1985b).

2.1.1 Modulation of FCS levels

In some experiments the cells were grown in DMEM supplemented with only 0.5%, 1% or 10% FCS, 2mM glutamine, penicillin (100U/ml), streptomycin (100 µg/ml) and fungizone (amphotericin B – 2.5µg/ml). These experiments were to determine the effect of differing levels of FCS in the cell culture media upon CLAN incidence and so the lowest concentration of FCS could subsequently be used throughout.

2.2 Preparation of 3D collagen matrices

It is over thirty years since the introduction of a new in vitro model of contraction and wound healing, the fibroblast-populated collagen lattice (Bell et al., 1979). The introduction of cultured fibroblasts into a 3D collagen matrix leads to the eventual, dynamic reduction in size of that matrix caused in part by the reorganisation of the cellular matrix (Bell et al., 1979). This extracellular matrix remodelling is measured by the reduction in area of the populated cell lattices over time. This gives an excellent in vitro model for cellular contraction and wound healing and contraction is dependent on subcellular actin for cell-mediated contraction. Collagen matrices were prepared with rat tail type I collagen (Sigma, UK) at 5 mg/ml in 0.1% (vol/vol) glacial acetic acid stock solution (VWR, UK). To prepare a collagen matrix at a final concentration of 1.5 mg/ml for each assay, 2.1 ml of concentrated culture medium (15 ml of 10x MEM, 35 ml sterile distilled water, 1.5 ml penicillin/streptomycin, 1.5 ml glutamine, 1.5 ml fungizone, and 3 ml of 7.5% (vol/vol) sodium bicarbonate) was added to 3.6 ml of collagen solution at 4°C. To this mixture, 0.9 ml of serum containing the appropriate amount of cells was added and to raise the pH drop wise

addition of 10ul NaOH was added to the whole mixture. Gel contraction studies were performed in 24-well plates in which each well received 0.25 ml of this final mixture (Sterilin, Stone, UK) and then was transferred to a humidified 37°C, 5% CO_2 incubator where the matrix set within 1 minute. After 10 minutes the matrices were overlaid with 1ml (24 well) of complete medium with or without DEX 10^{-7}M, detached from the base using a sterile pipette tip and floated. At set time points the matrices were measured using Image J software (NIH available at: http://rsb.info.nih.gov/ij/index.html) after taking a digital photograph of the matrices. Different cell densities were initially examined to determine optimum concentration.

2.2.1 Preparation of 2D collagen matrices

Collagen matrix formation followed the above protocol except 0.9 ml of cell-free FCS was used in the matrix formula. After matrix formation, cells were seeded onto the matrix in complete media with or without the addition of DEX 10^{-7}M and allowed to settle for 30 minutes in the incubator. Matrices were then detached, floated, and returned to the 37°C incubator. At set time points the matrices were measured using Image J software (NIH available at: http://rsb.info.nih.gov/ij/index.html) after taking a digital photograph of the matrices. Different cell densities were initially examined to determine optimum concentration.

2.2.2 F-actin staining of collagen matrices

Collagen matrices were removed from the wells and fixed in 10% Neutral Buffered Formalin (10% NBF) for 3 hours after which time they were washed in Phosphate Buffered Saline (PBS) for 1 hour with gentle agitation. Matrices were then permeabilised with 0.1% Trition-X 100, washed and incubated with 1% Bovine Serum Albumin (BSA) in Tris-Buffered Saline (TBS) pH 7.6 overnight at 4°C after

which they were stained with Phalloidin Alexa-488 (Invitrogen) 1:40 for 2 hours, washed 3 times with TBS, mounted on a slide with mounting media (Vectashield) and coverslipped. Images were taken using a laser scanning confocal microscope (Biorad MRC 600 Confocal) using either a X40 objective or X60.

2.3 Trypan blue

$1x10^5$ BTM cells per flask were seeded into T75 tissue culture flasks and grown to complete confluence after which time cells were washed twice with warm PBS and then medium supplemented with 1% FCS in complete medium containing either DEX 10^{-7}M, TGF-β2 2ng/ml (R&D Systems, UK) or medium alone was added to the cultures. At the indicated time points shown the cells were trypsinized (0.25% trypsin and 0.02% EDTA), resuspended and an aliquot of 500µl of cell suspension was added to 100µl of 0.4% trypan blue, mixed and allowed to stand for 5 minutes. After which cells were counted using a hemocytomer. Under a microscope cells were counted: live cells exclude the dye, whereas dead cells are stained blue. Live cells and dead cells were counted and expressed as percentage viability.

2.3.1 (3-(4,5-Dimethylthialthiazol-2-yl)-2,5-diphenlytetrazolium bromide MTT

BTM cells were seeded into 96 wells at $1x10^4$/well and after 24 hours DEX, TGF-β2 or control was added to the wells. At set time points, 20µl of MTT (5mg/ml) was added to the wells and incubated at 37°C for 4 hours after which time the crystals were solubilised by addition of 200µl of Dimethyl Sulfoxide (DMSO) to the wells and left at room temperature for 5 minutes. The absorbance was then measured at 570nm using a spectrophotometer. This assay works on the basis of living cells reducing the yellow substrate to a purple formazan through the activity of mitochondrial enzymes such as mitochondrial reductase.

2.3.2 Cellular apoptosis assay

BTM cells were seeded at $1x10^4$/ cells per well in four-well Lab-Tek chamber slides that allow immunovisulaisation (Nunc), when they reached confluence cells were incubated with DEX 10^{-7}M, TGF-β2 2ng/ml or control medium and at the set time periods fixed in 10% NBF for 30 minutes. Fixed cells were then washed three times with PBS after which Propridium Iodide 1μg/ml (Sigma) was added for 15 minutes, cell were then washed with PBS three times before mounting medium (Vectashield) was added and coverslipped. Cells were imaged using confocal microscopy. Cells were quantified by nuclear staining and apoptotic cells identified by shrunken nuclear condensation and expressed as % apoptotic cells.

2.3.3 Annexin-V staining

Loss of plasma membrane asymmetry is a universal phenomenon in apoptosis. This assay works on the basis that apoptotic cells express phosphatidylserine (PS) that is normally kept on the inner leaflet of the membrane, however, when the cell becomes apoptotic this translocates to the outer leaflet and can bind Annexin-V, therefore making Annexin-V a sensitive assay for apoptosis (Vermes et al., 1995). BTM cells were cultured in T75 flasks and when confluence was reached DEX 10^{-7}M, TGF-β2 2ng/ml or control was incubated with the cells. At the set time points the cells were trypsinised (0.25% trypsin) and resuspended at $1x10^6$/cells/ml with Annexin-V binding buffer 10mM HEPES, 70mM NaCl, 1.2mM $CaCl_2$ pH 7.4 (Invitrogen) and 5μl of FITC-Annexin-V was added along with 10μg/ml of Propridium Iodide and incubated in the dark for 15 minutes at room temperature after which 400μl of Annexin-V binding buffer was added and mixed. Fluorescence was measured at 530nm and 580nm using Flow Cytometer (FACS, Becton Dickson).

2.3.4 Caspase 3 Immunocytochemistry

BTM cells were seeded in Lab-Tek (Nunc) slides at $1x10^4$/cells per well, after reaching confluence cells were incubated with either DEX 10^{-7}M, TGF-β2 2ng/ml (R&D systems) or control and at set time points fixed with 10% NBF. Cells were then washed in TBS and permeabilised with 0.1% Triton X-100 (Sigma, UK) for 5 minutes, washed in TBS 0.1% Tween 20 and incubated with 5% Normal goat serum for 1 hour, washed with TBS 0.1 % Tween 20 and incubated overnight with Rabbit Anti-caspase 3 antibody (Abcam Ab13847) 5μg/ml. Cells were then washed with TBS three times and incubated with Goat anti-Rabbit Alexa-488 antibody (1:200 dilution) for 1 hour at room temperature, washed three times with TBS 0.1% Tween 20 in 0.05% BSA (wt/vol). Negative control was with the primary antibody step omitted. Cells were then incubated for 15 minutes with Propridium Iodide 1μg/ml and washed with TBS 0.1% Tween 20. After this mountant was added and the slides coverslipped. Cells were imaged using a confocal microscope using X20 magnification (Biorad)

2.4 CLAN identification

BTM cells were seeded in four-well Lab-Tek slides (Nunc) at $1x10^4$/cells per well and once confluent DEX 10^{-7}M, TGF-β2 2ng/ml (R&D systems) or control was added to the cells for up to 14 days. Cells were fixed in 10% NBF at set time points, cells were permeabilised with 0.1% Triton X-100 for 5 minutes and incubated with phalloidin Alexa-488 (Invitrogen) 1:40 for 40 minutes in TBS 0.1% Tween 20, cells were then washed three times with TBS 0.1% Tween and incubated with Propridium Iodide 1μg/ml for 15 minutes after which the cells were washed three times with TBS 0.1% Tween 20 and mounted with a coverslip. Cells were quantified for

CLANs using our rigorous definition of at least five hub points and three triangulated arrangements of spokes (Wade et al., 2009) using confocal microscopy (Biorad MRC 600 Confocal). This was performed in at least eight different fields of view within each well and at least four wells per treatment group under examination.

2.4.1 TGF-β-induced CLAN inhibition experiments

BTM cells were seeded at $1x10^4$/cells per well in Lab-Tek chamber slides in DMEM containing 10% FCS. Once confluence was reached the cells received either TGF-β2 2ng/ml, TGF-β2 & SB-431542 10μM (Tocris bioscience), TGF-β2 & LY-364947 20μM (Tocris bioscience) or anti-TGF-β2 neutralising antibody 1.4μg/ml (R&D Systems) for up to 7 days in DMEM containing 1% FCS. In separate experiments cells were treated with TGF-β2 2ng/ml, or TGF-β2 & SIS3 25μM (selective Smad3 inhibitor) or SIS3 25μM alone for up to seven days. On the seventh day cells were fixed with 10% NBF and permeabilised with 0.1% Triton X-100 for 5 minutes and incubated with phalloidin Alexa-488 (Invitrogen) 1:40 for 40 minutes in TBS 0.1% Tween 20, cells were then washed three times with TBS 0.1% Tween and incubated with Propridium Iodide 1μg/ml for 15 minutes after which the cells were washed three times with TBS 0.1% Tween 20 and mounted with a coverslip. Cells were quantified for CLANs using our rigorous definition of at least five hub points and three triangulated arrangements of spokes (Wade et al., 2009) as previously outlined above.

2.5 Western Blotting

Proteins are separated on the basis of size in SDS-PAGE performed under reducing conditions (Laemmli, 1970). The polymerisation of acrylamide is initiated by the addition of ammonium persulfate and the base N,N,N',N'-

Tetramethylethylenediamine (TEMED). TEMED catalyses the decomposition of the persulfate ion to give a free radical which initiates the polymerisation reaction. Proteins are separated by their size. Smaller proteins pass more easily through the pores of the gel. Larger proteins are retarded by frictional resistance. Proteins were transferred to a nitrocellulose membrane by means of a current. Proteins bind irreversibly and can be probed. BTM cells were cultured in T75 flasks until confluent. Once confluence was reached cells received either nothing; or SIS3 25μM for one hour prior to the addition of TGF-β2 2ng/ml to the SIS3 pre-treated culture or normal media culture for 2 hours. After 2 hours incubation cells were washed in ice cold PBS and then lysed in lysis buffer containing 1% SDS and protease and phosphatase inhibitor cocktail containing EDTA (Sigma), subjected to 5 seconds sonication and then protein determined using the bichoronic acid method to confirm protein levels for protein standardisation among lanes. 25μg of total protein lysate was subjected to 12% PAGE at 120V for 3 hours (Bio-rad mini protean II). After electrophoresis the proteins were transferred to a nitrocellulose membrane by wet transfer. The subsequent nitrocellulose membrane was washed in Tris-buffered Saline with 1% Tween (TBS-T) and then blocked overnight in 5% (wt/vol) BSA in TBS-T at 4°C with slight agitation. The next day the membrane was washed three times x5 minutes and incubated with Rabbit anti-phosphosmad-3 antibody (Abcam Ab51451) 1:500, which recognises the phosphorylated form of Smad-3 only, in 5% BSA for 1 hour and then washed in TBS-T three times and subsequently incubated with Goat anti-Rabbit secondary antibody labelled with horseradish peroxidase (1:15000 dilution) for 1 hour at room temperature. Finally the membrane was washed three times with TBS-T and immersed in TBS before the addition of the ECL

chemiluminesent substrate (Pierce, UK). The bands were visualised using a chemi-doc image system (Biorad, UK).

2.6 Aqueous Humour experiments

Bovine aqueous humour was removed from bovine anterior chambers that had arrived as whole globes from a local abattoir within 3 hours stored on ice. A sterile 25-gauge needle was inserted into the eye and a 1ml syringe was attached and aqueous humour was drawn from the anterior chamber using the syringe as previously described and great care was taken to avoid iris contact (Hogg et al., 1995b). Between 600-700µl of aqueous humour from each eye was retrieved and pooled immediately into siliconised tubes, immersed in liquid nitrogen and frozen at -80°C. Storage for up to a year was found to have minimal effect on aqueous humour CLAN promoting ability. Undiluted bovine aqueous humour was found to be an ineffective sustaining media so we therefore decided to dilute the isolated aqueous humour 1:1 with media. BTM cells were seeded at $1x10^4$ /cells per well in four-well Lab-Tek chamber slides. Once confluence was reached cells received Bovine Aqueous Humour diluted 1:1 (vol/vol) with DMEM in 1% FCS or Aqueous Humour supplemented with anti-TGF-β2 antibody 1.4µg/ml (Sigma) or standard tissue culture medium supplemented with anti-TGF-β2 antibody 1.4µg/ml for up to 7 days. At 3 and 7 days the cells were fixed in 10% NBF and stained for CLANs and quantified as outlined previously in this thesis.

2.6.1 Decorin experiments

BTM cells were seeded at $1x10^4$/cells per well in four-well Lab-Tek chamber slides. Once confluence was reached cell were incubated with recombinant decorin (R&D systems) at 1ng/ml, 500ng/ml or 25µg/ml for up to 7 days and fixed and stained for

CLANs as previously outlined. After finding the higher concentration induced an effect 25μg/ml recombinant decorin was used and incubated with confluent BTM cells for up to 7 days or vehicle control which contained 0.04μM HCL as the final concentration in the medium. After seven days incubation cells were fixed and stained for CLANs as above.

2.6.2 Cyclic Mechanical stretch

The TM is under constant mechanical stretch so we tried to recreate that environment by using a cyclic mechanical stretch to mimic the in vivo situation of pulsatile stretch and relaxation using a computer regulated bioreactor. The cells were seeded on an elastomer base which, because of hydrophobicity, had to be coated with an extracellular matrix. Initial investigation used Laminin. In the end we used fibronectin coated silicone membranes in six-well plates (Flexcell™). See figure 2.1

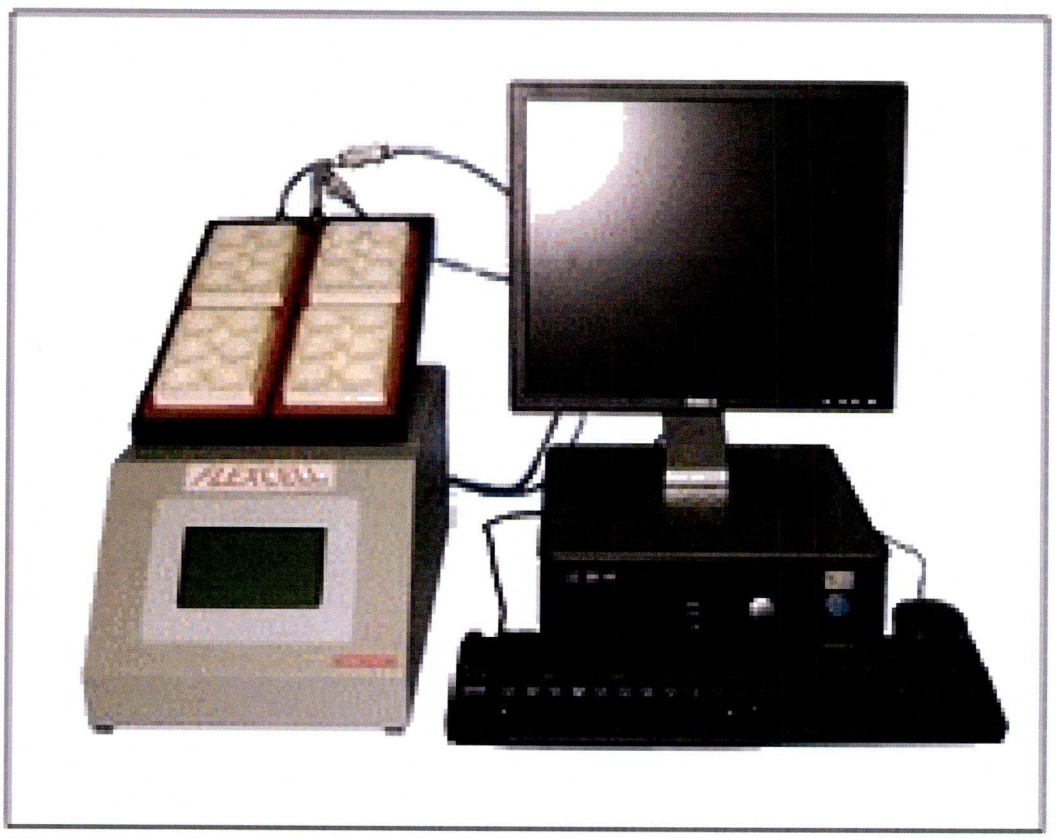

Figure 2.1 Flexcell™ mechanical stretching system. This image shows the components of the mechanical stretching device including the computer operating system and the base plate with the silicone elastomer based six well plates. Does not show the vacuum pump needed for the force generation required to drive the air vacuum to stretch the elastomer base.

BTM cells were seeded at $1x10^5$ cells/well in six well plates coated with the substrate. Once the BTM cells reached confluence they were treated with either nothing (control) or DEX for 14 days. After 14 days culture post confluence with either control or DEX 10^{-7}M the plates were placed onto the Flexcell™ FX5000 system (Flexcell corporation, Hillsburough, NC, USA). This system uses vacuum pressure to deform to flexible-bottomed culture plate yielding up to 33% substrate elongation. The non-stretch Flexcell™ plates were placed in the housing but did not receive mechanical stretch. However, the other plates DEX and control received cyclic mechanical stretch of 10% elongation 1Hz for a period of 12 hours. This regime of stretch was chosen to replicate the pulsatile mechanical forces found in vivo (Coleman and Trokel, 1969, Johnstone, 2004). After 12 hours of cyclic mechanical stretch media was removed and stored at -80°C for later analysis and the cells were immediately fixed in 10% NBF for 1 hour. Cells were then washed twice with TBS and the membrane was removed using a corneal trephine usually used for taking corneal buttons. This was found to remove the membrane quite nicely with limited disruption. The removed membrane was placed onto a glass slide and stained for CLANs as previously described except there was an extra wash step with TBS at the end before the mountant was added.

2.6.3 TGF-β2 quantitation

Once the cells had been stretched the conditioned medium was removed and analysed for TGF-β2 content using ELISA (R&D Systems, UK). This ELISA kit measures active and not 'latent' TGF-β2 therefore giving a more accurate

assessment. This assay is a quantitative immunoassay based on a sandwich ELISA. Medium from the cells was added to polypropylene tubes and to activate the latent TGF-β2 to the active immunoreactive form 1M HCL was added to each sample (25µl) and incubated at room temperature for 10 minutes. After which the reaction was neutralised by the addition of 1.2M NaOH/0.5M HEPES buffer and mixed well. This mixture was then added to the wells of the plate and any active TGF-β2 was bound to the anti-TGF-β2 antibody that is immobilized onto the base of the plate, after washing away any unbound proteins an enzyme-linked polyclonal antibody specific for TGF-β2 was added. After another wash to clear any unbound antibody-enzyme reagents a substrate is added and any colour change is proportional to the amount of TGF-β2 present in the initial step. This was then measured on a spectrophotometer (Sterlin). The amount of TGF-β2 is quantified against known standards using a standard curve.

2.6.4 IL-6 quantification

Once the cells had been stretched the conditioned medium was removed and analysed for Interleukin-6 (IL-6) content using ELISA (R&D Systems, UK). This assay is a quantitative immunoassay based on a sandwich ELISA. Medium from the cells was added to the wells and any active IL-6 was bound to the anti-IL-6 antibody that is immobilized onto the base of the plate, after washing away any unbound proteins an enzyme-linked polyclonal antibody specific for IL-6 was added. After another wash to clear any unbound antibody-enzyme reagents a substrate is added and any colour change is proportional to the amount of IL-6 present in the initial step. This was then measured on a spectrophotometer (Sterlin). The amount of IL-6 is quantified against known standards.

2.6.5 IL-1β quantification

Once the cells had been stretched the conditioned medium was removed and analysed for Interleukin-1β (IL-1β) content using ELISA (BenderMed Systems, Austria). This assay is a quantitative immunoassay based on a sandwich ELISA (Adlbrecht et al., 2007). Medium from the cells was added to the wells and any active IL-1β was bound to the anti-IL-1β antibody that is immobilized onto the base of the plate, after washing away any unbound proteins an enzyme-linked polyclonal antibody specific for IL-1β was added. After another wash to clear any unbound antibody-enzyme reagents a substrate is added and any colour change is proportional to the amount of IL-1β present in the initial step. This was then measured on a spectrophotometer. The amount of IL-1β is quantified against known standards.

2.7 Hsp70 quantification

Hsp 70 protein levels have never been quantified in TM cells of any species before and were hypothesised to be induced after cyclic mechanical stretch. After the BTM cells were stretched they were lysed in ice cold lysis buffer containing 1% SDS and protease and phosphatase inhibitors: 1 mM iodoacetimide, 1 mM benzithonium chloride, and 5.7 mM PMSF (Sigma, UK). After brief sonication the lysate was quantified for total protein using the BCA method. 25μg of total protein was subjected to 12% SDS-PAGE. After electrophoresis the proteins were transferred to a nitrocellulose membrane by wet transfer. The subsequent nitrocellulose membrane was washed in Tris-buffered Saline with 1% Tween (TBS-T) and then blocked overnight in 5% (wt/vol) non-fat milk (Marvel) in TBS-T at 4°C with slight agitation. After overnight blocking the membrane was washed and incubated with Mouse anti-Hsp70 antibody (Stressgen, Canada) 1:5000 for 1 hour, the membrane

was washed three times and incubated with secondary rabbit anti-mouse labelled with Horse Radish Peroxidase for 1 hour at room temperature. Finally the membrane was washed three times with TBS-T and immersed in TBS before the addition of the chemiluminesent substrate (Pierce). The bands were visualised using a chemi-doc image system (Biorad).

2.7.1 Nuclear Factor-Kappaβ expression

NF-kβ is a central transcription factor that is an important regulator of many inflammatory and tissue stress responses. Lysates after stretch were subjected to 10% SDS-PAGE, transferred to a nitrocellulose membrane and then probed with a Rabbit anti-Nf-kβ p65 subunit phosphorylated on serine276 (Abcam, Ab30623) 1:100 overnight in 5% BSA, after washing the nitrocellulose membrane was incubated with Goat anti-Rabbit labelled with Horse Radish Peroxidase for 1 hour at room temperature. Finally the membrane was washed three times with TBS-T and immersed in TBS before the addition of the chemiluminesent substrate (Pierce). The bands were visualised using a chemi-doc image system (Biorad).

2.8 TGF-β2 and mechanical stretch

BTM cells were seeded at $1x10^5$ cells/well in six well plates coated with the matrix substrate fibronectin. Once the BTM cells reached confluence they were treated with either nothing (control) or TGF-β2 (2ng/ml) (R&D systems) for 14 days. After this time they were treated to cyclic mechanical stretch regime as previously described and the fixed and stained for F-actin and examined for CLANs.

2.9 CLANS and morphology

BTM cells were seeded at $1x10^4$ cells/well on glass bottomed Iwaki six well plates (Iwaki, Japan). This gave superior imaging as the refractive index was better. Pre-confluent BTM cultures then received DEX 10^{-7}M, TGF-β2 2ng/ml or decorin 25μg/ml for seven days after which time the cells were fixed with 10% NBF and then stained with phalloidin Alexa-488, washed with TBS-T and a small circular coverslip was applied to the centre of the well to cover the indent. The fixed and stained cells were then subject to fluorescence microscopy through the base of the glass well in the plate. Selection was always done in fluorescence mode and then the exact same image was taken in phase contrast mode. Selection of fields was always done in fluorescence mode and based on the presence of a cell with a CLAN or a cell with clear stress fibres only. If the boundary of the cell was clear this was drawn round with a mouse cursor and measurements were taken using Image J software (NIH, USA). The cells were categorised as belonging to three distinct shapes epitheloid (round), spindle (an elongated polarised form) and kite shaped cells (polarised with a distinct triangular head, polygonal). Circularity was calculated in image J (NIH, USA) by using the circularity measurement after tracing the perimeter of the cell. A circularity of 1 indicates a perfect circle, as the value approaches 0.0 it indicates and increasingly elongated polygon. The circularity is calculated from the formula: $4\pi(\text{area}/\text{perimeter}^2)$.

2.9.1 Time lapse imaging of TM cells

Cells were seeded onto glass bottomed Iwaki six-well plates (Iwaki, Japan) and then treated with DEX 10^{-7}M, TGF-β2 or decorin 25μg/ml for 7 days after which the plates were placed into a microscope holder inside an incubator that controlled the temperature (37°C) and live phase contrast images of the BTM cells within the culture dish were recorded over 20 hour period using a Zeiss microscope with a X20

objective. This was performed using a microscope stage that was programmed to take an image every 60 seconds in a defined area of the well of the six-well plate. After the taking of one image the microscope stage would move to another pre-defined area of the well and image another area and so on until the end of the 20 hour filming period that we had programmed. At the end of the experiment the images of the different areas of the well from each time point had to be ''pieced together'' to form a video time lapsed movie. This was performed by the use of Image J (NIH, USA) software to combine the separated images from the previous experiment into a movie. The stage was 'drifting' slightly due to rudimentary equipment, however, this only became a problem after 20 hours in initial experiments to optimise and as such no lime lapse ever went over 20 hours of filming. Thus the drift was not an issue. At the end of the phase contrast filming period the cells were fixed in 10% NBF and stained according to previous method and a coverslip mounted in the middle of the indent. After staining the cells were analysed on the basis of clear fluorescent staining, their appearance was easy to classify and they could be followed without confusion for the entire filming period evolution.

We then looked at the three classifications of cell shape and followed their life history in the culture. An arbitrary scale for locomotion of the cells was employed where M* cells moved at 4μm/hour or less, M** reached up to 12μm/hour, whereas above that M*** cells were faster still and some could reach a movement rate of 25μm/hour for short periods, M**** is for cells that moved extremely quickly in the culture. The speed of the cells movement in culture was calculated by following its movement and measuring the distance over time knowing the scale of the area.

2.9.2 Resettling experiment

BTM cells were grown to confluence and then trypsinised and resuspended in 1ml of complete culture medium containing no CLAN inducers. Cells were agitated and seeded onto four-well Lab-Teks in complete media containing no exogenous agents. The definition of CLANs is often in a confluent culture so here after only 1, 2, 4 and 6 hours of culture on the substrate BTM cells were fixed and stained for F-actin as above and imaged using confocal microscopy to determine differences between 'settling' actin patterns and stable cultured cells that had reached confluence previously using confocal microscopy. The rationale behind this experiment is that CLANs are often defined as being only in confluent TM cell cultures and often, after exposure to a specific glucocorticoid. However, others have shown that CLAN-like structures are found in freshly plated cultures after only one hour of culture (as they adhere to the tissue culture substrates) cells were found to express structure that clearly resembled CLANs. The question is are these structures, although superficially similar to CLANs, really the same thing? This experiment set out to determine the answer to this question.

2.9.3 PCR Array

To identify possible signalling pathways Reverse Transcription (RT) PCR array profiling was performed. BTM cells were cultured either with nothing (control) or TGF-β2 2ng/ml for seven days after which cells were harvested and RNA collected. 1μg of BTM RNA was reverse transcribed using reverse transcriptase and the subsequent cDNA samples were loaded onto a RT^2 PCR array for Human TGFβ BMP signalling pathway (SABiosciences). This RT^2 profiler array profiles the expression of 84 genes related to signal transduction in the TGFβ BMP pathway.

3. Results

3.1 Morphological characterisation

The BTM cells grew vigorously from the explants and were predominantly bipolar although epithelioid and kite shaped cells were also to be found in the cell outgrowths (figure 3.1). At confluence the cells were somewhat flattened and formed a monolayer with a minimum of overlapping between cells. The BTM cells grew well in standard culture conditions and at confluence could be split up to 1 in 16 and usually reached confluence after 1 to 2 weeks similar to (Grierson et al., 1986). There is no specific surface maker to date for TM cells and hence we could not use immunocytochemistry to characterise the cells.

3.2 Collagen contraction models

Collagen contraction models were used to determine cellular contraction of the cells in both a 3D and 2D environment. This is an accepted model of in vitro contraction (Bell et al., 1979). Tissue contraction is a dynamic event characterised by both intracellular and extracellular events. A range of cell densities were initially employed to determine the optimum concentration. It was noted that compared to fibroblasts these cells are not as contractile and myofibroblasts are far more contractile cells possibly due to an increase in α-smooth muscle actin content. Contraction of the collagen matrices is both cell and sometimes serum dependant with tractional forces generated by the cells themselves. It was determined that the best model of cell contraction was when ~50% of the area of the matrix was contracted after 7 days in culture medium, allowing the sensitivity of the assay to determine subtle differences in area of the matrices. Figure 3.2 shows that the

appropriate cell density for seeding was $3x10^5$ cells/ml of matrix for 3D collagen matrices. Therefore, subsequent experiments where performed at this cellular density. Figure 3.3 shows that in 2D matrices $10x10^4$ cells/ml gave the appropriate response and were used in subsequent experiments. Cell free collagen matrices did not contract. The BTM cells were found to form a monolayer on the 2D collagen matrices and this monolayer was not apparent in the 3D collagen matrices; the 3D matrices had dendritic like processes emanating from the cells in a finger-like manner. This may be the reason for the increased contraction due to functional gap junctions in the 2D matrices.

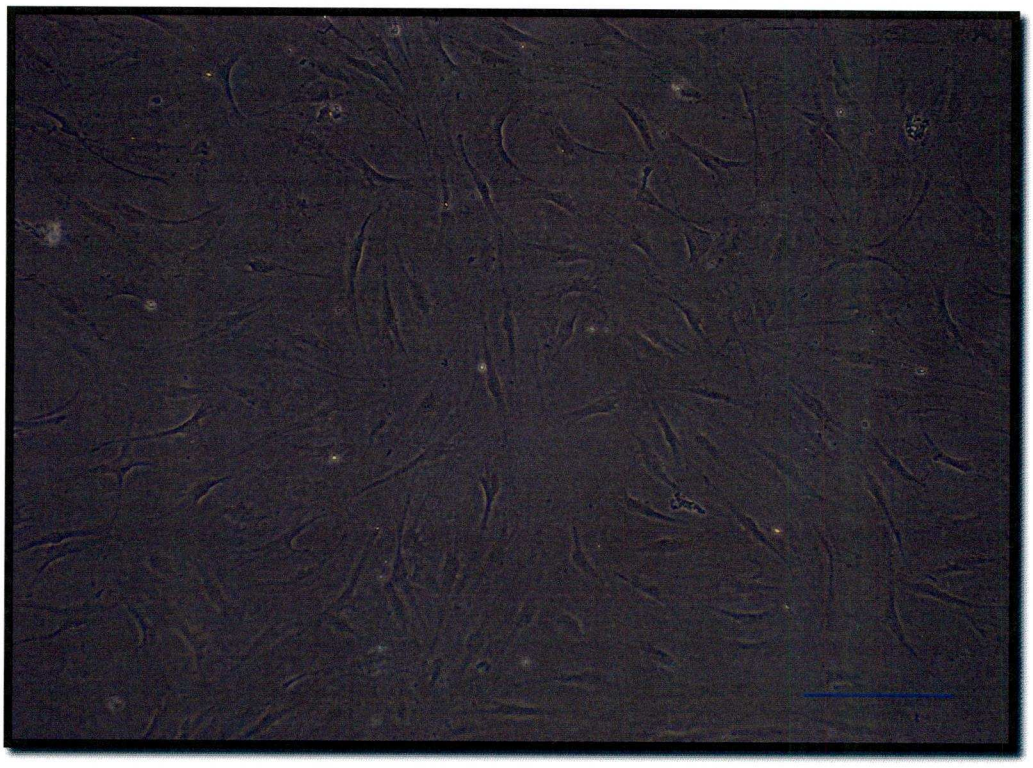

Figure 3.1 Phase contrast image of primary BTM cells. Preconfluent after four days in standard culture conditions. Cells are predominantly bipolar. Scale bar = 20μm.

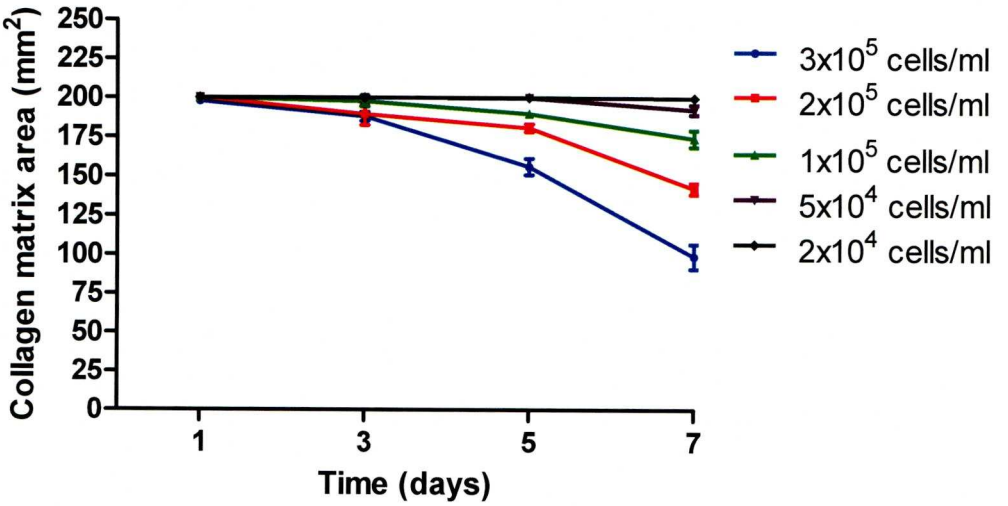

Figure 3.2 Contraction of BTM cells in 3D collagen matrices. Graph illustrating BTM cell-populated collagen matrices at different seeding densities of BTM cells/ml of collagen. Shows both time and dose dependant decrease in area of the matrices. 300,000 cells gave 50% contraction at day 7 and were used for subsequent experiments. Data presented are the mean +/- S.E.M (N=8 experiments).

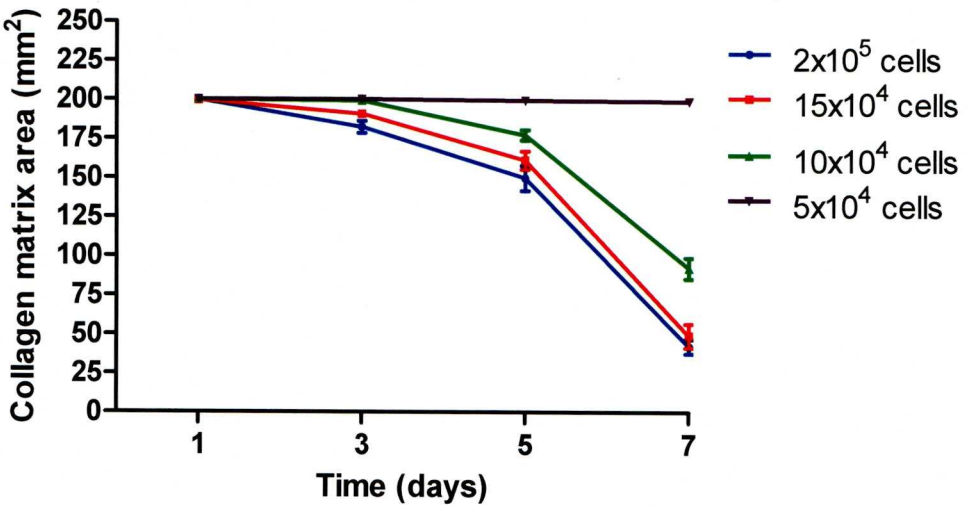

Figure 3.3 Contraction of BTM cells on 2D collagen matrices. BTM cells were seeded upon collagen matrices at different densities and measured at certain time points. Graph illustrating BTM cells seeded upon matrices results gave a more robust contractile response when compared to 3D collagen matrices. Data presented are mean +/- S.E.M (N=8 experiments).

3.3 Collagen contraction in 3D matrices

After determining the appropriate cell number for contraction experiments 3D matrices were populated and incubated with and without DEX 10^{-7}M. This has previously been determined as the optimum concentration for CLAN induction (Wade et al., 2009). The results indicated that there were no significant differences between DEX-treated BTM cells and control treated cells in the populated matrices except at day 5 (Student's t-test). Figure 3.4 illustrates the contracted area of the DEX-treated and control treated collagen matrices.

3.3.1 Collagen contraction in 2D matrices

The appropriate BTM cell number was added to the surface of the collagen matrices and incubated with and without DEX 10^{-7}M. In this model inhibition of collagen matrix contraction was evident at days 5 and 7. It was clear that at day 5 the DEX-incubated matrices had over 50% inhibition of contraction compared to control and by day 7 over 70% inhibition of contraction of the collagen matrices had occurred both $P=<0.05$ (Student's t- test). Figure 3.5 demonstrates the inhibition of contraction is clearly apparent on days 5 and 7. This may be due to alterations in gap junctions due to the DEX administration. It is known that DEX upregulates ZO-1 and occludin expression in endothelial cells (Romero et al., 2003) and also alters gap junctions in TM cells (McCartney et al., 2006, Zhuo et al., 2010). There was poor reproducibility with both 2D and 3D collagen gels. This is one of the weaknesses of the collagen contraction assay.

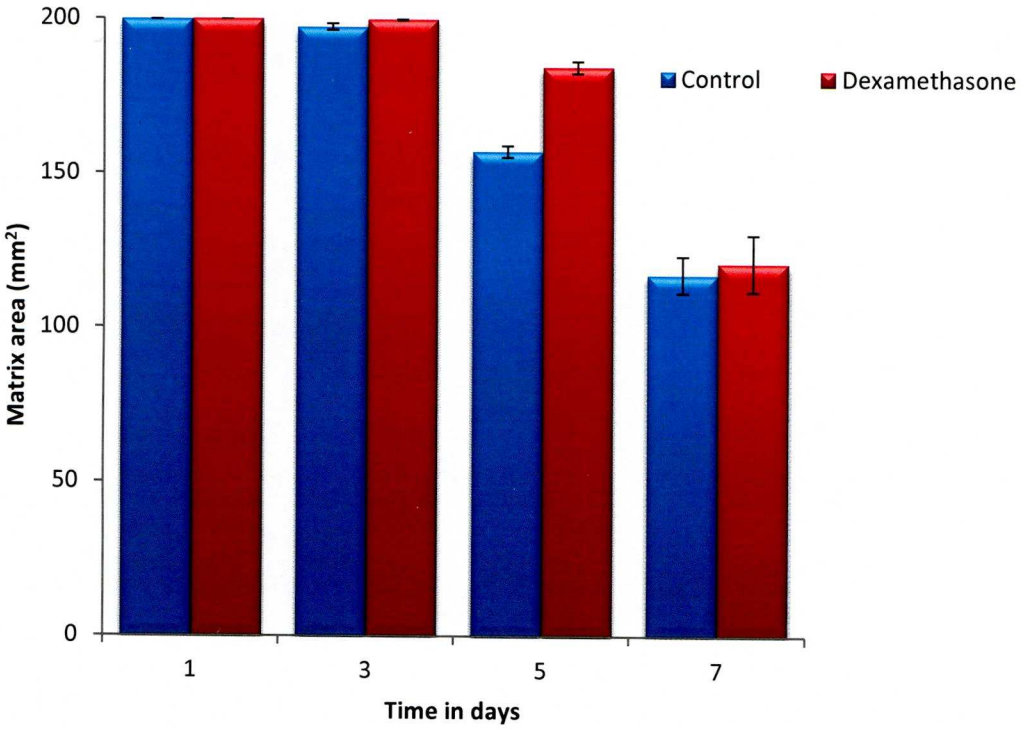

Figure 3.4 Histogram showing mean matrix area for BTM populated collagen matrices either in the presence or absence of DEX 10^{-7}M. BTM cell were populated in collagen gels that were placed in 24-well plates and measured at set time points in the presence or absence of DEX. Data expressed as mean+/-SEM (N=12). There is no significant difference between DEX-treated and control matrices except for day 3 P=0.029 Student's t test.

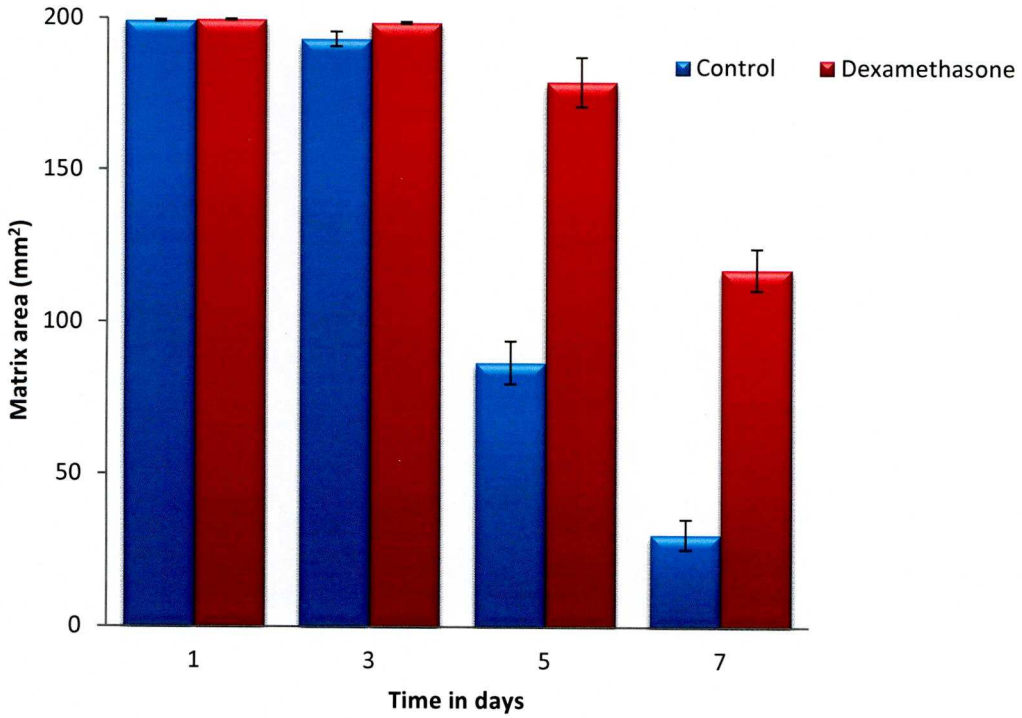

Figure 3.5 Histogram showing mean matrix area for BTM cells seeded 'on' collagen matrices either in the presence or absence of DEX 10^{-7}M. Data expressed as mean +/- SEM (N=12). There was a significant difference in matrix contraction between control and DEX-exposed matrices after 3, 5 and 7 days in 3D collagen matrices ($P<0.05$).

3.4 Contraction-inhibited matrices contain CLANs

A logical next step was to demonstrate the presence (or absence) of CLANs within the collagen matrices. After cessation of the experiment the matrices were fixed and stained as indicated in the methods section. Figure 3.6 shows a confocal image of a CLAN on a contraction-inhibited matrix stained with phalloidin-FITC. The 'hub' points for CLANs are clearly evident. The left hand side of the image shows another CLAN. The prominent pattern in the control matrices that were not exposed to DEX was that of stress fibres. It was however difficult to image CLANs in the collagen matrices due to high 'background' staining and therefore it should be noted that no quantitative CLAN incidence within or upon the gels could be performed. Thus quantitative data regarding CLANs in or upon gels is lacking.

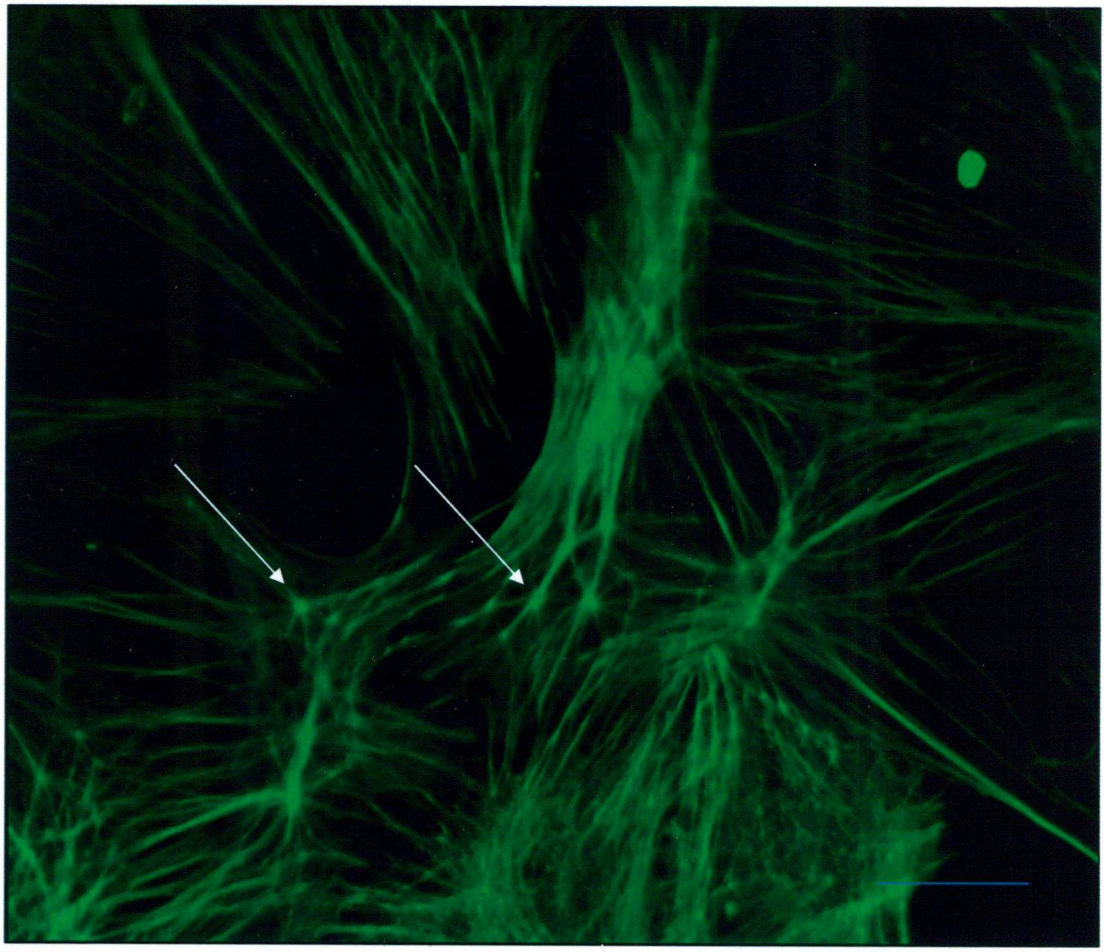

Figure 3.6 CLANs on a DEX-treated collagen matrix. The 2D collagen matrix was fixed and stained for F-actin with phalloidin-FITC and visualised using confocal microscopy. The 'hubs' and 'spokes' are clearly evident. Scale bar =20μm. Arrows are identifying hub points of the CLANs.

3.5 Cell viability

3.5.1 Trypan blue exclusion

It was important to evaluate the effect of dexamethasone/CLANs on cell survival as CLANs may be associated with cell death; therefore we undertook assays to assess the effect of the glucocorticoid on cellular apoptosis. General morphological characterisation of cells after treatment, using phase contrast microscopy did not reveal any gross changes associated with cell death. Trypan blue exclusion was initially used to determine any gross changes in cell death. Trypan blue works on the exclusion of the dye when the cell membrane is not compromised and not dead. When the cell is dead the dye can enter the cells as the membrane integrity is compromised; however it cannot distinguish between an apoptotic and a necrotic cell. After treatment with DEX and TGF-β2 (a cytokine that was later found to induce CLANs) there was no decrease in cell viability. Viability was always over 97% in these culture conditions. This demonstrated that no gross cell death was occurring based on this relatively insensitive assay (figure 3.7).

3.5.2 MTT assay

The conversion of MTT to an insoluble formazan, which is then solubilised and read at 570nm spectrophotometrically, is dependent on mitochondrial enzymes to reduce this and as such is a sensitive assay for cellular viability. Figure 3.8 shows that incubation for up 14 days in culture results in no decrease in cellular viability or increase in cell number with exposure to DEX and TGF-β2.

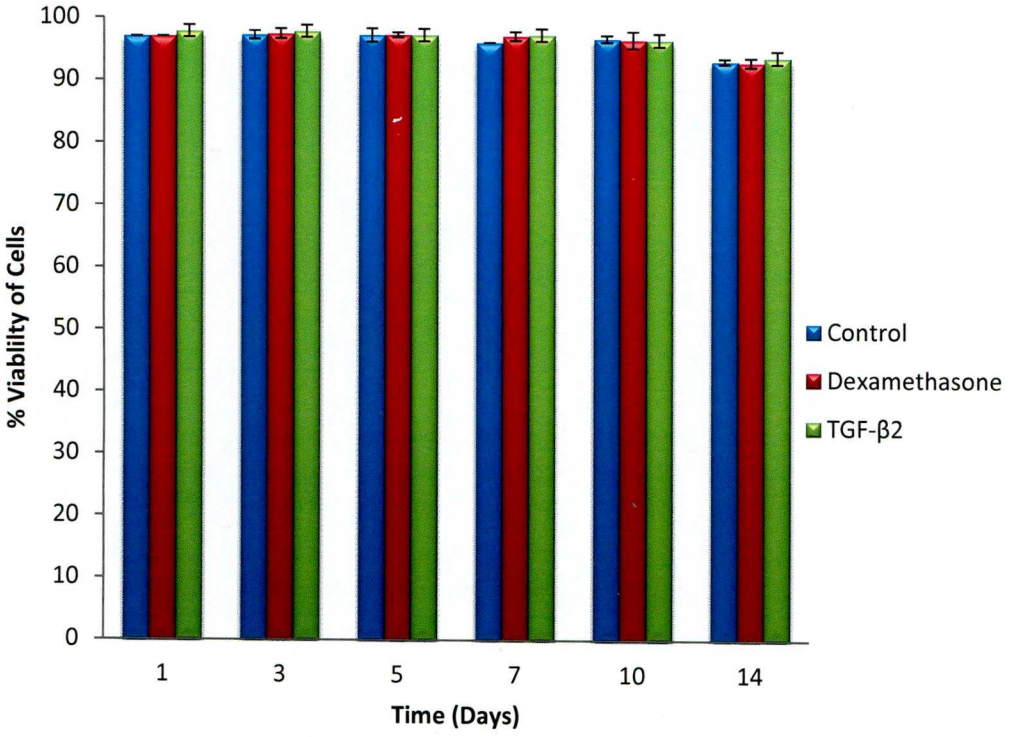

Figure 3.7 Viability of BTM cells over time. BTM cells were cultured to confluence in tissue culture plastic flasks and then incubated with DEX 10^{-7}M, TGF-β2 2ng/ml or control media containing 1% FCS and at various time points cell viability was assessed using trypan blue exclusion dye and expressed as % viability. Data presented are the mean ±SD. No significant difference between any of the treatments was observed at any time point examined (P>0.05) (N=8).

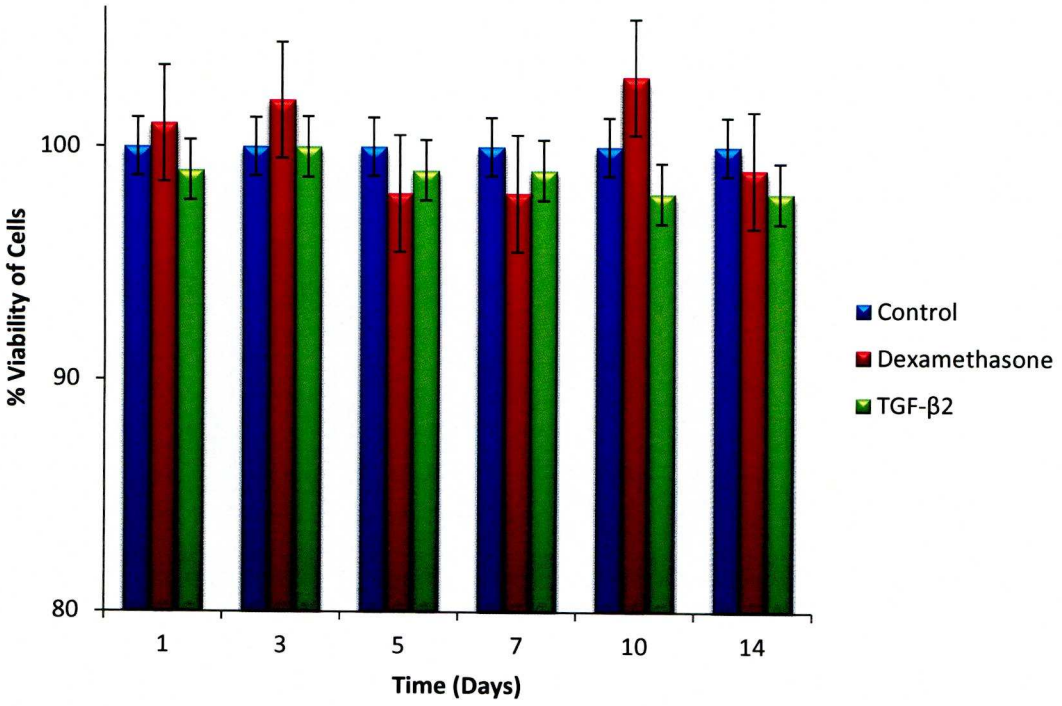

Figure 3.8 Viability of BTM cells over time assessed by MTT assay. MTT reduction assay results converted to % viability compared to control treated cells (100%). BTM cells where grown to confluence and then treated with DEX 10^{-7}M, TGF-β2 2ng/ml or control medium containing 1% FCS and at set time points examined for MTT. Data presented are the mean ±SD (N=10). No significant differences were determined between treated and control groups (P=>0.05).

3.5.3 Determination of apoptosis

After determining no clear obvious gross changes in cell death, investigations of apoptosis using morphological and nuclear signs characteristic of apoptotic cell death were undertaken using the nuclear marker propridium iodide, such as nuclear condensation. This was pursued as cell loss in POAG is a hallmark of the disease and no investigations to date have found a reason for the cell loss (Grierson and Howes, 1987) and we hypothesised that CLANs are associated with apoptosis. It was found that very low levels of apoptosis occurred in BTM cells in normal medium in vitro and no significant differences were found between control, DEX or TGF-β2 treated groups. Although there was a trend towards increased apoptosis, based on morphological appearance, this was very small and not significant (figure 3.9).

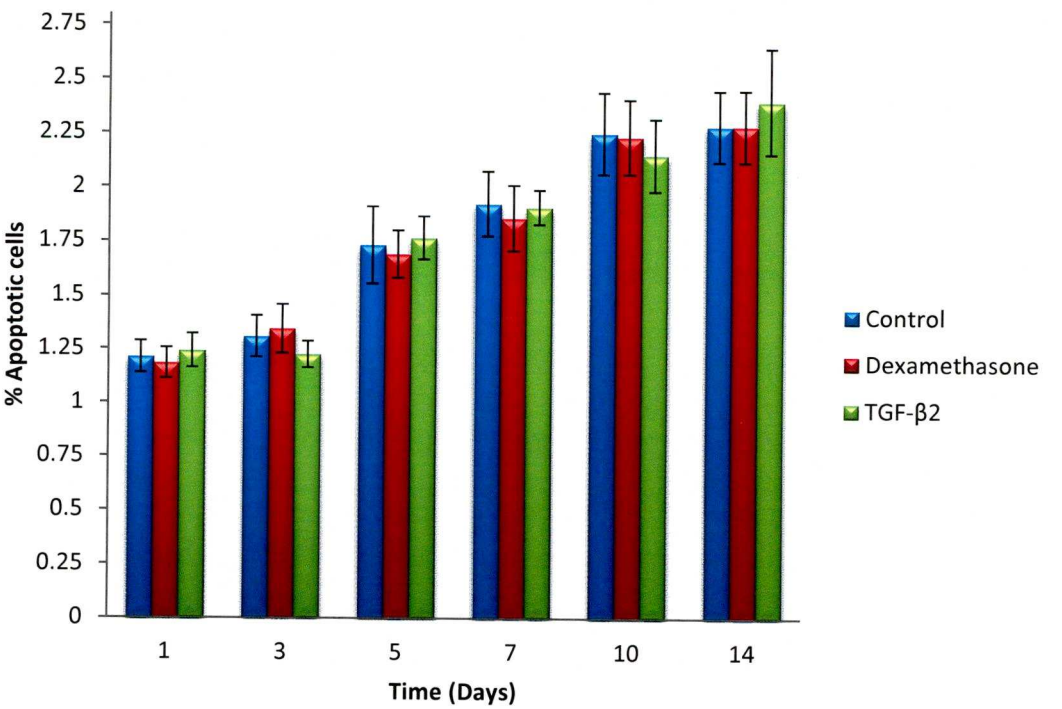

Figure 3.9 Histogram illustrating the % apoptotic cells as determined by morphological criteria up to 14 days in culture. There is an increase trend of apoptosis over time in culture conditions, however this is small and there is no significant difference in apoptosis between treatment groups. Data presented are the mean±SD (N=12).

3.5.4 Annexin-V analysis

We next used Annexin-V staining to determine apoptosis as Annexin-V binds to PS that is flipped to the outside of the membrane, mediated by the enzyme flippase and as such is a reliable marker of apoptosis (Fadok et al., 1992). Data presented in figure 3.10 show an increasing trend of apoptosis over time in culture and there were no differences between any of the groups tested.

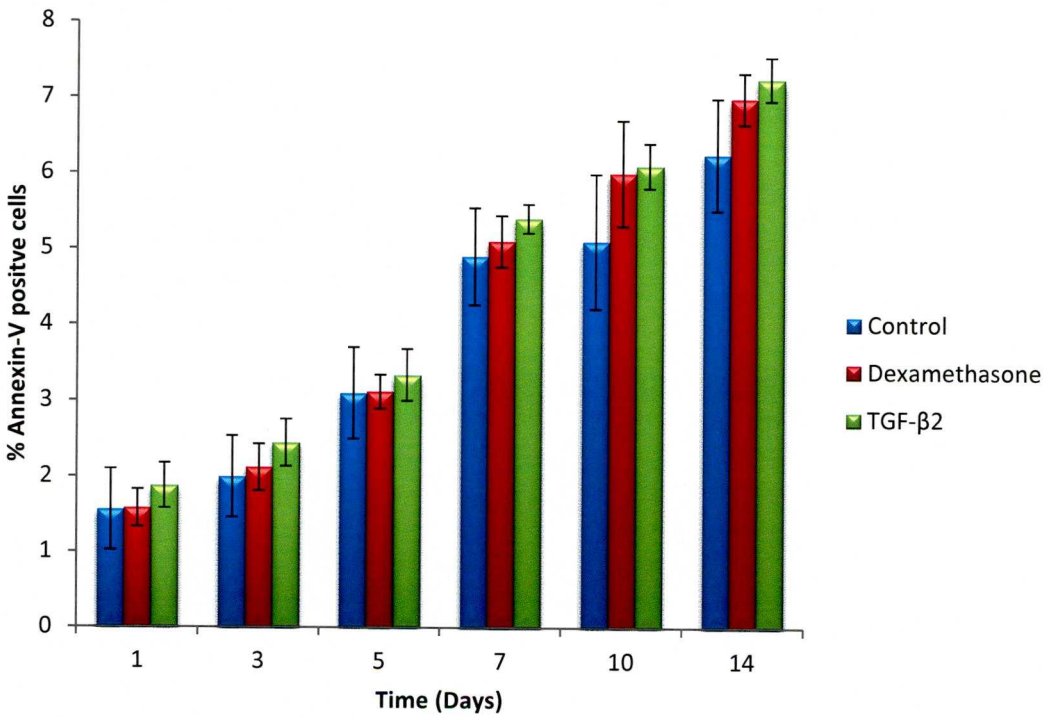

Figure 3.10 Annexin-V positive BTM cells. BTM cells where treated with either control, DEX 10^{-7}M or TGF-β2 2ng/ml with 1%FCS in the medium for up to 14 days in culture and examined at each time point using flow cytometric analysis as detailed in the methods. There is an increasing trend for apoptotic cells over time however there is not a significant difference between any treatment groups analysed. Data are the mean± SEM (N=5).

3.5.5 Caspase 3 staining

Caspase 3 is an execution caspase in the apoptotic pathway therefore we used a cleaved caspase 3 antibody to determine apoptosis immunocytochemically (figure 3.11). This was found to be a very rare event in any of the cultures examined using the anti-caspase 3 antibody and no differences between groups. On average less than 5% of cells between any of the treatment groups were caspase 3 positive.

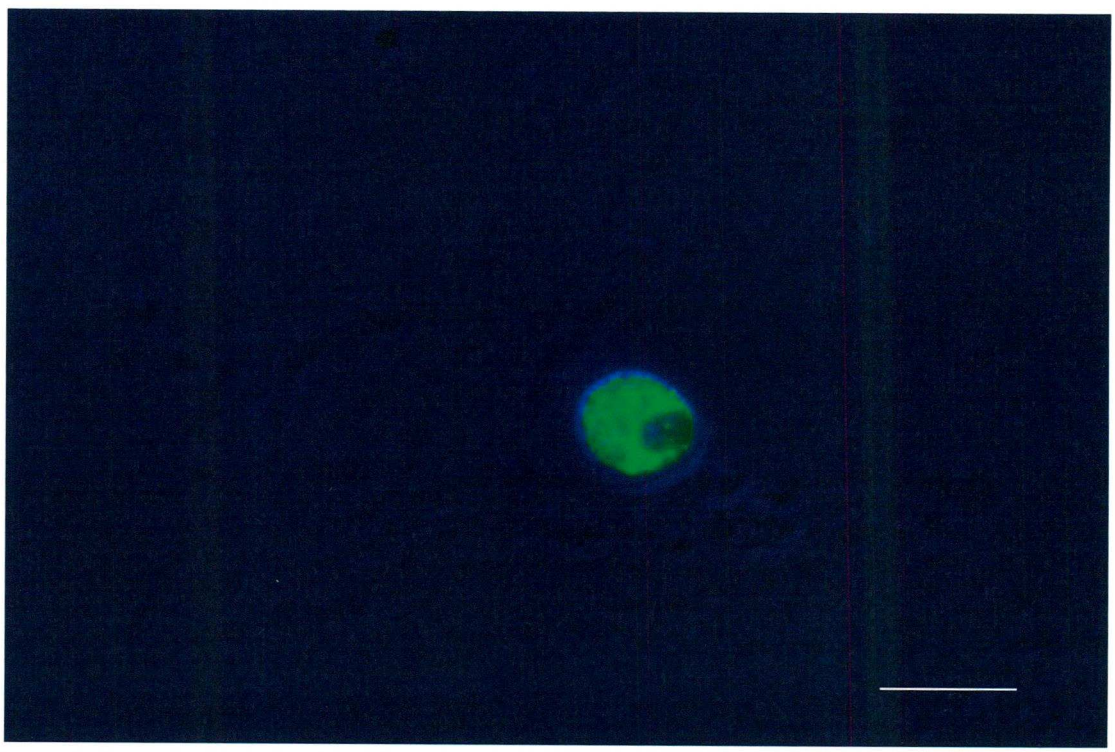

Figure 3.11 Active caspase 3 activation in an apoptotic BTM cell after exposure to DEX. BTM cells where grown to confluence in tissue culture plastic wells and then exposed to DEX 10^{-7}M, TGF-β2 2ng/ml or control in 1% FCS after which the cells were washed with cold TBS and permeabilised with 0.1% Triton X-100, probed with anti-active caspase 3 antibody (5μg/ml) and left overnight after washing cells were incubated with a secondary antibody labelled with Alexa-488 antibody (green) and imaged with a confocal microscope. The green is active caspase 3 in the cell nucleus. Scale bar= 20μm

Caspase 3 was also probed using Western blotting techniques and could not be detected in these cells using this antibody as it probably did not recognise the epitope as the antibody worked for RPE cells that were serum starved.

3.6 Other CLAN inducers

DEX and other corticosteroids were the only known CLAN inducing agents known at the outset of this study and so we sought to find other CLAN inducing compounds.

3.6.1 Differing serum levels

Varying the amount of FCS in the standard culture medium was initially used to determine the effects on CLAN incidence and so we could use the lowest concentration of FCS in subsequent experiments. Analysis revealed that in 0.5% FCS in our normal culture medium (the lowest concentration used) only 3.7% of BTM cells at 14 days contained CLANs. Medium containing 1% FCS however, produced twice as many (7.4%) CLANs and in 10% FCS there was a further increase to 13.6% of BTM cells with CLANs at the 14 day time period. Figure 3.12 shows this low level but progressive and significant (P=<0.05 or better) step wise increase in the incidence of BTM cells containing CLANs with around a 3 fold increase between low and standard levels of serum in our culture medium. We used 1% FCS in subsequent experiments. These CLAN incidences are higher than that seen with human TM cells and seem to be more sensitive to CLAN induction compared to that of human TM and are much larger. Routine evaluation of 0.5% FCS cells and 1% FCS cells using trypan blue exclusion as previously described determined cell viability to be 94% and 96% respectively. Therefore, showing these cells to be hardy and resilient to serum-reduced conditions.

3.6.2 TGF-β2 induction of CLANs

TGF-β2 is a pleotropic low molecular weight cytokine that is highly expressed in the aqueous humour and increased levels have been determined in aqueous humour from POAG patients (Min et al., 2006, Tripathi et al., 1994b), therefore we hypothesised that TGF-β2 induced CLANs in BTM cells.

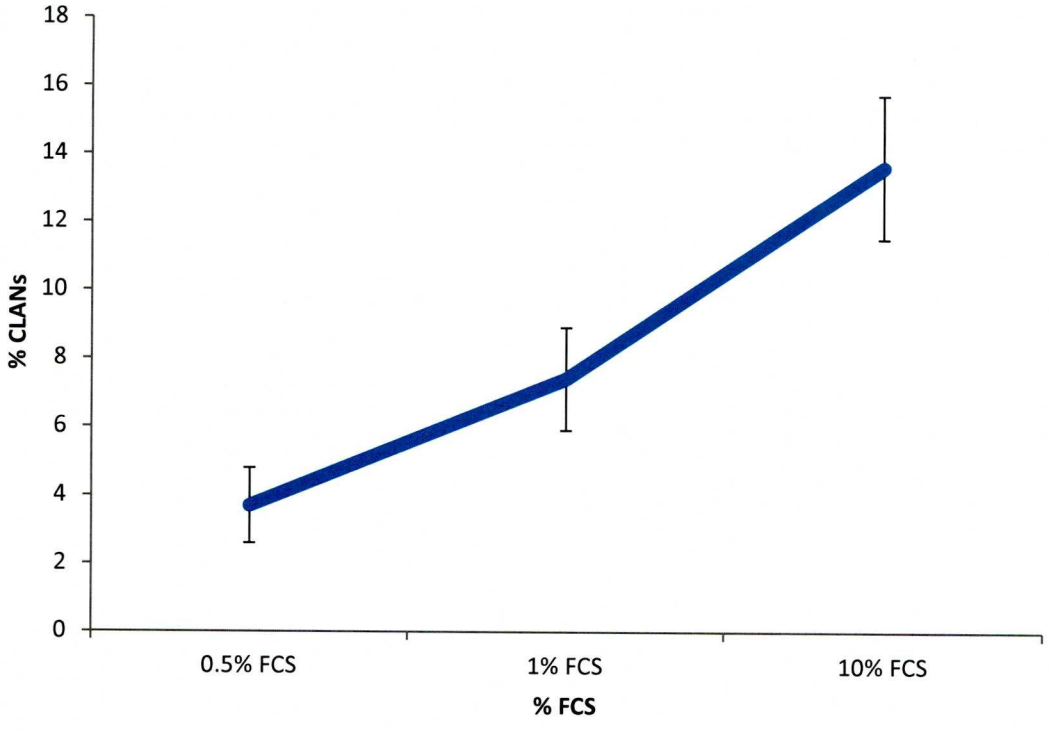

Figure 3.12 Graph showing that BTM cells incubated in increasing levels of FCS in vitro produced CLANs. BTM cells were grown to confluence in culture before they were washed in PBS and the medium replenished with 0.5, 1 or 10% FCS supplemented medium for seven days after which they were fixed and stained for F-actin according to methods. There is a significant increase in % CLANs with increased concentrations of FCS (P=<0.05 between all groups Student's t test). Data presented are the mean±SD (N=4).

Dose response curves with TGF-β2 induced a similar incidence of CLANs from 2ng/ml to 10ng/ml. Therefore the lower end of the response curve was subsequently used. This concentration also correlates with the reported amount in aqueous humour. Time response curves showed that at each time point under examination the TGF-β2 CLAN induction effect was significantly greater than that produced by an optimum concentration of DEX ($P<0.01$) (figure 3.13). After 7 days in culture around 50% of TGF-β2 exposed cells contained CLANs, which was comparable to the maximum CLAN response after 14 days in culture (longer period). Indeed after 10 days exposure to TGF-β2 the CLAN induction was 59% compared with DEX and control treated cultures and this was very significant ($P=<0.01$). Figure 3.13 shows the induction of CLANs over time by TGF-β2 compared to DEX (our "gold standard" CLAN inducing agent) and a culture medium containing 1% serum but without any of the other agents as a baseline control.

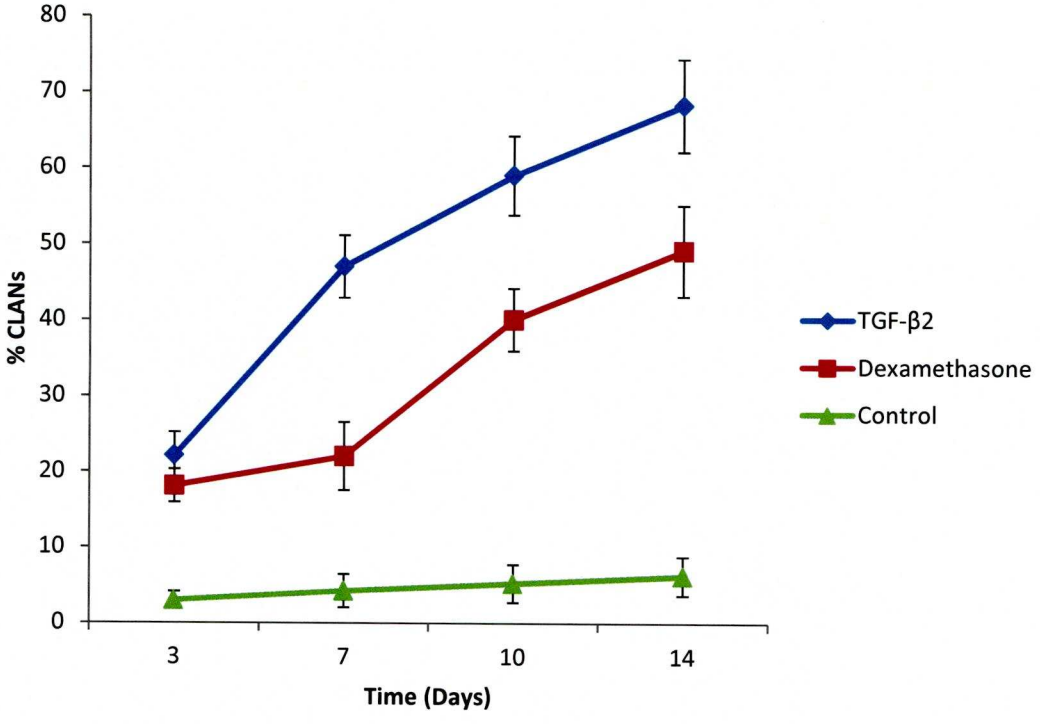

Figure 3.13 Incidence of CLANs after DEX and TGF-β2 exposure. Graph illustrating the increase of CLANs over time in BTM cells incubated with the multifunctional cytokine TGF-β2 2ng/ml, DEX 10^{-7}M or control medium containing 1% FCS. Significant differences are observed between TGF-β2-exposed cultures and DEX and also control (P=<0.01) Data presented are the mean ±SD (N=4). At all time points TGF-β2 is a more potent inducer of CLANs in comparison to DEX.

These polygonal triangular arrangements of F-actin induced by TGF-β2 incubation in vitro, could not be distinguished from DEX-induced or indeed, basal medium-induced CLANs and therefore it was justified to call them "CLANs" and not CLAN-like structures. Arrangements of hubs and spokes were variable ranging from insubstantial structures to very large structures. For quantitative requirements, reliability and repeatability needs an arbitrary definition of what constitutes the smallest CLAN. We established the minimum requirement as being five or more hubs and three triangulated arrangements of spokes radiating from the hubs. Although we may well have undercounted CLANs our inter and intra-observer errors were less than 10%. Figure 3.14 demonstrates a spectacular CLAN induced by 7 days DEX exposure, clearly evident are the polygonal networks occurring in arrangements of 5 and 6 as outlined in section 1.0. TGF-β2 was capable of induction of very large CLAN territories where the CLAN extended through a large proportion of the cell cytoplasm. Territories of 50 or more hub sites were occasionally observed at the longest exposure times. Figure 3.15 displays a TGF-β2 induced CLAN. Confocal z-series through CLANs induced by TGF-β2 demonstrated that even the biggest CLAN territories had relatively little height so CLANs that occurred in over 3x1μm confocal slices were uncommon. At 14 days incubation with TGF-β2 there was an increased in CLAN 'hotspots' or clusters of CLAN-containing cells in specific regions within the culture, compared to the more uniform distribution of CLANs were found in cultures exposed to DEX. The reason for the CLAN 'hotspots' is unknown, however, it may represent heterogeneity within the culture.

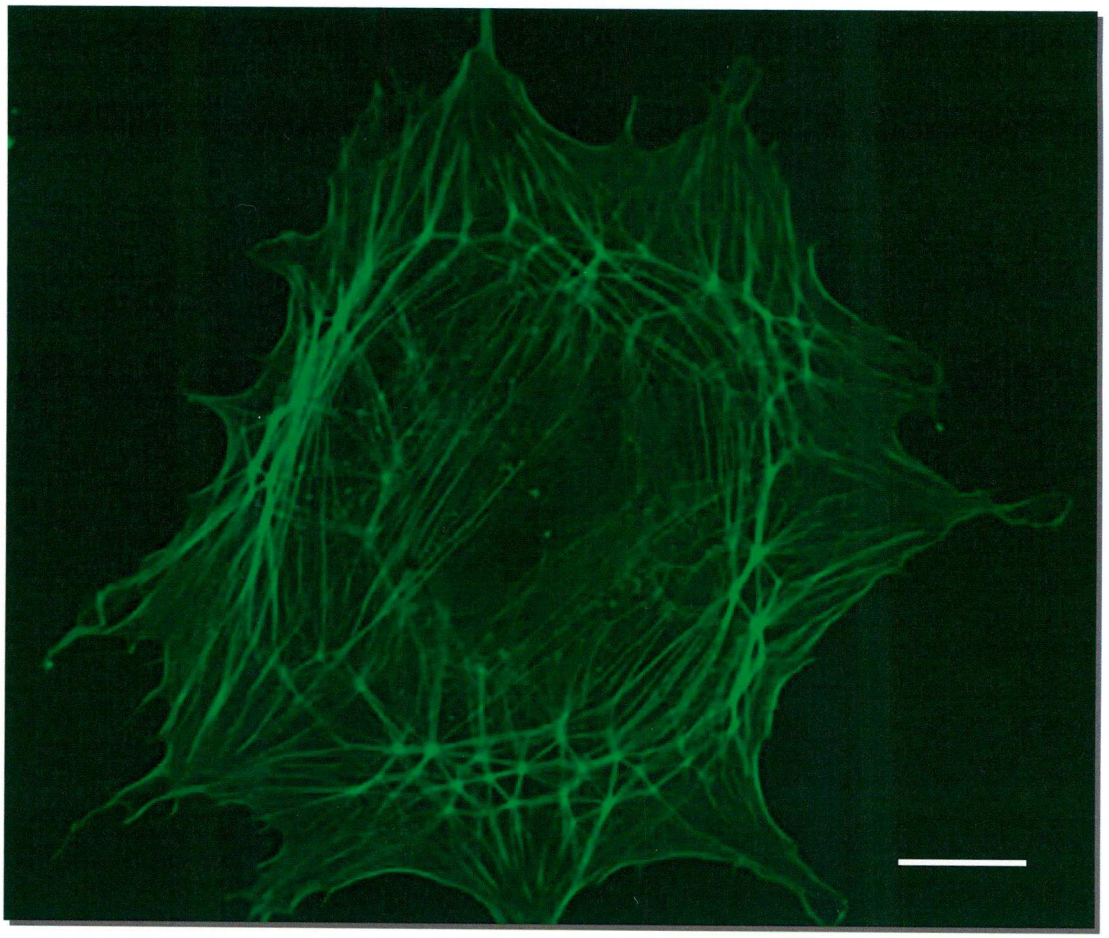

Figure 3.14 DEX-induced spectacular CLAN. Demonstrates a spectacular perinuclear CLAN after seven days exposure to DEX 10^{-7}M. F-actin is labelled with phalloidin-FITC. The actin 'hubs' and 'spokes' are clearly visible in triangulated forms and spans the cytoplasm. Note the BTM cell is 'epithelioid' in appearance. The constituent geodesic units are very obvious. Scale bar= 20μm

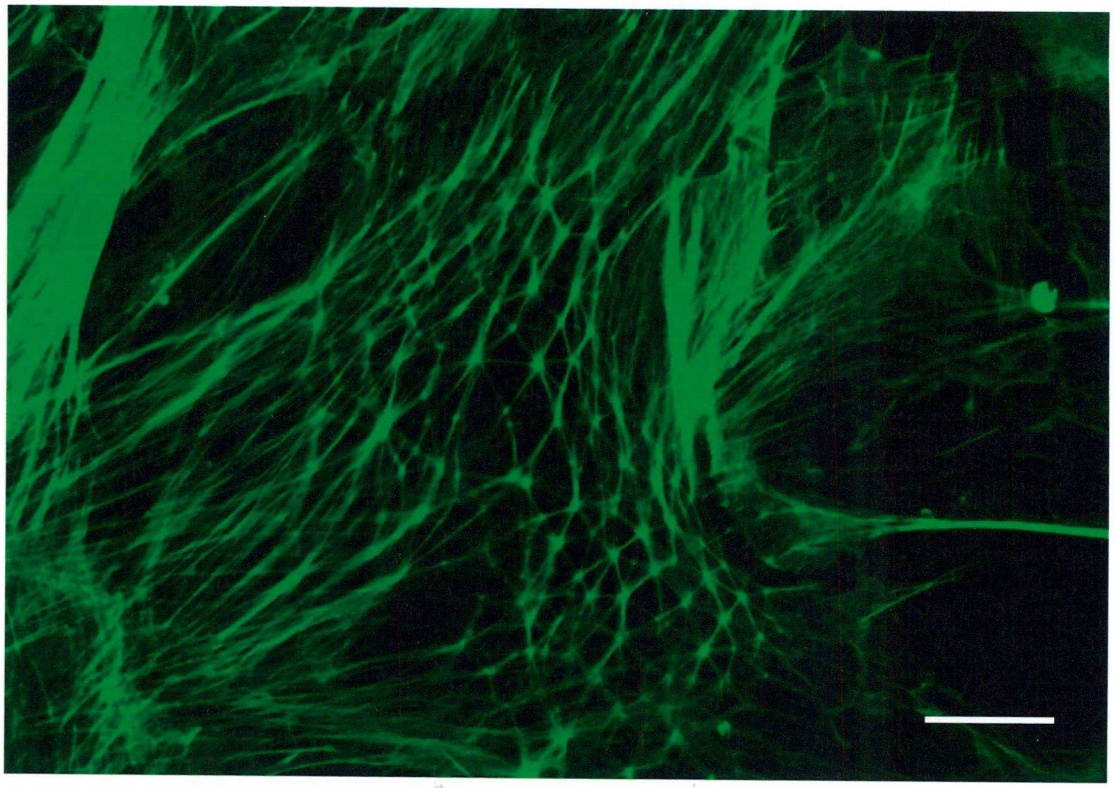

Figure 3.15 A large TGF-β2 induced CLAN in a single BTM cell. This image illustrates the huge network CLAN that is often found in TGF-β2 treated cultures. The punctate 'hubs' and 'spokes' are clearly visible with particularly bright 'hubs' The BTM cells were cultured for one week with TGF-β2 2ng/ml with 1%FCS after confluence was reached and then fixed in 10% NBF and subsequently stained for F-actin. Scale bar =20μm.

Thus TGF-β2 treatment leads to a profound CLAN inducing effect in the BTM cells (as was hypothesised) and the magnitude of the induction is larger than that of DEX. Moreover, although the CLANs were the same phenotypically and indistinguishable from one another they did appear to span a larger area of the cellular cytoplasm and also occur in hotspots or "clusters" of cells in specific regions within the cultures. The reason for these "clusters" of CLAN-containing BTM cells is unknown but may be related to small variations in surface topography in the culture plate.

3.6.3 Inhibition of TGF-β2 CLANs using small molecule inhibitors and a neutralising antibody

To further explore the pathways of TGF-β2 induction of CLAN we used TGF-β receptor inhibitors, an anti-TGF-β2 antibody that neutralised TGF-β2 and a small molecule inhibitor of Smad-3 activation. Smad 3 is a transcription factor activated upon TGF-β signalling. It was shown that TGF-β receptor I inhibitor SB-431542 reduced CLANs to 34% (P=<0.05) and incubation of TGF-β2 in the presence of LY-364947 suppressed CLANs to 31% which was statistically significant compared to TGF-β2 exposure alone (P=<0.05). Combining both inhibitors together to increase inhibition of TGF-β signal transduction lead to cell death. Also the neutralising anti-TGF-β2 antibody reduced CLANs to 12%, a reduction in CLAN incidence of over 100% (P=<0.0001). These inhibitors and the antibody were at least partially effective at suppressing CLAN incidence. Figure 3.16 shows the reduction in CLANs with all the agents evaluated.

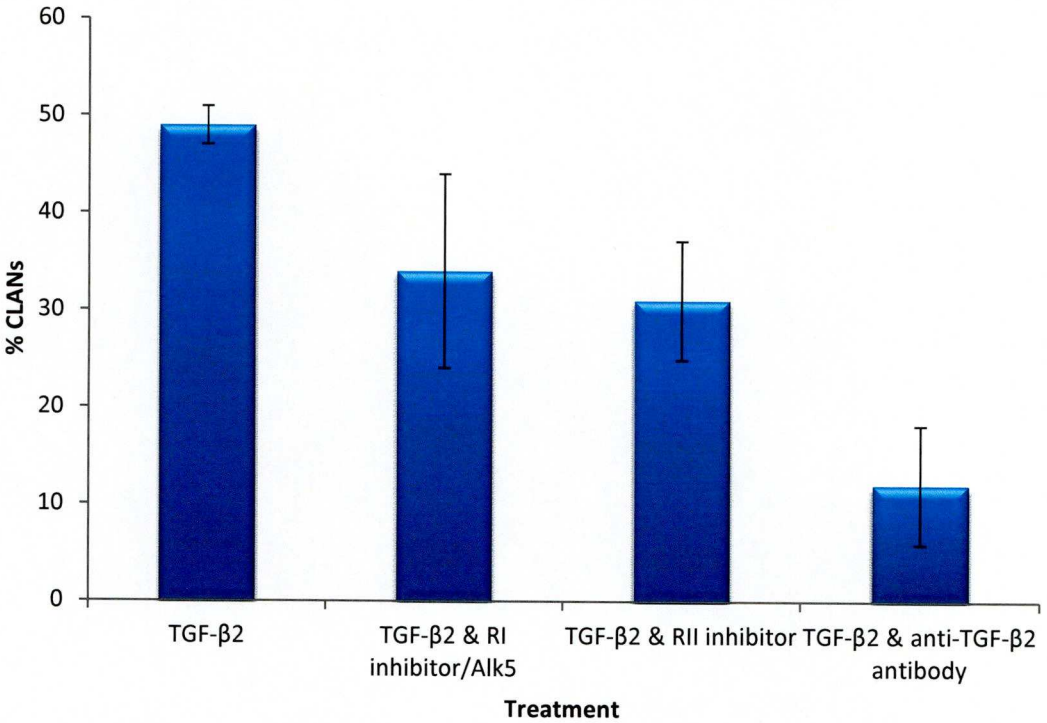

Figure 3.16 TGF-β blockade retards TGF-β2-induced CLANs. Histogram showing the incidence of CLANs with TGF-β2 ± receptor inhibitors. Cells were treated with either TGF-β2, or TGF-β2 & SB-431542 10μM or TGF-β2 & LY-364947 20μM or anti-TGF-β2 neutralising antibody 1.4μg/ml for 7 days after which the cells were quantified for CLANs. A statistically significant inhibition of CLAN incidence is observed with incubation of any of the agents, however, the anti-TGF-neutralising antibody appears to be more effective at CLAN suppression than the TGF-β receptor antagonists (P=<0.0001 ANOVA). Data presented are the mean ±SD (N=5).

At higher concentrations the neutralising antibody had deleterious effects on the cells leading to cell death so the concentration used in this study was never greater than 1.4 μg/ml and exposures were not longer than 7 days but even so a pronounced (5 fold) reduction in CLANs was determined. To check the viability of the cells with receptor blockade general morphological characteristics were examined in culture at the end of the incubation period and the cells appeared healthy with no evidence of cell apoptosis. It was noted however that many cells appeared more epithelioid in the TGF-β2 treated group. In separate experiments the BTM cells viability was checked by trypan blue exclusion, as previously described, and found to be consistently over 97% for both receptor antagonists.

We further examined which pathway CLANs were being generated through by using a specific inhibitor of Smad-3 (Jinnin et al., 2006). TGF-β2 induced CLANs were totally negated with this pharmacological inhibitor and no CLANs could be found. This was a total suppression and highly statistically significant (P=<0.0001). Smad-3 is essential for transducing the TGF-β2 signal into CLANs. The prevailing pattern of actin was that of stress fibres running along the axis of the cell which is the predominant pattern of architectural actin in TM cells. Figure 3.17 shows the data showing Smad-3 suppression of TGF-β2 CLANs. On morphological examination of the cells they appeared healthy with no obvious signs of cell death or cell detachment from the substrate. Again in separate experiments cells were treated and examined by trypan blue exclusion and viability was consistently over 96% when incubated with SIS3. Therefore, the cells where healthy and viable. Figure 3.18 shows the cells actin cytoskeleton after 7 days treatment with the molecules.

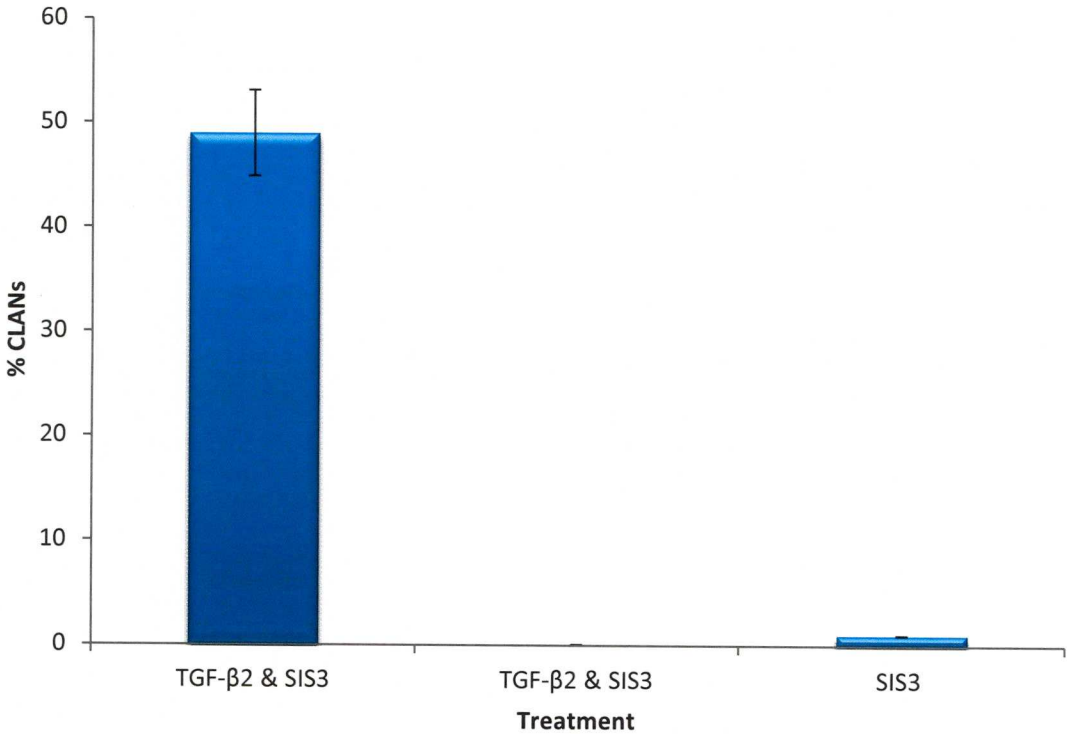

Figure 3.17 Histogram showing the attenuation of CLANs in BTM cells in vitro. Cells were treated with either TGF-β2 2ng/ml, TGF-β2 & SIS3 25μM or SIS3 alone after 7 days the cells were fixed and stained and CLANs evaluated. There is a significant difference between TGF-β2 treated cultures and TGF-β2 & SIS3 and SIS3 alone (P=<0.001). Data presented are the Mean ±SD (N=5).

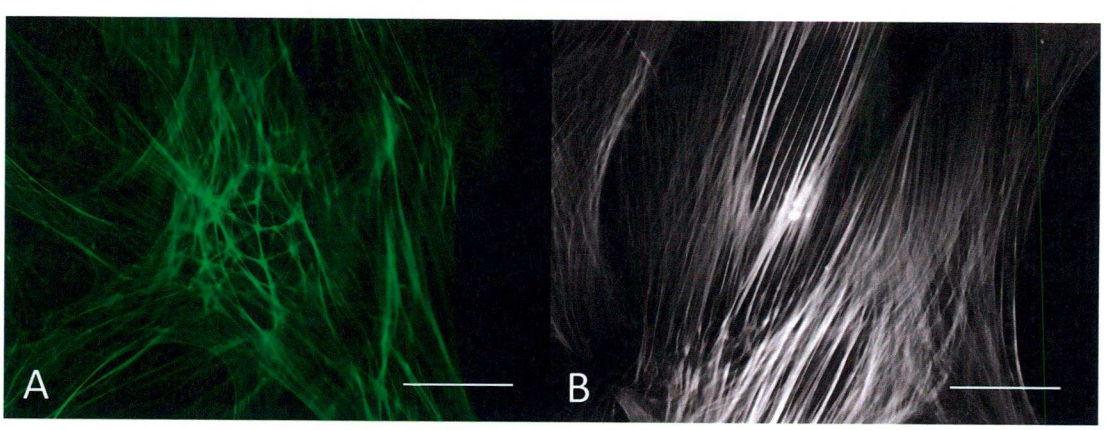

Figure 3.18 Smad-3 phosphorylation inhibits CLAN formation. Representative immunoflourescent images of F-actin in BTM cells treated in (A) with TGF-β2 2ng/ml and in (B) TGF-β2 2ng/ml & SIS3 25 μM for 7 days. The image in A shows a clear CLAN with bright fluorescent 'hubs'and the image in B shows the pattern that was found in all cells of actin stress fibres. Scale bar in A= 20μm and in B=15μm

3.6.4 SIS3 attenuates Smad-3 phosphorylation

After previously demonstrating that the inhibitor of Smad-3 suppressed CLANs we sought to confirm this by immunoblotting techniques for phosphorylation of Smad-3 as an indication of activation as phosphylated Smad-3 translocates to the nucleus to alter gene expression for a plethora of genes. Phospho-Smad-3 was at the predicted molecular weight of 50 KDa. Figure 3.19 shows that after 2 hours incubation with TGF-β2 Smad-3 is phosphorylated, and preincubation with SIS3 completely negates this phosphorylation of Smad-3. We could not perform a loading control due to the fact the GAPDH antibody did not recognise the epitope from BTM cells and actin could not be used due to the obvious nature of the experiment.

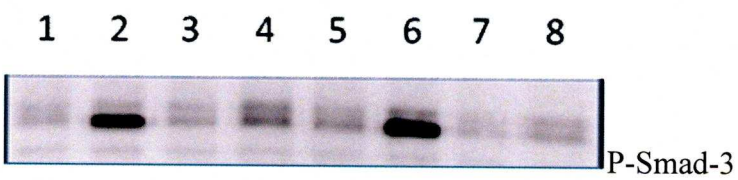

Figure 3.19 Representative Western blot of Phospho-Smad-3 in BTM cells from 2 separate experiments. Lane 1 was treated with control medium, lane two was treated with TGF-β2 2ng/ml, lane 3 was pre-treated for one hour with SIS3 then incubated with TGF-β2 2ng/ml for 2 hours, lane 4 received SIS3 alone. Lanes 5, 6, 7 and 8 represent the same treatments but from a different culture. The cells were treated as in the methods, lysed and 25μg of total protein was resolved using 10% PAGE and transferred to a nitrocellulose membrane after which the membrane was probed with a phospho-specific anti-Smad-3 antibody overnight before incubation with a secondary antibody labelled with HRP and exposed using chemidoc image analysis. It is clear that Smad-3 is phosphorylated after TGF-β2 exposure and pre-treatment with SIS3 negates this phosphorylation and activation.

3.6.5 CLAN inhibition using a neutralising antibody to TGF-β2

This lab has already shown that in vitro exposure to aqueous humour leads to an increase in CLAN incidence (Wade et al., 2009). This is not surprising as in vivo these cells are constantly bathed in aqueous humour as it circulates throughout the chamber angle. To determine if the factor present in aqueous humour induced CLAN formation was indeed TGF-β2 it was decided to neutralise the TGF-β2 using our neutralising antibody. We used bovine aqueous humour diluted 1:1 with complete media supplemented with 1% FCS. Previous work has revealed that 100% aqueous humour is a poor sustaining media (Wade et al., 2009). After incubation for 3 and 7 days with bovine aqueous humour CLAN incidence was 11% and 40% respectively, however coincubation with our TGF-β2 neutralising antibody reduced CLAN incidence to 8% and 11% at the equal time points as figure 3.20 illustrates a total reduction of over 50%. Control basal medium coincubated with anti-TGF-β2 antibody showed a similar CLAN incidence.

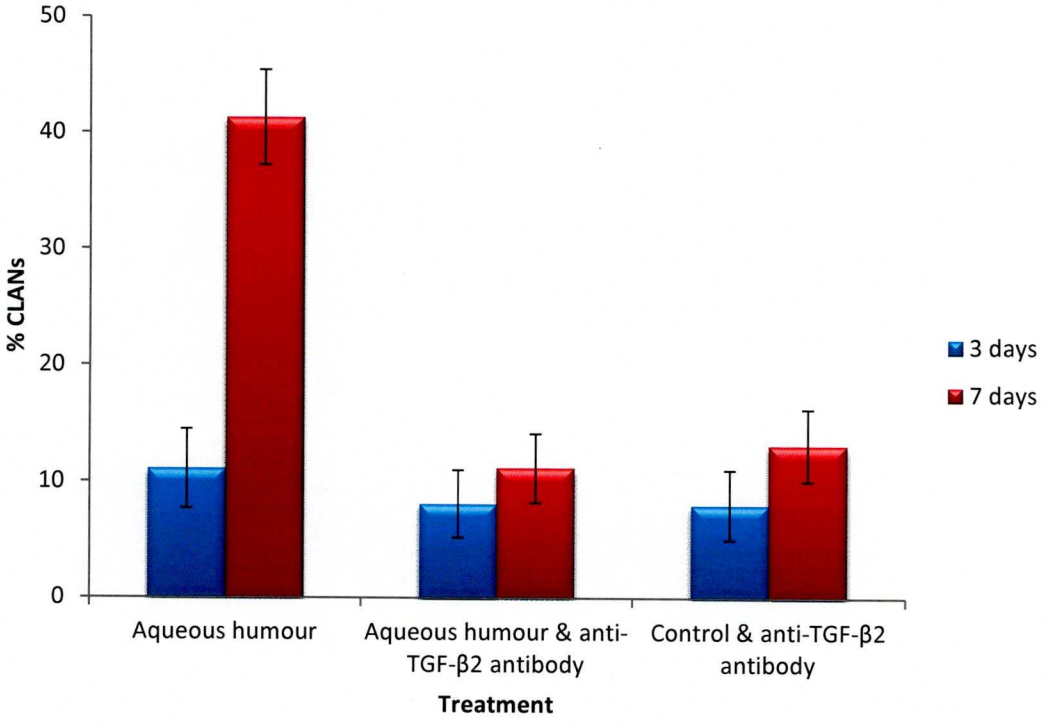

Figure 3.20 Aqueous humour contains CLAN-promoting TGF-β2. Column chart showing CLAN incidence in BTM cells after 3 and 7 days culture with bovine aqueous humour only, aqueous humour & anti-TGF-β2 antibody, or control medium & anti-TGF-β2 antibody 1% FCS. It can be seen that incubation of the aqueous humour with the neutralising antibody suppresses CLAN incidence at both time points (P=<0.05). Data presented are the mean ±SD (N=5).

Morphological examination of BTM cells incubated with aqueous humour revealed the cells to be a little larger and more round refractile compared to control medium and after 7 days in culture, but on the whole the cells grew well in aqueous humour medium mix. Previous work by this group showed that heat denatured aqueous humour totalled negated the CLAN producing effect of aqueous humour (Wade et al., 2009). Therefore, it suggested that the effect due to a protein(s) in the fluid. We have explored this further in this study to show that a CLAN producing factor is TGF-β2.

Qualitative examination of CLANs produced by aqueous humour revealed them to be identical to both DEX and TGF-β-stimulated CLANs, except like TGF-β2-induced CLANs they appeared peculiarly large. These large CLANs extended right throughout the cell cytoplasm in certain BTM cells. There were very obvious 'hubs' and 'spokes' of actin present in all CLANs identified in these treated cultures with polygonal triangulations in positioned groups of five or six. Figure 3.21 shows an aqueous humour-induced CLAN extending over a large area of the cell. This was not an infrequent finding in aqueous humour treated cultures.

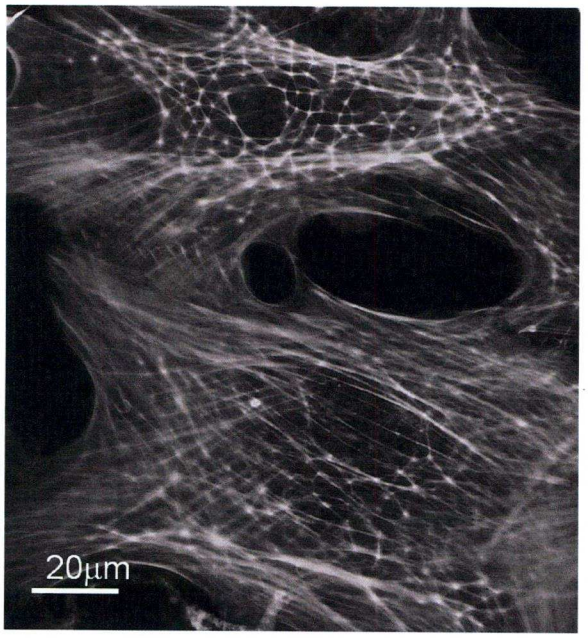

Figure 3.21 Aqueous humor elevates CLAN incidence. Image of a particularly large CLAN in BTM cells following exposure to aqueous humour diluted 1:1 with complete media supplemented with 1% FCS and stained with phalloidin-FITC. Note the pore formation. Source Natalie Pollack.

3.6.6 Unexpected induction of CLANs by decorin.

Decorin is a small leucine-rich proteoglycan that is an inhibitor of TGF-β2 and has been proposed as a negative regulator of TGF-β2 signalling (Yamaguchi et al., 1990). We therefore undertook studies to determine whether decorin was a potential inhibitor of TGF-β2-induced CLANs. On its own however, at low concentrations such as 1ng/ml of decorin produced no effects on the actin distribution patterns; medium concentration 500ng/ml showed no obvious effects on actin, however, high dose decorin 25μg/ml produced quite dramatic effects on the actin arrangement of the cultured BTM cells (figure 3.22). Addition of decorin resulted in 22% and 69% of BTM cells having CLANs at 3 and 7 days respectively compared to vehicle control which only produced 2.2% and 3% at the equivalent time points. Figure 3.22 demonstrates that decorin induces CLANs progressively over time.

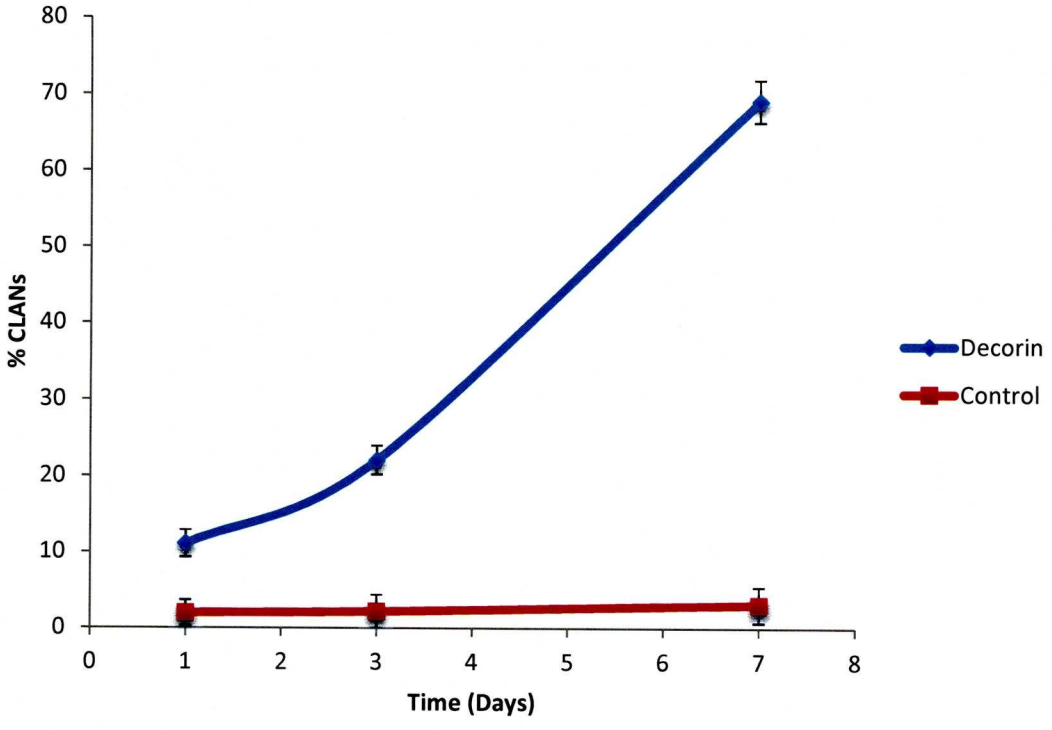

Figure 3.22 Change in CLAN incidence over time after incubation with the proteoglycan decorin or control. BTM cells were incubated with decorin 25µg/ml or control which contained 0.04µM of HCL vehicle for a period of seven days. Decorin induced significant incidences of CLANs at all time points examined compared to control cultures (P=<0.05 compared to control at 1, 3 days; P=<0.0001 compared to control at 7 days). Data presented are the mean ±SD (N=5).

The phenotype of CLANs that is generated by exogenous decorin was identical to DEX, TGF-β2 and aqueous humour induced-CLANs. In common with both TGF-β2 and aqueous humour, there was a small population of decorin-induced CLANs that extended over a large area of the cell. Figure 3.23 shows typical CLANs from decorin incubated BTM cells. This was a surprising result as we initially thought decorin would inhibit CLANs as it is a negative regulator of TGF-β2 (Yamaguchi et al., 1990). To clarify if that was a class effect biglycan another proteoglycan was incubated with BTM cells, however no increase in CLAN incidence occurred above control medium levels at all concentrations examined. Decorin is present in the TM and aqueous humour and often associates with collagen (Tanihara et al., 1995, Wirtz et al., 1997) although its actual concentration is unknown. Few studies have looked at decorin in the TM.

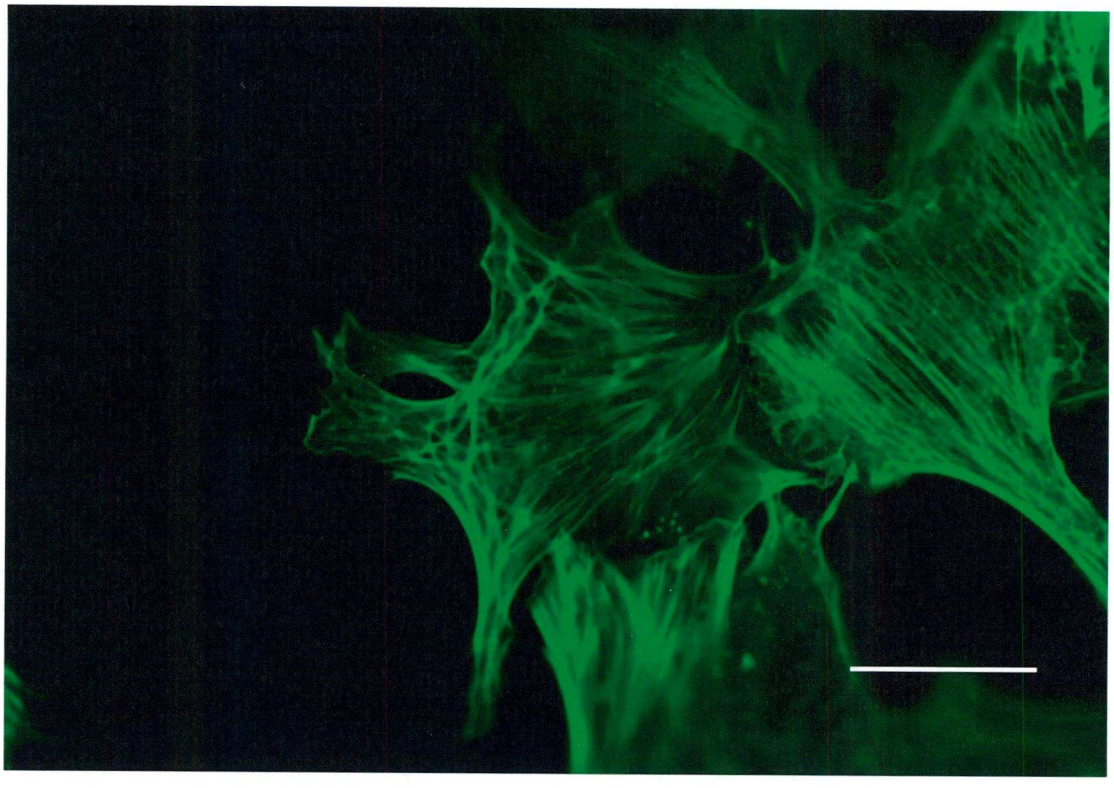

Figure 3.23 Decorin induces CLANs in BTM cells. Image of decorin-induced CLAN in BTM cell after staining for F-actin with phalloidin-FITC after incubation with decorin 25μg/ml for 3 days. The 'hubs' and 'spokes' are clearly evident and the polygonal nature is clear. Note the stress fibre containing cell on the right. Scale bar = 30μm

3.7 Cyclic mechanical strain induces CLANs

3.7.1 Physiological stretch leads to CLANs

The trabecular meshwork as an intact tissue is under mechanical stretch and as such may modulate its cytoskeleton to respond to such biomechanical signals (Tumminia et al., 1998). Thus we sought to determine if cyclic radial mechanical stretching of confluent BTM cells results in induction of CLANs. The hypothesis was biomechanical signals are integrated and transduced into CLANs. Using a Flexcell™ stretching equipment cells were subjected to 10% mechanical strain (1 cycle/1sec) for a period of 12 hours. This stretch regime was chosen to replicate the pulsatile biomechanical forces to which the normal TM is exposed in vivo and 10% mechanical stretch is thought to be physiological (Johnstone, 2004, Coleman and Trokel, 1969). Initial investigations using laminin-coated silicone elastomer revealed that the cells were detaching from the elastomer membranes, where cells where attaching to the substrate they later rounded up and appeared to have elongated cell processes. Further analysis revealed that cells were not viable even when we used laminin coated membranes. Because the silicone is highly hydrophobic and thus proper cell attachment and function would not occur we decided to use fibronectin-coated silicone membranes. Initial investigations determined full cell attachment, with cells being well spread and confluent, with high cell viability (see figure 3.24). Once cells were confluent they remained in culture for 14 days with or without additional incubation of DEX prior to the 10% stretch regime being applied.

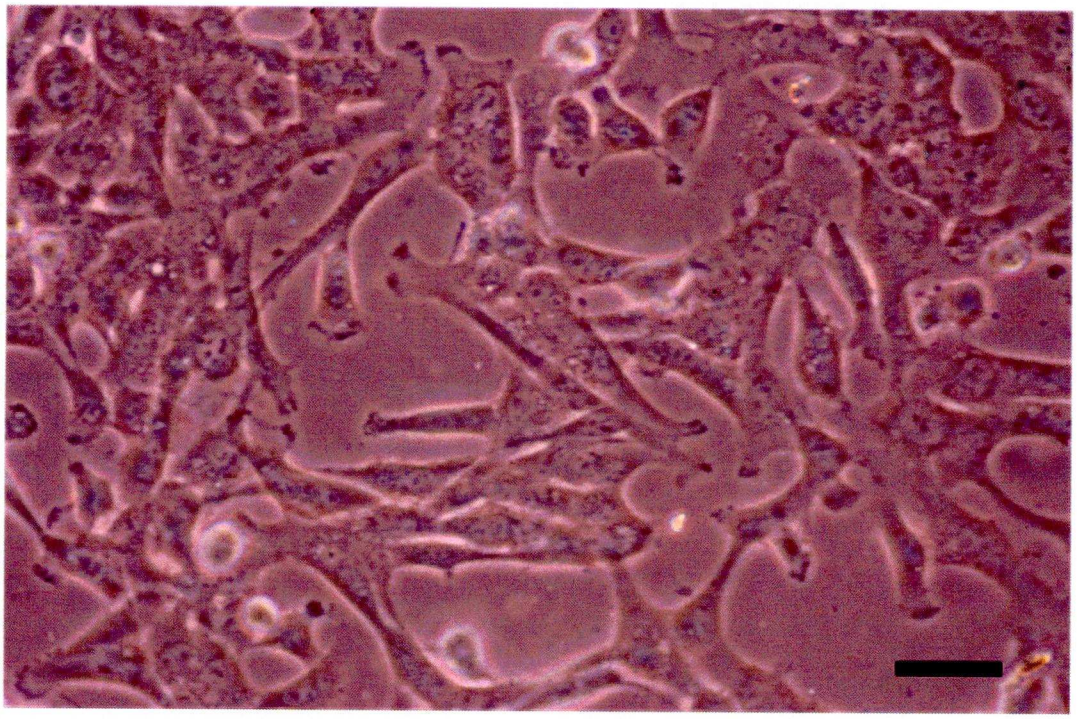

Figure 3.24 BTM cells grown on fibronectin-coated silicone membranes after 24 hours. Phase contrast image shows cells well spread on surface of substrate and pre-confluent. Scale bar = 90μm.

Results of our stretch regime on CLAN incidence reveals that stretch increased CLANs to 40.5% compared to 20% grown on the same substrate and placed in the hold but not exposed to cyclic stretch regime, representing a 100% increase in CLAN incidence compared to un-stretched control (P=<0.01). BTM cells exposed to stretch and pre-incubated with DEX for 14 days resulted in 53% CLANs compared to control this is significantly different (P=<0.01). Cells that were incubated with DEX and were not subjected to stretch (but exact same conditions) the CLAN incidence was 49% CLANs in equivalent cultures that did not receive cyclic stretch. Figure 3.25 shows this upregulation of CLANs by stretch regardless of DEX incubation.

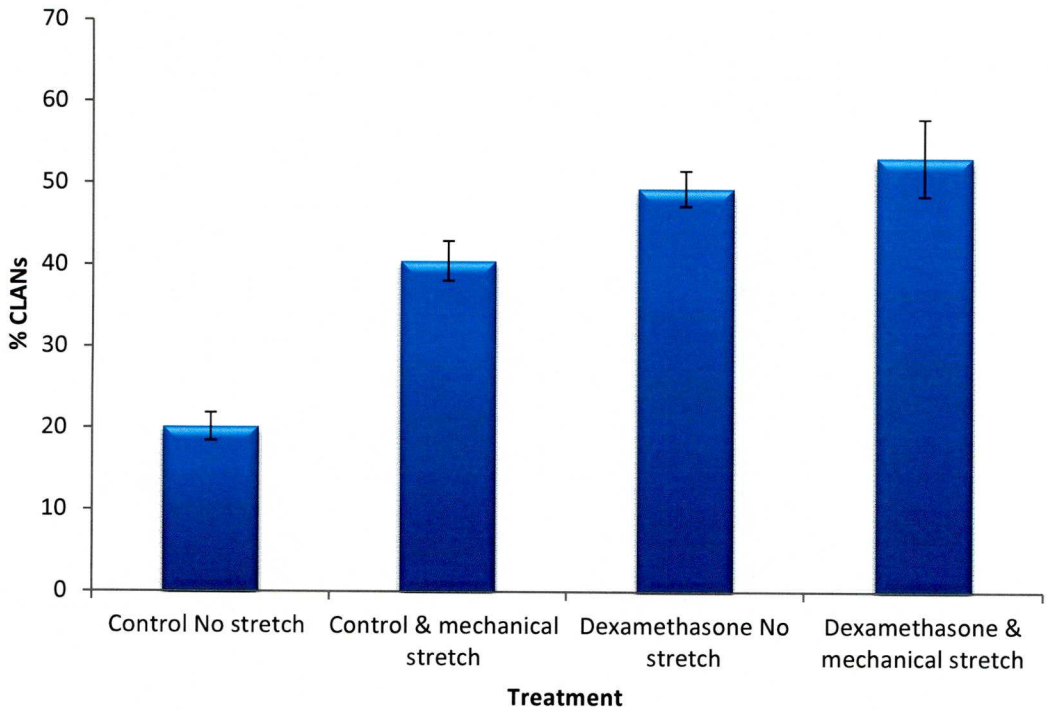

Figure 3.25 CLAN incidence in BTM cells after mechanical stretch regime incubated with or without DEX. Cells were cultured in fibronectin-coated silicone elastomer based flexcell inserts for mechanical stretch, after confluence cells where incubated in the presence or absence of the CLAN inducer DEX 10^{-7}M for 14 days after which the cells where subjected to cyclic mechanical stretch at 10% elongation 1Hz/ 1 sec for 12 hours after which the cells were fixed and stained for actin cytoskeletal rearrangement. It can clearly be seen that cyclic mechanical stretch upregulates CLANs compared to equivalent cultures of non-stretched cells (P=<0.01 ANOVA) There is an increase with DEX and mechanical stretch. Data presented are the mean ±SD (N=5).

Phenotypically these CLANs were similar to DEX, TGF-β2 and decorin produced CLANs, however, they did not appear to span the whole area of the cell and it was not apparent that they were appearing in hotspots or 'clusters'. The conspicuous dominant pattern of actin in the control treated and unstretched membrane was that of stress fibers running along the axis of the cells. However in this unstretched culture CLANs were clearly evident at around 20% of cells containing CLANs comparing this to our usual basal level of CLANs incubated on normal tissue culture plastics (and no matrix substrate) (figure 3.12) of 6.2% CLANs means there is large change in CLAN numbers, therefore indicating that extracellular matrix may play a facilitative role in formation of CLANs at least in vitro (Filla et al., 2006) or the rigidity of the substrate induces CLANs. Such CLANs were present after only 12 hours of stretch suggesting *de novo* generation of CLANs can occur relatively quickly.

General morphological analysis on the culture using phase contrast microscopy after DEX and mechanical stretch revealed that the cells were healthy and with no obvious change in directional cell alignment that has been reported for other cells types (Standley et al., 2002).

3.7.2 TGF-β2 is upregulated in response to stretch

Conditioned media was collected from the cells after the exposure to cyclic mechanical stretch and analysed for TGF-β2 expression. Secreted TGF-β2 was found to be 500pg/ml in control cultures not exposed to mechanical stretch, however mechanical stretch led to an upregulation of TGF-β2 expression in culture medium that was 657pg/ml which was statistically significant (P=<0.05 ANOVA) (figure 3.26). DEX treated membranes not exposed to stretch was 601pg/ml and DEX-

exposed and stretched levels were 556pg/ml. Incubation with DEX and mechanical stretch resulted in less TGF-β2 secretion than DEX alone; however, this was only a small decrease and clearly not significant as figure 3.26 demonstrates.

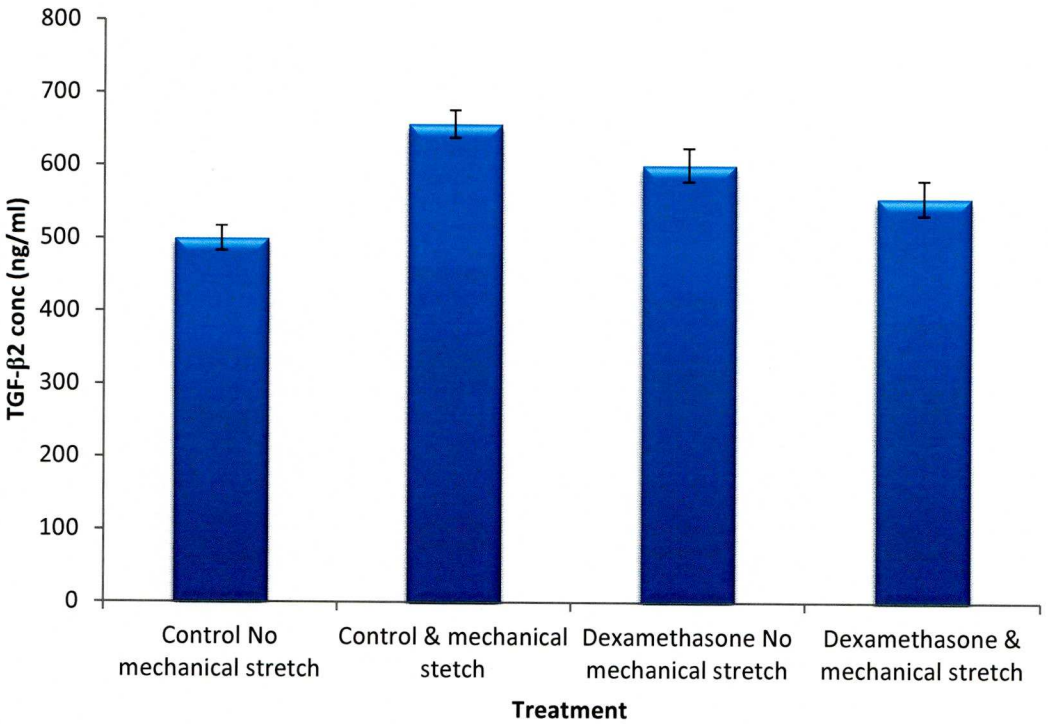

Figure 3.26 TGF-β2 concentrations in conditioned medium taken from BTM cells after exposure to radial mechanical stretch. BTM cells were subjected to cyclic mechanical stretch 10% elongation, 1Hz/sec for 12 hours with or with DEX pre-treatment 10^{-7}M. Data presented are the mean ±SD (N=5). A statistically significant difference is observed between control and mechanical stretch (P=<0.05 ANOVA).

3.7.3 IL-6 quantification

IL-6 is a pleiotropic cytokine that has been speculated to play a role in homeostatic regulation of the TM and of pathological significance (Liton et al., 2005b). We sought to determine is regulation in response to cyclic mechanical stretch. IL-6 was below the limit of detection in the ELISA for control cells not exposed to stretch, however after being subjected to mechanical stretch IL-6 levels were 2488pg/ml and 4351pg/ml with DEX treatment alone and 5842pg/ml with mechanical stretch and DEX treatment (figure 3.27).

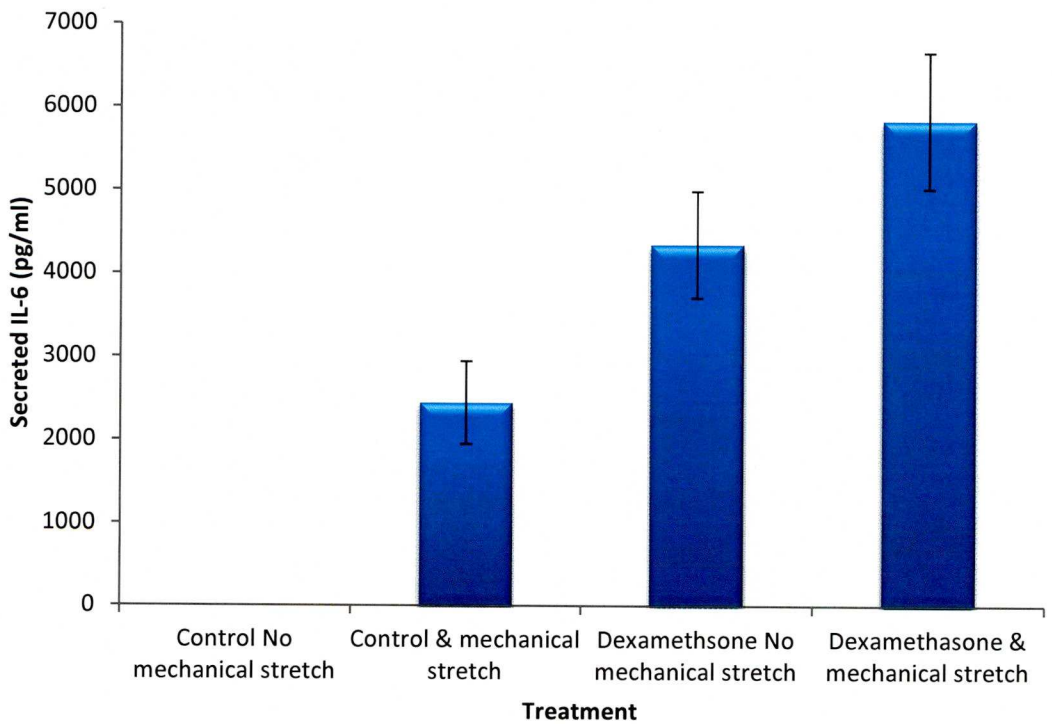

Figure 3.27 IL-6 concentrations in medium after various stimuli. Secreted IL-6 concentration in media from mechanical stretched BTM cells after 12 hours of 10% elongation, 1Hz/sec mechanical stimulation on silicone elastomer. IL-6 was measured using ELISA. IL-6 is seen to be increased after mechanical stimulation (1cycle/sec), DEX alone and no stimulation and DEX and stimulation. Data presented are the mean ±SD. (N=5). Significant differences are between all groups (P=<0.01ANOVA).

The pattern of IL-6 expression was somewhat different to that of TGF-β2 secretion into the media with a large increase in expression after both DEX treatment and mechanical stretch, both known to increase CLAN numbers. It has been suggested that there is cross-talk between TGF-β and IL-6 in human TM cells and this could be the case here (Liton et al., 2009). No study to date has looked at the association of DEX/CLANs and IL-6 expression.

3.7.4 IL-1β quantification

IL-1β has been shown to play a role in mediating changes in the outflow system both ex vivo and in vitro (Hosseini et al., 2006) so we therefore examined this cytokine after cells had been subjected to cyclic mechanical stretch in vitro. Figure 3.28 shows that basal levels of IL-β were 27.2 (SD 9.4) pg/ml and an increase of over 400% was demonstrated after 12hrs of stretch that was statistically significant (P=<0.01). Interestingly significant increases were observed with DEX exposure and not stretched (554% increase). A huge increase in IL-1β was seen of over 780% with DEX exposure and cyclic mechanical stretch suggesting a synergistic effect.

Using RT-PCR arrays we found that compared to control untreated IL-6 mRNA was 2.5 fold elevated with both DEX and TGF-β2 exposure (n=2). Therefore, demonstrating a common target gene of both inducers. Unfortunately none of the other 83 TGF-β BMP pathway target genes were significantly altered in this array at this time point. We could not do this for BTM stretched cells though.

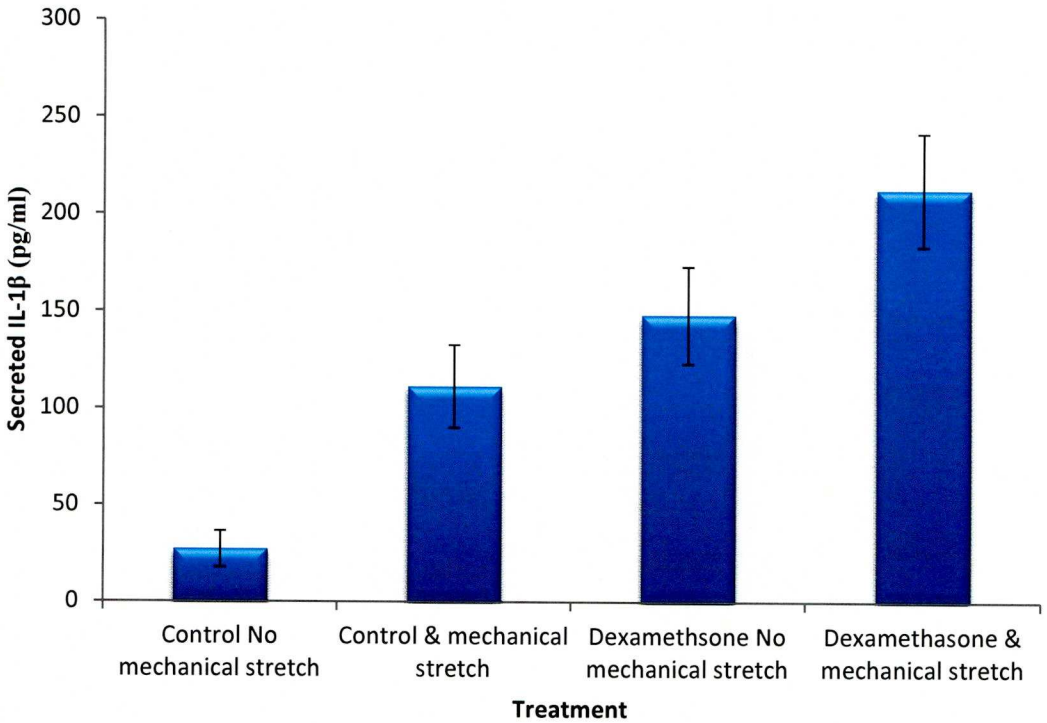

Figure 3.28 IL-1β concentrations from BTM cell conditioned medium. BTM cells were cultured on silicone elastomer plates pre-incubated with or without DEX 10^{-7}M prior to exposure to cyclic mechanical stretch 10% elongation, after 12 hrs the media was collected and analysed for IL-1β content using ELISA. There is a clear upregulation of IL-1β after mechanical stretch alone, DEX, or DEX and mechanical stretch. Data presented are the mean ±SD (N=5).

3.7.5 Hsp70 expression

Hsp70 is among the most abundant intracellular proteins and is one of the most highly conserved genes. However, they are induced by a variety of cellular insults such as heat shock, oxidative stress, hypoxia/reoxygenation and also biomechanical stress. We therefore determined the Hsp response mediated by mechanical stress in vitro. Previous work has only noted hugely increased expression of Hsp 70 mRNA in TM cells after mechanical stretch (Luna et al., 2009). However mRNA levels do not necessarily reflect post-transcriptional protein levels. Western immunoblots indicated that BTM cells do indeed contain Hsp70 in addition also display elevated intracellular levels of Hsp70 in response to cyclic mechanical stretch (figure 3.29). Constitutive levels of Hsp70 in control untreated cultures was just identifiable, a positive control of recombinant Hsp70 was also ran to clarify it was Hsp70, this migrated at the correct molecular weight of 70kDa.

This is the first demonstration of Hsp70 protein levels in the TM of any species after mechanical stretch. A previous study identified Hsp70 as differentially expressed after mechanical stretch using gene arrays in human TM cells (Luna et al., 2009). They also validated using RT-PCR after a candidate gene approach; however they did not check the protein Hsp70 levels.

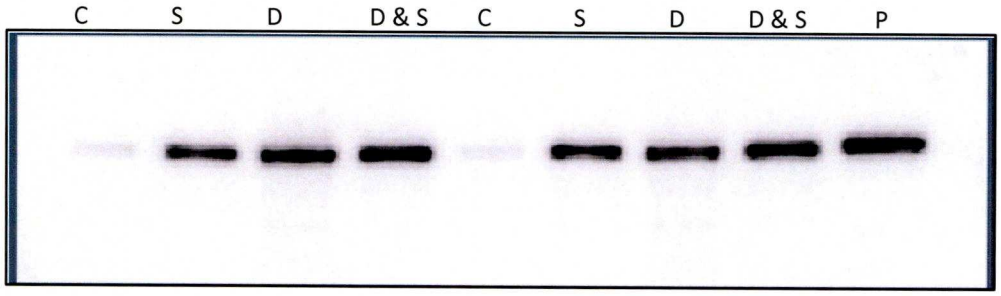

Figure 3.29 BTM cells express Hsp70 protein and is highly induced by cyclic mechanical stretch. Representative immunoblot of Hsp70 from BTM cells that were cultured on fibronectin coated silicone elastomer plates after which they were incubated with or without DEX 10^{-7}M for 14 days and subsequently exposed to 10% elongation cyclic mechanical stretch for 12 hours. BTM cells were lysed and total protein determined and 25µg of protein lysate was loaded into each well ran on a 10% PAGE and immunoblotted onto a membrane and subsequently probed with anti-Hsp70 antibody. C Control, S stretch D Dexamethasone D&S Dexamethasone & stretch. P positive control was recombinant Hsp 70. The immunoblot shown is from two independent experiments. No loading control could be performed as GAPDH could not be identified.

3.7.6 Downstream signalling activation

After determining that cytokines were elevated from BTM cells that had been subjected to cyclic mechanical stress and also DEX exposed cultures that had not been exposed to stress but contain CLANs, we decided to check the activation of the critical transcription factor Nuclear Factor Kappa-β Nf-kβ) as a downstream activator of such cytokines. Nf-kβ is a central transcription factor that when activated, the phosphorlylation of its constituent subunit p65 (RelA), leads to dissociation from IKBα and translocation from the cytoplasm to the nucleus. Using immune blotting techniques it was shown that the p65 subunit of Nf-kβ was highly phosphorylated after 12 hours of cyclic mechanical stretch as figure 3.30 shows. Note that DEX alone also leads to Nf-kβ phosphorylation.

Thus activation through cyclic mechanical stretch leads to elevated transcriptional activator Nf-kβ subunit that likely accounts for the increased expression of the cytokines that may induce CLANs in a cellular autocrine manner.

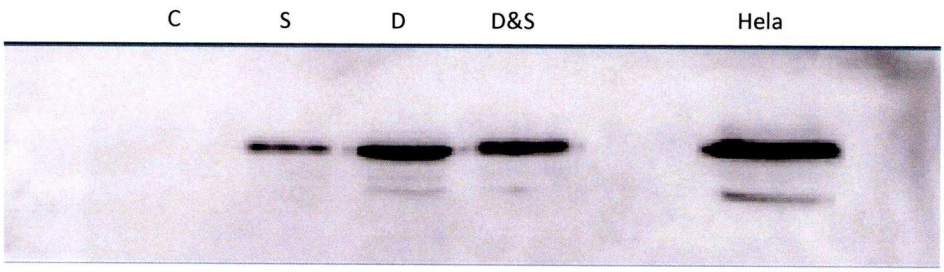

Figure 3.30 BTM cells express phosphorylated Nf-κB p65 subunit. Representative immunoblot of phospho-p65 from BTM cells that were cultured on silicone elastomer membranes and subjected to stretch, DEX alone or DEX & mechanical stretch after which they were lysed. 25μg total protein loaded and subjected to standard immnoblotting techniques. C Control, S stretch D Dexamethasone D&S Dexamethasone & stretch. Hela cell lysate was run as a positive control for Nf-kβ p65 phosphorylated. It is clear that stretch induces phosphorylation as does DEX alone or DEX plus mechanical stretch.

3.7.7 TGF-β2 and mechanical stretch

In totally separate experiment cells were pre-treated with the CLAN inducer TGF-β2 for 14 days before exposure to the same stretch regime as described. Results indicate that stretch alone resulted in 41% CLANs, however pretreatment with TGF-β2 resulted in 66% CLAN containing cells which is significantly different compared to control unstretched cells (P=<0.05) (figure 3.31). This is a significant difference compared to control. However, incubation with TGF-β2 and not receiving mechanical stress resulted in an incidence of 63%. There is a small difference between TGF-β2 preincubation and stretch and TGF-β2 alone however this is not significant.

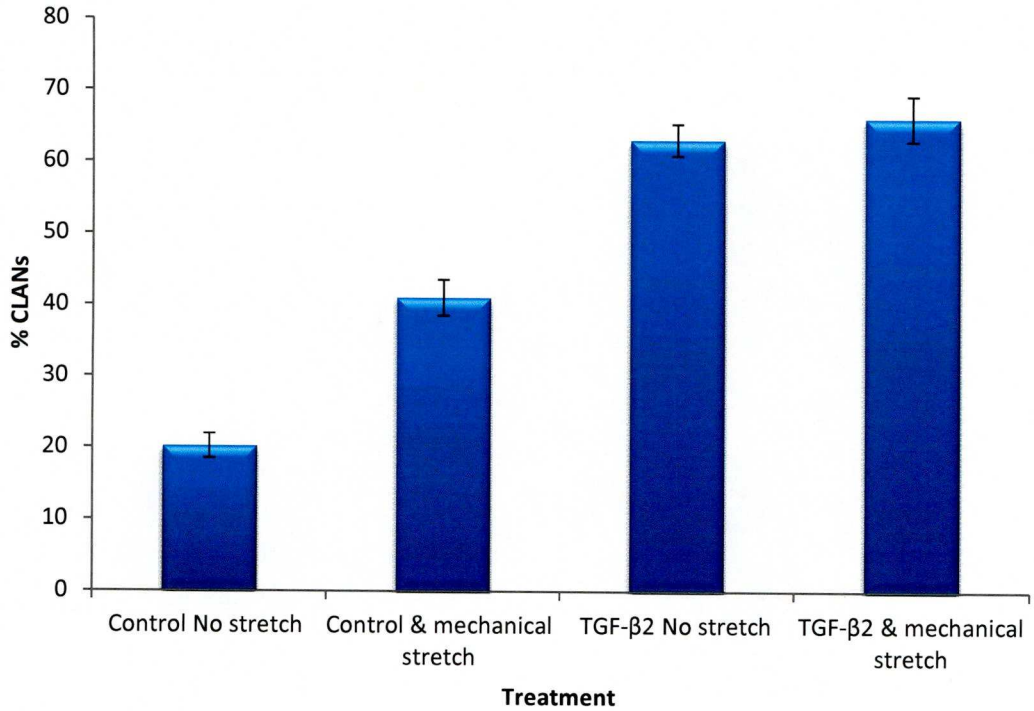

Figure 3.31 CLAN incidence in BTM cells after mechanical stretch regime incubated with or without TGF-β2. Cells were cultured on fibronectin-coated silicone elastomer based flexcell™ inserts for mechanical stretch, after confluence cells where incubated in the presence or absence of TGF-β2 for 14 days after which the cells where subjected to cyclic mechanical stretch at 10% elongation 1Hz/ 1 sec for 12 hours. The cells were fixed and stained for F-actin cytoskeleton rearrangement. TGF-β2 does not increase mechanical stretch induced CLANs (P=<0.01) Data presented are the mean ±SD (N=5).

3.8 Morphological interrogation of CLAN-containing cells

3.8.1 CLAN containing BTM cells display an altered morphological phenotype.

It was evident that all our stimulants of CLAN formation caused some level of shape change in the cultures exposed to the CLAN stimuli. A question arose as to whether BTM cells containing CLANs were at all different in appearance from those cells rich in stress fibres and whether there was any relationship to the cell-shape changes produced by our CLAN induction agents. Two investigations were conducted on pre-confluent BTM cultures specifically to test whether or not CLAN-containing cells could be predicted on the basis of how they looked. Pre-confluent BTM cells were grown on multi-well glass-bottomed plates and exposed either to DEX, TGF-β2 or decorin to induce CLAN formation. The cells were then fixed and after staining with phalloidin to identify F-actin, fields were photographed initially by fluorescence and subsequently the exact same fields were re-photographed to obtain phase contrast images. Selection of fields was always done in fluorescence mode and based on the presence of a cell with a CLAN or a cell with clear stress fibres only. Almost invariably in BTM primary cultures, even when comparing those established from different eyes and at different passage number, three distinctive cell appearances were identified by phase contrast microscopy that we called spindle (an elongated polarised form), epithelioid (a flat, rounded cell) and kite shaped cells (polarised with a distinct triangular head, polygonal). Figure 3.32 illustrates the idealised cells. After treatment with DEX, TGF-β2 and the proteoglycan decorin the incidence of spindle (40%) and epithelioid (40%) were much the same but each was twice as abundant as kite shaped cells (20%).

Pairs of digitised images were examined and in fluorescence mode a cell was selected solely on the basis of the phalloidin staining showing a cell with clear-cut obvious stress fibres but clearly no CLANs. We then alternated to phase contrast and if the boundaries of the cell were clear a mouse cursor was taken round the cell margins and the measurement parameters recorded. At this point we categorised the cell as belonging to one of the three identified forms. Subsequently the libraries of paired digitised were reassessed, this time the selection was for the presence of a CLAN within a cell and, as we already knew that CLANs can co-habit with stress fibres, the presence or absence of prominent stress fibres was not an influential part of this selection. Again after selecting the cell it was drawn around in phase contrast mode and classified into one of the three identified shapes.

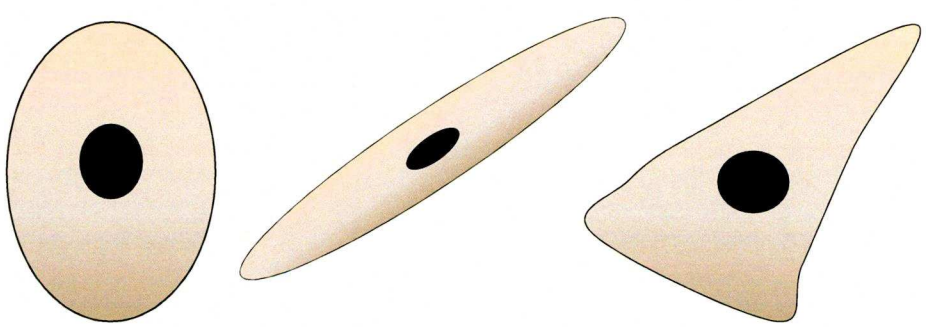

Figure 3.32 Idealised shapes of BTM cells. The cartoon depicts the idealised shapes of the three types of cells we categorised the BTM cells as being in on the left is the epithelioid cell, in the middle the spindle shaped cell and on the right hand side of the cartoon is the kite shaped cell.

Figure 3.33 illustrates that CLAN containing cells have a different phenotype to non-CLAN containing cells. BTM cells that are kite shaped are just as likely to have stress fibres as they are to have CLANs so neither actin arrangement is a predictor of this cell shape. However, BTM cells containing stress fibres tend predominantly to

be spindle shaped whereas those cells with CLANs tend primarily to be epithelioid (figure 3.34). Intriguingly the pattern is repeated remarkably consistently irrespective of whether the CLAN inducing agent is DEX, TGF-β2 or decorin. As might be expected from the results of our classification findings, image analysis showed that CLAN-containing cells were significantly more rounded (0.63) (a circularity of 1 indicates a perfect circle, as the value approaches 0.0 it indicates an increasingly elongated polygon) than stress-fibre only containing cells for each of the CLAN inducing agents used in this part of my investigation (P=<0.01) figure 3.35. Therefore this added a level of support to the concept that CLAN-containing cells tend to be rounded, although the data was less dramatic. Indeed another parameter measured was total area of the BTM cell and this was found to be increased in CLAN containing/epithelioid cells.

The previous data indicated epithelioid shape was highly indicative of the presence of a CLAN but there were non-epithelioid BTM cells that had CLANs and some epithelioid (not many) cells did express a stress fibre pattern of actin only so round flat cells were not entirely specific. The decorin exposed cells exhibited the highest incidence of epithelioid cells with CLANs (79.2%) and the lowest incidence of epithelioid cells with clear prominent stress fibres only (5.9%) whereas DEX was slightly weaker with 70.4% of epithelioid cells containing CLANs and 9.7% with stress fibres but definitely devoid of CLANs. Thus cellular shape of BTM cells may be used a predictor of CLAN-containing cells.

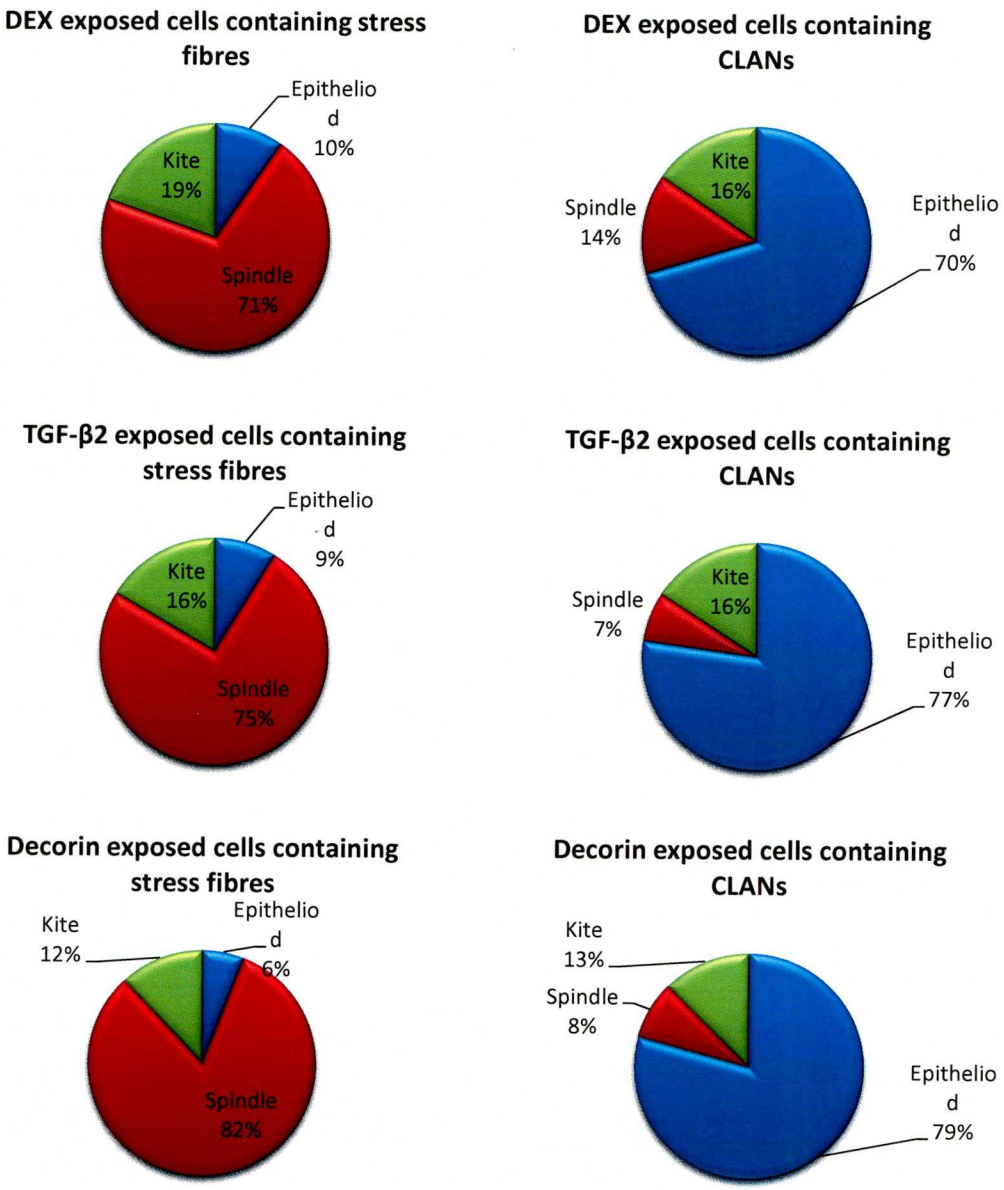

Figure 3.33 CLAN induction mediates altered morphology. Following classification into three distinct groups based on shape of BTM cells after stimulation with the three different types of CLAN inducers it was found that, irrespective of the CLAN-inducing agent used, CLAN-containing cells displayed a more epithelioid morphological phenotype. BTM cells which contained stress fibres were spindle shaped. Analysis was on at least 100 cells.

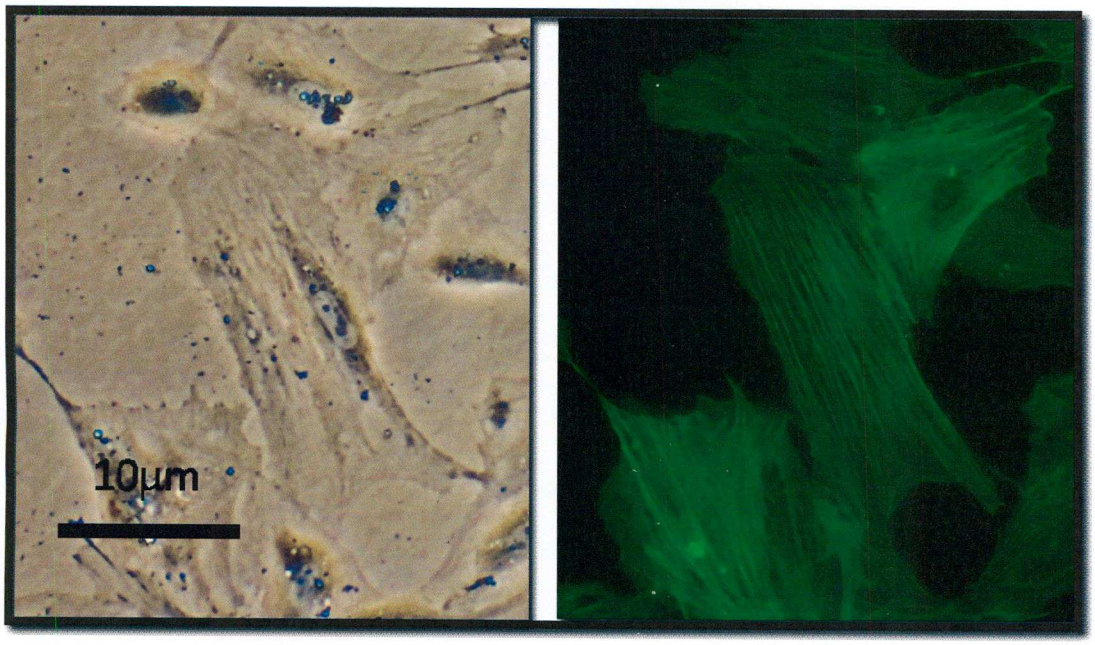

Figure 3.34 Representative image of stress fibre-containing BTM cell in both phase and fluorescence in the same field of view. This image is a BTM cell that in fluorescence mode (right) contains clear cut stress fibres running parallel and switching to phase contrast mode it is clear that the same cell is spindle shaped (left). The cell nucleus is clear on the phase contrast image. This was a common pattern throughout the experiments.

3.8.2 Imaging reveals divergent shifts in phenotype

A further study was conducted using phase contrast time-lapse imaging to follow the BTM cells for 20 hours after treatment with CLAN inducing agents, prior to fixation and staining with phalloidin. Within the filming period most BTM cells maintained their cell shape throughout however, it was clear that a large proportion of cells changed shape from spindle to epithelioid or epithelioid to spindle. This held for all our CLAN stimulants so arbitrarily we chose to follow the lineages of 100 cells from a DEX treatment experiment to test these qualitative impressions. The cells were selected on the basis that their end fluorescence staining was clear, their appearance was easy to class and they could be followed without confusion for the entire filming period. We had 20hour traced histories on 55 epitheliod-shaped cell, 31 spindle and 14 kite (based on appearance at the termination of filming). Whereas most of the epithelioid appearing BTM cells remained in that form throughout filming (87.3), the other 2 were less constant with 58.1 spindle cells being without change and hardly any (14.3%) kite-shaped cells. The kite shape appeared to be an intermediate that formed when epithelioid was changing to spindle and vice versa. It was also a form adopted by a mobile BTM cell when it changed direction or came to an abrupt halt. Within confluent areas of cells the constituent BTM cells usually maintained a stable shape during the 20 hours of filming. It was in the in the pre-confluent areas where the cells were more dynamic both in terms of shape-change and clearly in terms of cell movement. Even in low serum containing media we observed cell division particularly in the pre-confluent areas. It was observed that subsequent to cell division, daughter cells did not contain CLANs or stress fibres but had a peculiar perinuclear halo of intense fluorescence.

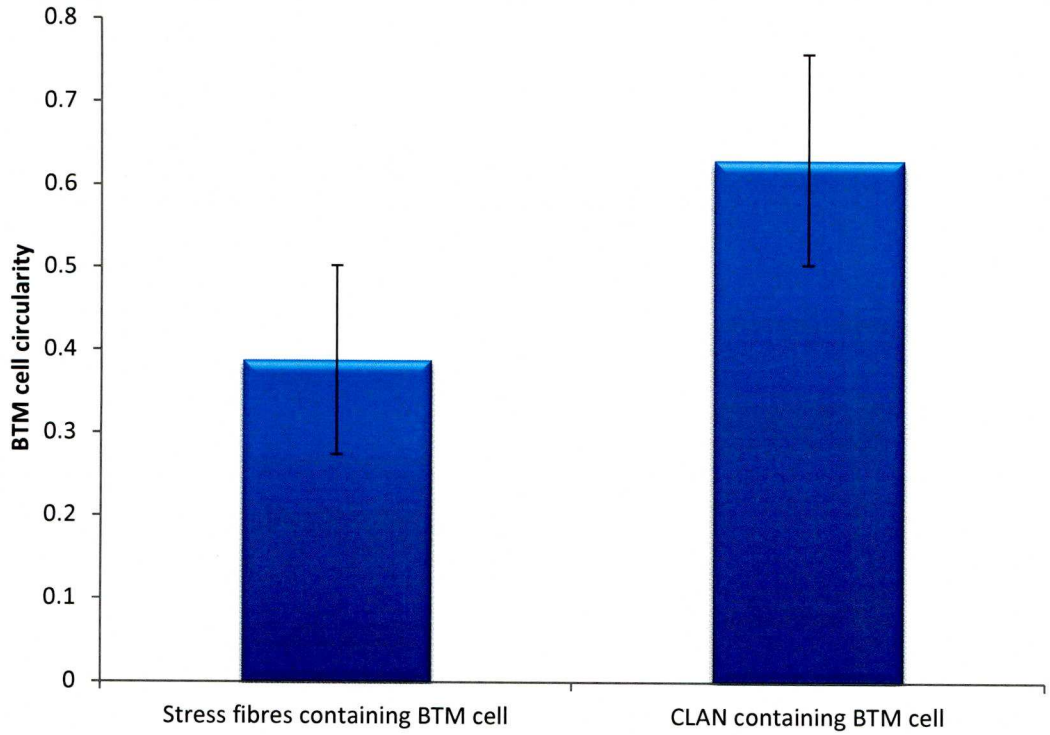

Figure 3.35 Circularity of BTM cells exposed to CLAN inducers. BTM cells were exposed to a variety of CLAN inducers and after fixation of F-actin visualisation for actin were measured detailed in methods and circularity calculated with Image J software using the formula: $4\pi(\text{area}/\text{perimeter}^2)$. Data are mean and SD (N=100) Circularity is a dimensionless unit.

Regardless of which CLAN-inducing stimulant was used, it was obvious from the time-lapse examination that individual BTM cells showed a wide range of mobility in the pre-confluent parts of the cultures that ranged from stationary (S) to highly mobile (M****). An arbitrary scale for locomotion was employed where S was a cell that could undergo shape change or ruffling but moved less than a cell length in 20 hours. M* cells moved a 4μm/hour or less, M** reached up to 12μm/hour, whereas above that M*** cells were faster still and some could reach a movement rate of 25μm/hour for short periods. We labelled cells that moved extremely quickly M****, an exceptional event in the cultures, irrespective of treatment, but these rapid cells on phalloidin staining exposed a diffuse actin pattern and never expressed CLANs or stress fibres in their cytoplasm. Analysis of the 100 cell-time-lapse DEX-exposed series started with the phalloidin immunofluorescence and was entirely in line with earlier observations that the CLAN structures were predominantly associated with epithelioid cells and the other pattern of actin arrangement, stress fibers, were restricted to spindle shaped cells. 58.8% of the 51 epithelioid cells containing CLANs that were followed, were classified as being stationary and the rest (41.2%) were mobile, just about (M*). However the spindle shaped cells only 10.7% were stationary and, of the rest, 20% were M*, the majority were rather mobile (M**) and a number (15.3%) were M*** Table 3.1.

CLAN containing epithelioid BTM cells clearly appeared to have a fairly rigid and non-malleable cytoplasm and they tended only to undergo shape alteration if they had contacted another cell or a mass of cells. Spindle shaped cells underwent sliding and stretching constantly and even when not travelling large distances they altered their shape and stretched backwards and forwards. Within confluent areas of the culture epithelioid cells would ruffle whereas the spindle shaped cell undertook

polarised elongation and retraction all the time. It also appeared that epithelioid cells with rare stress fibres and devoid of CLANs were all highly tractable; while spindle shaped cells containing CLANs were stationary. Only a small number of kite shaped cells were followed and among these only 5 cells contained CLANs in their cytoplasm of which 2 were stationary and 3 mobile whereas 9 had stress fibres and all of these were mobile including 3 that had been graded at M*** level. These observations indicate a functional deficit in CLAN containing cells, at least in vitro.

Table 3.1 Morphological correlation with actin patterning in BTM cells.

		Cell shape and actin arrangement present					
		Epitheloid		Spindle		Kite	
		CLAN	Stress Fiber	CLAN	Stress Fiber	CLAN	Stress Fiber
Movement level	Stationary	31	0	1	3	2	0
	M*	20	3	1	6	3	4
	M**	0	1	0	15	0	2
	M***	0	0	0	5	0	3
Total cells		51	4	2	29	5	9
Overall total		55		31		14	

BTM cells were induced with DEX to produce CLANs in a percentage of cells after which the cell were monitored using phase contrast time lapse photography for a time period of 20 hours. The movement levels of the cells were arbitrarily assigned a code according to the mobility on culture. It is clear stress fibre containing cells are more mobile in cultures compared to CLAN containing cells. (N=100).

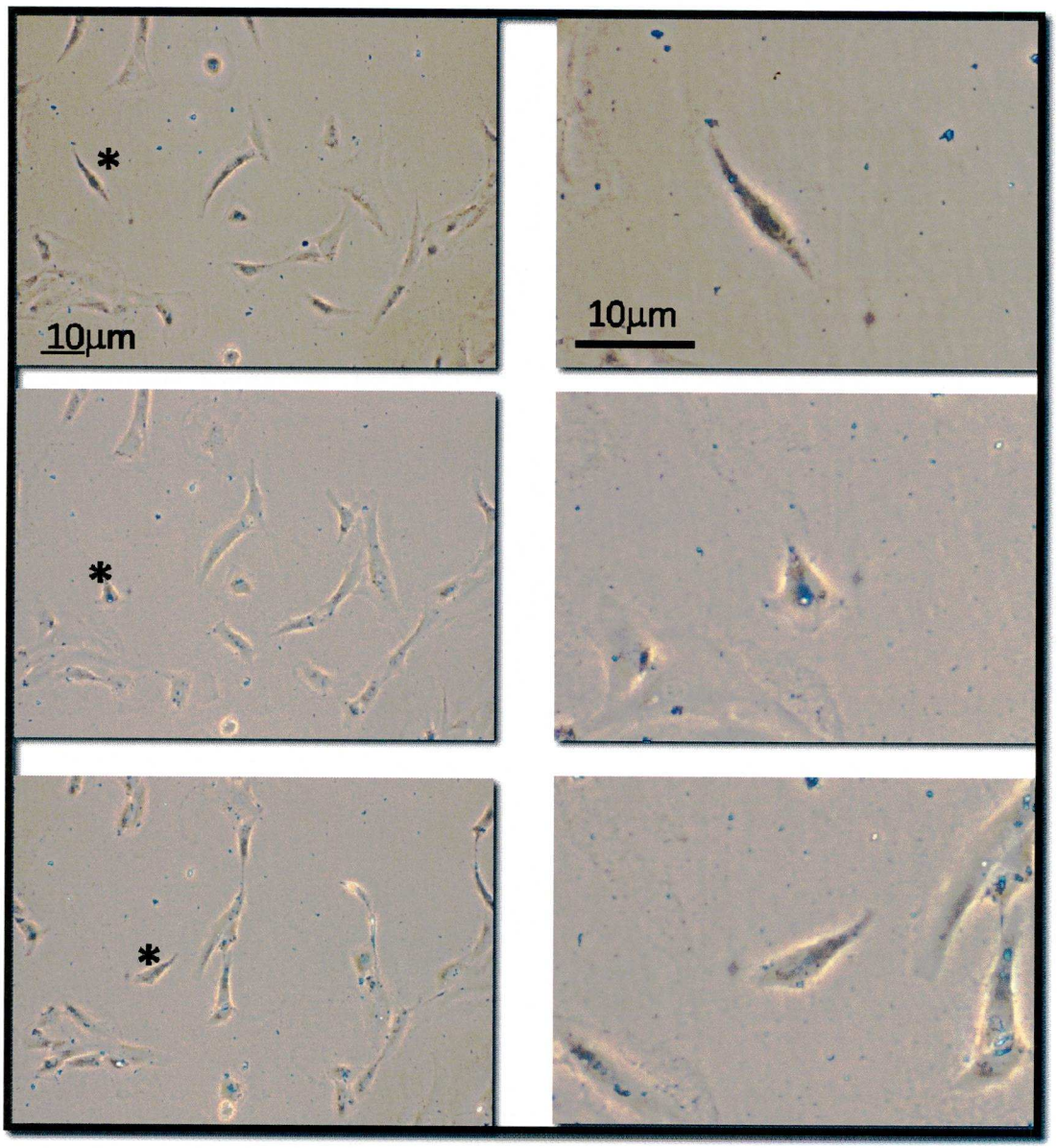

Figure 3.36 Spindle shaped BTM cell in culture. Time lapse cinematography demonstrates that a spindle shaped category of BTM cell is highly mobile in vitro showing a high level of pliablilty. The panels on the left show the cell (*) over time and the right hand panels show the same cell at higher mag. Each image is 20 minutes apart. Actin drives the motility.

3.9 PAAs Vs CLANs

As stated in section 1.0 CLANs are found only in confluent cultures of TM cells. Similar structures have been observed in other cells as a precursor to stress fibre formation (Lazarides, 1976, Ireland and Voon, 1981) and we have termed these similar structures Polygonal Actin Arrangements (PAAs). PAAs may have height as a property. A key argument in the literature is whether the transient PAAs seen in freshly plated cultures after being removed from their substrate with agents such as trypsin and CLANs, usually defined as in confluent cultures are the same thing. Or are the polygonal PAAs described in the literature an earlier manifest of CLANs in culture?

To examine this further we trypsinised BTM cells from their substrate and resuspended them in culture and fixed and stained the for the F actin distribution. This 'settling' experiment revealed spectacular polygonal arrangements of actin in the cells cytoplasm that involved much of the area of the cell (figures 33.7-3.38). These PAA 'CLAN-like' structures were more 'dome like' and appeared to have height as focussing through the cell some hubs and spokes within the same cell were in focus and other hubs and spokes not. Although this is in 2D imaging and confocal Z-stacking through a single cells was not possible with the confocal microscope they had the appearance of having height. These polygonal arrangements are striking and appear very similar to structures observed elsewhere (Filla et al., 2009, Filla et al., 2006). These structures have been described as CLANs, however, they may not be phenotypically the same thing and their numbers diminish over time in culture. After 12 hours these temporary geodesic structures have diminished and the majority of cells contain stress fibres. Upon pharmacological induction they then express CLANs. It is totally possible that they are CLANs and are just an acute version of the

same thing after mechanical disturbance and upon exposure to a CLAN inducing agent they then express CLANs. As outlined in section 1.0 CLANs are defined as being in confluent cultures of TM cells. Height is not a defining criterion.

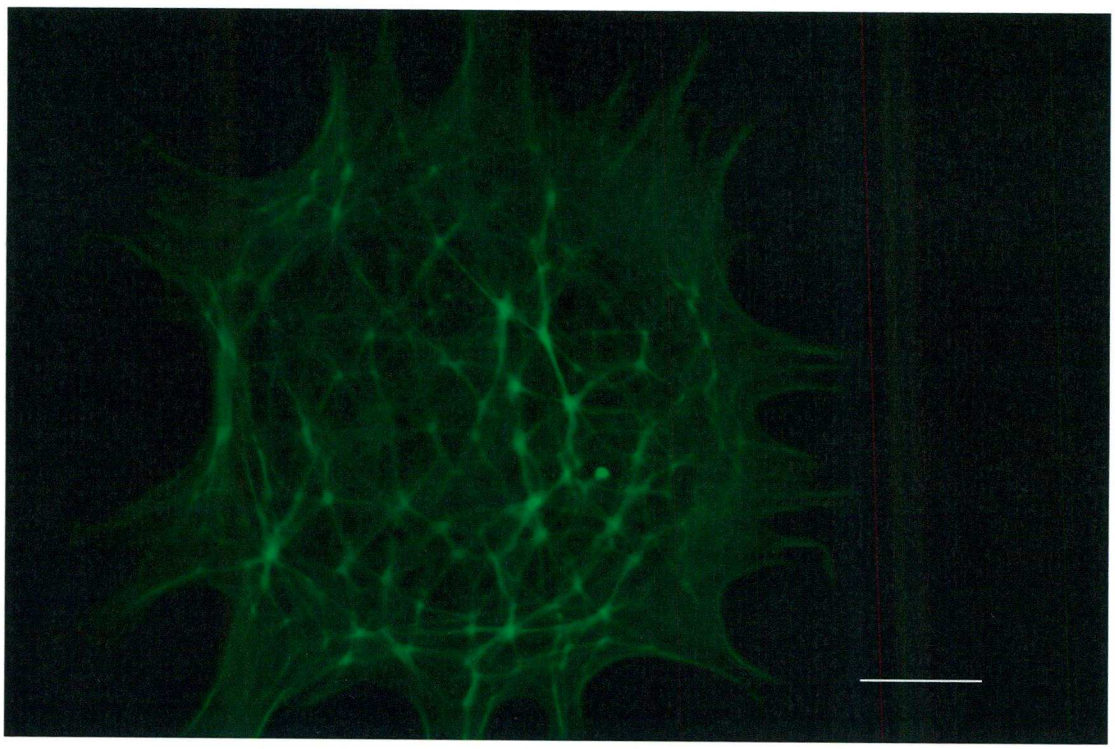

Figure 3.37 A spectacular PAA in an isolated BTM cell in culture. The BTM cell was previously trypsinised from tissue culture plastic and seeded onto a plastic substrate to settle after three hours of adherence to the underlying substratum the cell was fixed and stained for F-actin and imaged using fluorescent microscope. Scale bar= 10μm

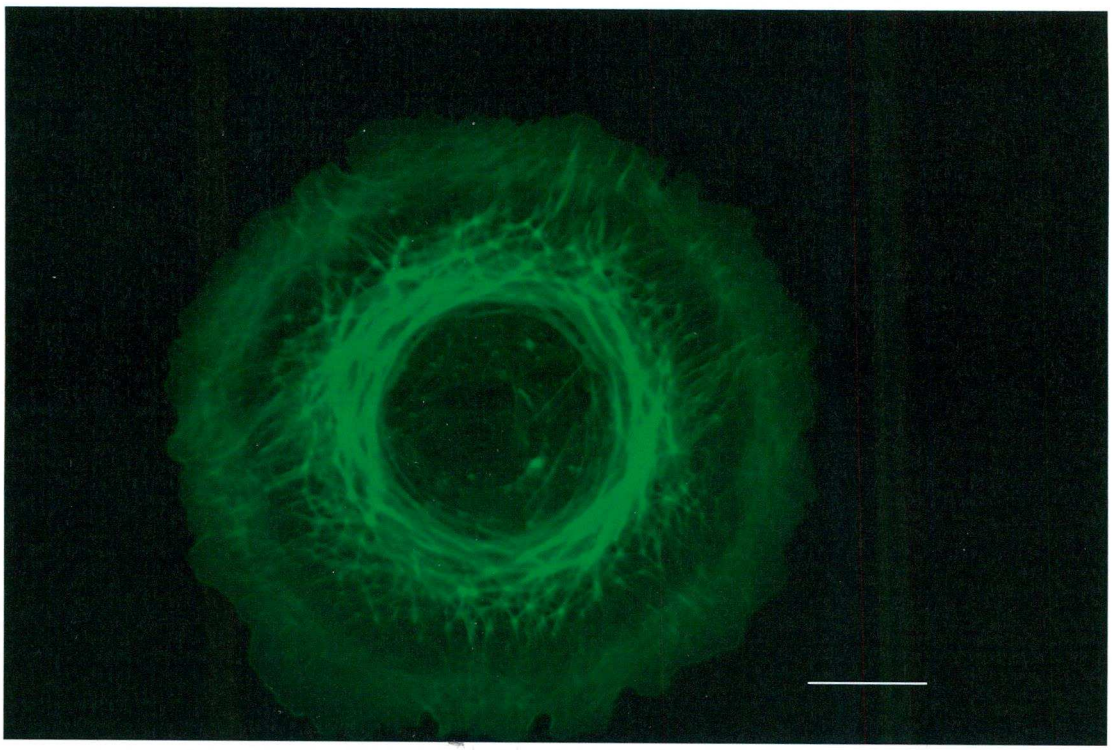

Figure 3.38 PAAs are common in early culture. A PAA in an isolated BTM cell after five hours adherence subsequent to trypsinisation and stained for F-actin arrangement. Small hubs and spokes are evident that are polygonal and encircle the nucleus of the cell. Scale bar = 10μm

4. Discussion

The TM is a smooth muscle like tissue exhibiting marked contractile properties both in vitro and in vivo (Lepple-Wienhues et al., 1991, Wiederholt et al., 2000, Rosenthal et al., 2005a). This contractile property is displayed both in human and BTM cells (Thieme et al., 2001). This cellular contraction is thought to regulate the aqueous humour outflow of the chamber angle and thus modulate IOP (Wiederholt et al., 2000). As such any dysregulation of the normal contractile function of the TM cells would have a profound effect on outflow facility and hence IOP. The actin cytoskeleton performs a vital part of the contractile apparatus of the TM cells both in vitro and in vivo and this is demonstrated profoundly by the addition of cytoskeletal disrupting drugs modulating contraction and functional competence (Cai et al., 2000, Johnson and Tschumper, 1993). CLANs are polygonal actin structures that have been demonstrated in the TM of both human and bovine cells, both in vitro and in situ (Clark et al., 1994, Wade et al., 2009). *It was hypothesised by us that the presence of CLANs in the cytoplasm will affect the contractility of BTM cells.* The use of BTM cells as opposed to human TM cells is better as they have a predisposition to the formation of CLANs and therefore serve as a useful model for the interrogation of functional effects. The first part of this study demonstrated, using an established in vitro model of cellular contraction to mimic the complex in vivo environment; that cells exposed to the CLAN inducer DEX exhibited a significant inhibition of cellular contraction when incubated in 2D gels and not 3D gels, except at day 5 (figure 3.5). There was more than 50 and 70% inhibition of contraction at days 5 and 7, respectively. Furthermore it was demonstrated that contraction-inhibited collagen matrices contain CLANs, whereas the normally contracted matrices predominantly contained stress fibre encompassing cells. However, it was difficult to quantify

CLAN-containing cells in the 3D collagen contracted matrices due to technical difficulties with regards to the imaging. The difference in inhibition between the two types of contraction models may relate to differences in their mechanism(s) of contraction. It may be that in a 3D arrangement of cells within a collagen matrix stress fibre induction predominates whereas in a 2D cell arrangement CLAN formation by appropriate stimuli is favoured (Ehrlich et al., 1989). Such an interpretation needs further exploring but it predicts that a stimulus that promotes stress fibre formation in a 3D arrangement would produce vigorous collagen matrix contraction while in 2D the induction of CLANs is associated directly or indirectly with the inhibition of matrix contraction. DEX administration to human skin fibroblasts has been shown to reduce the contractility of fibroblasts in the collagen matrix assay and this is largely irreversible (Coulomb et al., 1984). Also DEX exposure significantly reduces an actin-dependant process in TM cells: phagocytosis (Zhang et al., 2007). It is also possible DEX is altering MMP levels and thereby affecting the remodelling of the collagen matrix.

In vivo TM cells are in a 2D environment resident upon the collagenous beams (see section 1.3). These beams are composed of collagen but also elastic fibres upon which the contractile TM cells reside and form cell-cell interactions (Lutjen-Drecoll et al., 1981). Thus the 2D collagen matrix contraction system employed here is a more realistic recreation of the in vivo environment. In vivo TM cells also express gap junctions. Gap junctions are plasma membrane microdomains comprised of assemblies of channel proteins. These channels that are formed allow the passage of ions and small molecules up to ~1000Da (Kumar and Gilula, 1996). Hence small informational molecules facilitate communication between neighbouring cells. The principal structural component, the membrane protein connexin, forms the connexon.

Six connexins form one connexon, which traverses the plasma membrane of one cell and docks with the connexon of the other giving rise to a transmission pore. Recently pannexins have also been discovered to be integral proteins in gap junctions (Panchina et al., 2000). DEX has been shown to modulate gap junctions in vitro and also cell size in human TM cells (McCartney et al., 2006) and express the main junctional protein Cx43 (Kimura et al., 2000). Furthermore, a recent study demonstrated alterations of the integral gap junctional protein Cx43 and CLANs in glaucomatous human TM cells, although, they did not demonstrate any functional correlation (Zhuo et al., 2010). It is now known that there are many junctional protein interacting proteins; indeed it has been shown that Cx43 directly binds α- and β- tubulin and thereby alter their properties (Giepmans et al., 2001). Indeed the actin binding protein developmentally-regulated brain protein (drebrin) has been shown to be a binding partner of Cx43, thereby coupling gap junctions to the cytoskeleton (Butkevich et al., 2004).

Knockdown of drebrin results in impaired cell-cell coupling (Butkevich et al., 2004); drebrin binds both F-actin and facilitates the recruitment of other actin related proteins. Cortactin, another actin binding protein promoting nucleation, has been shown to interact with Cx43 and alter junctional formation in seminiferous epithelium (Vitale et al., 2009). Given that DEX is known to alter gap junctions in both normal and glaucomatous cells and that this is coupled to the cytoskeleton it could be that CLANs are generated through this pathway. Future work could examine the role of connexins in linking cytoskeletal rearrangements in TM cells. Contraction of TM cells and many other cells is dependent on an intact actin cytoskeleton and primarily stress fibres (Weinreb et al., 1986). Indeed when BTM cells were cultured in the same collagen matrices model employed here, Nakamura

found a clear relationship between contraction and the appearance of stress fibres in BTM cells (Nakamura et al., 2003, Nakamura et al., 2002). Addition of cytochalasin D attenuated this affect (Nakamura et al., 2003). Compounds that affect the F-actin architecture such as Latrunculin-B (Ethier et al., 2006), cytochalasin-D (Johnson, 1997), H-7 (Tian et al., 1998) and the Rho kinase inhibitor Y- 27632 (Lu et al., 2008) profoundly alter the TM system and increase outflow facility, however, such drugs have not yet reached the patient as 'global' disruption of F-actin can be very toxic. Another issue is corneal toxicity if it is to be used topically as most/all glaucoma medications are.

DEX is an excellent CLAN promoting agent both in human TM cells and BTM cells (Clark et al., 1994, Wade et al., 2009). Indeed BTM cells are more sensitive to the induction effects of CLANs and display higher constitutive levels of CLANs without any exogenous agents added to the basal culture media (Wade et al., 2009). However, they show an increased level of CLAN induction ability compared to human TM cell cultures, both in transformed cell lines and also primary cultures. The propensity to CLAN induction and possible link to POAG is backed up in a study that demonstrated that topical application of steroids to cow globes resulted in all cows responding with increased IOP (Gerometta et al., 2004). The appearance of CLANs is appreciable at the time points used here to measure. These geodesic F-actin arrangements likely alter cell biomechanical properties resulting in a less pliable cell (Meller and Theiss, 2006). This less motile cell cannot alter the extracellular matrix surrounding it and hence results in functional incompetence. It has been shown that anti-proliferative agents do not affect cell-populated matrices so it is unlikely that cell proliferation plays any role (Ehrlich et al., 1989). A functional cytoskeleton is a requirement for collagen gel contraction (Ehrlich et al., 1989) and a

linear relationship exists between stress fibres and contractility (Tomasek et al., 2002). It is likely that CLANs alter the isometric tension within the cell. As tissue culture probably suppresses CLAN formation rather than induces it, it could be suggested that in vivo in the whole intact tissue, CLAN-mediated inhibition of TM contraction is more profound.

The pathways that lead to CLAN formation in TM cells by the steroid DEX are elusive. However it has been noted that the addition of DEX to TM cells leads to an overall increase in cell size as well as promoting the formation of CLANs (Clark et al., 1994). Indeed the main target gene induced by DEX is myocilin (Clark et al., 2001) and this gene has been identified as mutated in a significant minority of POAG cases and was mapped to the chromosome 1q susceptibility locus (Stone et al., 1997). Myocilin has not be ascribed a function as yet and is likely a gain of function mutation rather than a loss of function. The gene for myocilin has glucocorticoid response elements, however DEX induction of myocilin is dependent on new protein synthesis, suggesting that transcriptional regulation by DEX is a secondary response, not a direct stimulation (Shepard et al., 2001). Myocilin contains a signal peptide sequence suggesting it is secreted by the cell and has been found in a number of organelles associated with the secretory pathway such as the ER. However, the protein is also found intracellularly. Interestingly, myocilin mutated in cultured TM cells was found to diminish myocilin secretion compared to wild type (Jacobson et al., 2001). This suggests a blockade on the normal protein secretory pathway. It has been suggested that myocilin affects Wingless in *Drosophila* int (Wnt) signalling (Kwon et al., 2009). Indeed Kwon et al demonstrated that recombinant mutated myocilin proteins incubated with human TM cells led to an increase in stress fibres (Kwon et al., 2009). This group then transiently transfected cDNAs of mutated

myocilin or wild type into HEK293 cells as a amenable model cell line and then took the conditioned medium and incubated 3T3 cells which led to an upregulation of stress fibre containing cells (Kwon et al., 2009). The stress fibre promoting effects of conditioned medium was due to secreted myocilin and was attenuated by the addition of secreted Frizzed Related proteins 1 and 3 (sFRPs). sFRPs are extracellular Wnt inhibitors. sFRPs are decoy receptors that contain soluble Wnt-binding frizzled domains therefore they inhibit the Wnt signalling pathway. This myocilin-induced increase in stress fibre containing cells was found to be β-catenin-dependant, as siRNA knockdown of β-catenin in 3T3 cells diminished stress fibre containing 3T3 cells. β-catenin is an integral part of the Wnt signalling pathway. Activation of the pathway occurs when Wnt ligands bind to frizzled receptors and co-receptors which then leads to recruitment of an adaptor protein, dishevelled, and recruitment of a scaffold protein axin, adenomatosis polyposis coli protein, this disrupts axin-mediated phosphorylation and to the subsequent stabilisation of β-catenin allowing it to translocate to the nucleus with the transcription co-factor, T-cell Factor to activate Wnt target genes (Katoh and Katoh, 2007).

A second component of the Wnt signalling pathway is activation of the small GTPases RhoA and Rac1 which leads to reorganisation of the cytoskeleton within the target cell downstream of receptor ligation (Moon et al., 2004). This component of the Wnt signalling pathway is often referred to as the noncanonical Wnt pathway and results in cell morphological changes and is involved in a number of morphological processes in vertebrate species including organ development. Indeed Kwon et al demonstrated that conditioned medium from HEK293 mutated myocilin transfected cells activates Rac1 and JNK phosphorylation and therefore activates the noncanonical Wnt signalling pathway ultimately leading to cytoskeletal modification

in 3T3 cells facilitating altered cell morphology (Kwon et al., 2009). Although these studies provide a mechanistic link between altered myocilin expression and alterations of F-actin architecture which are mediated through non-canonical Wnt signalling and downstream Rac1 activation they do not confirm this in the TM, the tissue responsible for outflow resistance. It has however been shown that human TM cells contain the Wnt signalling components for both pathways and is operative in the TM (Wang et al., 2008b). It could be suggested that in TM cells, as opposed to other cells, exposure to DEX leads to increased gene and protein expression of myocilin that acts upon the cell and surrounding cells to activate and initiate the noncanonical Wnt signalling pathway independent of β-catenin and downstream activation of Rac or Rho to induce CLAN formation. Thus unifying DEX exposure, myocilin expression with Wnt signalling and ultimately cytoskeleton rearrangement.

Microarray analyses of TM cells that have been exposed to long term DEX to identify differentially expressed genes have yielded few target genes. The most consistently up regulated gene was MYOC that codes for myocilin (Lo et al., 2003) along with α-1 anti-chymotrypsin, a serine protease inhibitor. Indeed decorin mRNA was also found to be up regulated after DEX exposure (Ishibashi et al., 2002). The different pattern of expressed genes after exposure to DEX may relate to different concentrations of steroid used in each study, time of exposure, passage number of the cells used in the studies and cell heterogeneity.

DEX primarily signals through its glucocorticoid receptor-α. The other isoform is glucocorticoid receptor-β which is a dominant negative regulator of glucocorticoid-α function and is a splice variant from the same gene (Derijk et al., 2001). One reason for the heterogeneity between cultures with respect to CLAN induction could be the relative expression of the receptor isoforms. Indeed it has been shown that TM cells

that overexpress the dominant negative glucocorticoid receptor-β secrete less myocilin (Zhang et al., 2005). It would have been interesting to have examined the CLAN incidence in the overexpressing β receptor TM cells.

Apoptosis

No thorough studies exist on the relationship with CLANs and apoptosis. The next section of the study sought to determine if CLANs are associated with cell death as this may underlie the loss seen in ageing and disease.

The time periods that were chosen correlated the known time points we know CLANs are present in appreciable numbers and we could not find any evidence of apoptosis in CLAN-rich cultures, regardless of the conditions used and using multiple assays to evaluate apoptosis. Apoptosis is a clear linear sequence of events that results in the eventual demise of the cell and these are easily distinguishable (Thompson, 1995). Myocilin, a DEX inducible protein that is significantly upregulated after exposure, has been shown to sensitise cells to oxidative stress-induced apoptosis (Joe and Tomarev, 2010).

It is not surprising that no association occurred with CLANs as when a cell has decided to apoptose the earliest biochemical event is dissolution of the actin cytoskeleton. Indeed actin is itself a substrate of caspases resulting in dissolution (Kayalar et al., 1996). We know human TM cells can undergo FAS-induced apoptosis through the extrinsic pathway and express pro-apoptotic and anti-apoptotic proteins and mRNA (Agarwal et al., 1999b), however this is the first examination of apoptosis in relation to CLANs/DEX/TGF-β2 exposure. Compared to other cell types, TM cell apoptosis has not been examined in great depth. It has been demonstrated that BTM cells exposed to dipivefrim hydrochloride, timolol maleate

and levobunolol hydrochloride, all common glaucoma medications, results in a small amount of cell death but often at supra-physiological levels (Kawa et al., 1993).

Another study which examined apoptosis in human TM cells found that the steroid triamcinolone acetonide resulted in an increase in apoptosis and decrease in cell proliferation (Wang et al., 2008a). However this was only noted at the higher concentration of 1mg/ml and could be due to the benzyl alcohol preservative. Also in an ex vivo organ culture model of the TM, in which tissue viability is maintained by perfusion of culture medium addition of ethacrynic acid to the perfusate resulted in some level of toxicity (Johnson and Tschumper, 1993). No study to date has looked specifically at the relationship between CLANs and apoptosis.

CLAN inducer and inhibitors

DEX is currently the only known CLAN inducer to date and as well as inducing CLANs it also has a host of metabolic effects on the TM cell (Clark et al., 1994). DEX was initially added to TM cells due to the fact that in a significant proportion of the human population (steroid responders) who are exposed topically to DEX develop elevated IOP. If the elevated IOP persists it results in a DEX-induced glaucoma that is clinically similar to POAG (Armaly, 1966). This part of the thesis investigation set out to discover new CLAN inducing agents and also to find inhibitors if at all possible.

Previous studies (Wade et al., 2009) demonstrated that even without DEX in the media, a few BTM cells developed CLANs and there were more in bovine than had been found in the non-glaucoma HTM cell lines that we worked with. Initial investigations centred on base-line CLAN induction by varying the amount of serum in the culture medium. This resulted in a dose dependant increase in CLAN

incidence as the concentrations increased and in the presence of "standard" medium containing 10% FCS there were around 13% of BTM cells had CLANs in their cytoplasm by 14 days. These data demonstrate a progressive and significant step wise increase in the incidence of BTM cells containing CLANs with the increasing serum levels in the culture medium. There were less CLANs present in the lowest concentration of FCS used, but to tease out the effects of addition of other compounds 1% FCS concentration was subsequently adopted for the rest of the experiments.

The investigation initially focussed on TGF-β2 as a possible CLAN inducer in BTM cells for multiple reasons. Firstly it is abundant in the aqueous humour (Min et al., 2006) and is significantly expressed in higher concentrations in aqueous humour from glaucomatous patients (Tripathi et al., 1994b). Secondly TM cells express functional receptors for growth factors including TGF-β (Wordinger et al., 1998). Moreover in porcine TM cells it has been found that such cells express the gene for TGF-β2 and also secrete the protein, albeit in a latent non-activated form (Tripathi et al., 1994a). Further TGF-β2 has a well-defined pathway through years of research on this molecule and its molecular effects which include activation of the canonical Smad pathway leading to transcriptional targets (Derynck and Akhurst, 2007). As a result it was hypothesised that TGF-β2 exposure would induce substantial numbers of CLANs in BTM cells. Evaluation of TGF-β2 as a CLAN inducing agent showed it to be highly effective because at levels as low as 2ng/ml it was able to induce CLANs in around 50% of confluent BTM cells following 7 days exposure to TGF-β2. By way of comparison it took twice as long to produce comparable numbers of CLANs with DEX treatment. Thus the induction of CLANs by means of exogenous TGF-β2 results in a greater magnitude of response than that of DEX our only other

known inducer. It is not known whether TGF-β2 would lead to decreased collagen gel contraction mediated by BTM cells as this has not been tested anywhere, however TGF-β1 does increase collagen gel contraction by BTM cells (Nakamura et al., 2002). This may not be surprising as TGF-β1 does not lead to increased CLAN incidence in TM cells.

Use of a TGF-β2 neutralizing antibody reduced the CLAN producing action close to baseline levels in BTM cells in both our TGF-β2 and aqueous humour experiments presumably by sequestering available TGF-β2. The first report of aqueous TGF-β levels in human cataract patients was in 1990 when the extremely high level of 4.5ng/ml (with 60% of the cytokine being in an active form) was reported (Jampel et al., 1990). Further investigations agreed that it was the TGF-β2 isoform of the cytokine that was the dominant form of TGF-β in aqueous, however at considerably lower levels for total and activated cytokine. One study showed values of 2.7ng/ml to be expressed in human aqueous humour (Tripathi et al., 1994b). Another study determined extremely high levels of TGF-β2, but conceded that this was unlikely to be mature, activated TGF-β2 (Kokawa et al., 1996). Research using aqueous humour from cataract patients determined the levels to be higher in cataract vs controls however, the actual ratio of latent (unactive) to mature (activated) seemed to be high (Maier et al., 2006). Values for total TGF-β2 in species other than man approximate the human levels but normal bovine aqueous humour seems to be a little higher with a range between 1.13 and 5.6ng/ml has been published (Hayasaka et al., 1998). The concentration used in this study fits easily into that range and is often used in investigations looking at the effects of TGF-β2 on extracellular matrix deposition and turnover in the TM (Wordinger et al., 2007).

The physiological action of TGF-β2 is mediated by TGF-β receptors type I and type II, both of these are serine and threonine kinases. Once latent and inactivated TGF-β2 is activated by cleavage, possibly through latent activator protein and TSP-1 (Schultz-Cherry and Murphy-Ullrich, 1993), it binds one or both of these receptors, this results in both receptors binding and increasing stabilisation with each other as a heterotetramer and results in phosphorylation of the receptors as a critical initiating downstream signalling event leading often to Smad recruitment and activation (Piek et al., 1999). Therefore the theory was tested that TGF-β2 CLAN inducing activity could be retarded by TGF-β RI and TGF-β RII inhibition using small molecule inhibitors of both receptors.

Inhibition of TGF-β RI resulted in a suppression of CLAN induction to 34% and inhibition of TGF-β RII reduced CLANs to 31% (P=<0.01) (figure 3.16). This CLAN inhibition by blockade of the TGF-β receptors is statistically significant compared to agonist treated cultures, however a more efficient attenuation of CLANs may have been possible with increased concentrations of the inhibitors. Routine observations of cells indicated that they were healthy and viable. However TGF-β2 treated cultures alone appeared more rounded compared to receptor antagonist-treated BTM cultures.

To further investigate the downstream signalling pathways involved in CLAN formation a newly characterised Smad-3 inhibitor that inhibits Smad-3 and has no effect on other Smad proteins or p38 was employed (Jinnin et al., 2006). Incubation with SIS3 mediated suppression of TGF-β2 induced CLANs. Indeed no CLANs were present in any culture examined. Blocking Smad-3, a downstream target of TGF-β2 signalling and central transcription factor, totally negated CLANs. Loss of CLANs was not due to adverse changes in our cells because from morphological examination

of cells they appeared healthy and the trypan blue exclusion assay showed that our BTM cells had a consistent viability of over 97 % viability. Smad-3 is an intracytoplasmic receptor regulated protein that upon phosphorylation it is activated and translocates to the nucleus to alter gene expression. Here this heterodimeric complex directs transcriptional activity of various genes in response to TGF-β stimulation. Therefore the phosphorylation of Smad-3 using a phosphospecific antibody to Smad-3 (Abcam serine 423/425) was investigated. The time point of two hours incubation was chosen as phosphorylation likely occurs early in the cell response to ligand stimulation, followed by significant gene expression and this may be a dynamic kinetic situation of oscillations. Results showed that TGF-β2 induced increased phosphorylation of Smad-3 and SIS-3-mediated suppression of this phosphorylation and hence activation which was coincident with CLANs induction and suppression. Thus, TGF-β2 induction of CLANs is dependent on Smad-3 pathways. So it would appear that TGF-β2 induced-CLANs require the Smad-3 pathway. This is the first time a study has demonstrated an effective CLAN inhibitor. The TGF-β2 responsive genes that are activated in TM cells leading to CLANs are unknown. However, fibronectin has been found to be upregulated in response to TGF-β2 exposure (Fuchshofer et al., 2007) and fibronectin has been shown to induce CLANs through interaction with integrins linking extracellular signals to the cytoskeleton (Filla et al., 2006). Thus TGF-β2-induced fibronectin may be elevating CLANs via interactions with specific integrins. Figure 4.1 illustrates the possible pathways of CLAN formation. In RPE cells a bone fide target gene of TGF-β has been identified as GEF-H1 that activates RhoA ultimately leading to altered cell migration and is Smad-dependant (Tsapara et al., 2010). It has been shown that Smad-7 is an inhibitory antagonist of TGF-β2 signalling thus providing negative

feedback to regulate local signalling. Indeed adenoviral overexpression of Smad-7 to the corneal endothelium of rats in vivo significantly reduced injury-induced corneal fibrosis (Saika et al., 2005, Sumioka et al., 2008). It is interesting that Fuchshofer et al. identified Smad-7 as being a key molecular switch that works in a negative feedback loop to suppress TGF-β2 induced signalling in human TM cells (Fuchshofer et al., 2009).

To determine that the protein factor in aqueous humour that responsible for CLANs is TGF-β2 an anti-TGF-β2 neutralising antibody co-incubated with aqueous humour was used in these experiments. A significant upregulation of CLANs in BTM cells was evident in cells exposed to aqueous humour. Incubation with the neutralising antibody retarded this upregulation, with cells having less than 10% CLAN-containing cells present with incubation with neutralising antibody.

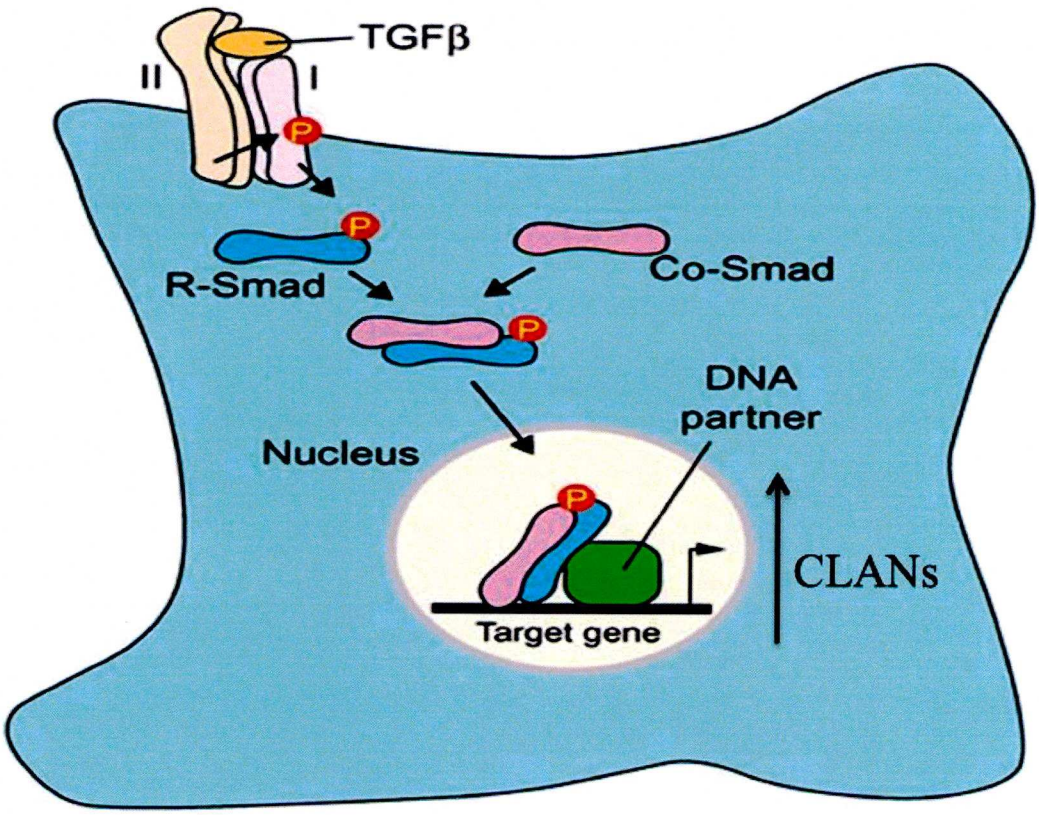

Figure 4.1 Possible pathway of CLAN formation. TGF-β2 binds to the TGF-β R I and RII this results in the activation of the receptors and dimerization leading to phosphorylation of R-Smad-3, this in combination with co-Smad, translocates to the nucleus to act as a transcription factor leading to gene expression of a plethora of genes with a subsequent increase in CLANs. Some of the target genes that have been identified in TM cells include ECM genes such as fibronectin (Fuchshofer et al., 2007). Fibronectin has been shown to promote CLAN formation via interactions with integrins in human TM cells. We have shown blockade upstream of the Smad-3 pathway results in partial inhibition of CLANs but specific inhibition of Smad-3 (SIS3) leads to total negation of TGF-β2 induced CLANs. However the target gene downstream that leads to CLANs is still elusive.

This confirms that CLANs are upregulated by aqueous humour, is consistently reproducible, and one of the factor(s) mediating this CLAN induction is TGF-β2. Previous studies measuring TGF-β2 levels in the aqueous humour where all from the small samples taken from the middle of the anterior chamber, so we have no clear idea of what the actual true TM pathway levels are. They are likely higher than the measured amounts in a variety of studies and freeze thawing of aqueous samples surely has an effect on the protein levels, also different total protein levels will lead to different results along with the sensitivity of the assay employed to measure the analyte.

On the other hand if TGF-β2 is the inducing agent then why is its ability to produce CLANs apparently greater in DMEM than in aqueous humour when at reasonably similar concentrations? In this study, TGF-β2 at 2ng/ml was always more effective at CLAN production at any time period in the target cells than optimum DEX, and even at lower concentrations like 1ng/ml it was at least as good as DEX. But in every experimental run with 100% aqueous humour, consistently it was significantly less than that of DEX-CLANs. This was puzzling. A reasonable and likely explanation is deficiency of activation of latent TGF-β2 in aqueous humour that we had. Such non-activation would lead to lower levels of functional active TGF-β2. Aqueous humour is a complex mixture of proteins and contains all manner of inhibitor and competitors

that could be suppressing the TGF-β2 activation or signalling (Klenkler and Sheardown, 2004, Freddo et al., 1990). Also freeze/thawing cycles of aqueous humour cannot be beneficial for the proteins.

Decorin is a small leucine-rich proteoglycan that has been documented as a natural inhibitor of TGF-β signalling and represents a negative feedback loop (Yamaguchi et al., 1990) and recently has been shown to supress pro-fibrotic TGF-β-induced gene expression in human corneal fibroblasts (Mohan et al., 2010). Therefore decorin was used to inhibit CLAN incidence in BTM cells based on previous evidence in the literature that it is a natural endogenous inhibitor of TGF-β2 signalling. It was surprising to notice that initial observations found that decorin resulted in a marked F-actin rearrangement into CLANs. Indeed after 7 days in culture CLANs were found in 69% of cells (figure 3.22). The CLANs were phenotypically the same with bright punctate hubs of actin and appeared quite large in relation to the cell. They were indistinguishable from other inducers of CLANs.

Phase contrast microscopy revealed that many cells appeared more rounded. However this was not a class affect as biglycan showed no increase above baseline CLAN levels. Decorin is a common component of the TM and has been localised at both the gene and protein level immunohistochemically (Tanihara et al., 1995, Wirtz et al., 1997). It is abundant and is a major component of the extracellular matrix that helps stabilise the matrix. Also it has been suggested as a modulator of response in glaucoma filtration surgery (Grisanti et al., 2005). Moreover its gene expression using gene chip arrays has been found to be significantly upregulated after treatment with DEX (Ishibashi et al., 2002). However, this was not confirmed at the protein level. This could lead to DEX-mediated upregulation of decorin that in an autocrine manner leads to CLAN biogenesis in TM cells. Recently recombinant decorin has

been shown to suppress TGF-β1-induced cytoskeletal changes and contraction of collagen lattices by hypertrophic scar fibroblasts (Zhang et al., 2009). The exact mechanism through which decorin regulates CLANs is currently unknown however decorin has been shown to cause shape changes in rabbit synovial fibroblasts especially rounding and this may lead to cytoskeleton modification (see later) (Huttenlocher et al., 1996) and also modify the shape of lung fibroblasts (Tufvesson and Westergren-Thorsson, 2003).

Stretch

The TM is under constant mechanical stretch and as such must respond to this constant stretch and distortion accordingly. Many studies have used mechanical stretch systems using TM cells of various species however they have normally only looked at MMP levels and modulation in this context as a function of extracellular turnover (Bradley et al., 2001). This study sought to determine if cyclic mechanical stretch induces CLANs using a commercially available system in an attempt to model the stretch and distension of outflow pathway cells that occurs in vivo. The hypothesis is that biomechanical cues are integrated and transduced and respond in producing CLANs. Stretch applied for only 12 hours was sufficient to create and increase in CLANs to 40.5% of the cell population, DEX alone (and no stretch) resulted in 49% and pretreatment with DEX and cyclic stretch resulted in there being 53% of BTM cells with CLANs. That there was no massive increase with DEX and stretch suggests that there is no synergistic effect occurring. With other CLAN inducing agents it often takes many days of exposure for the stimuli to induce appreciable numbers of CLAN, suggesting a chronic effect. However, in this system it has been shown that CLANs are induced after only 12 hours, it may be that the

initial biomechanical stimuli is sufficient to muster an early gene response resulting in formation of CLANs expediently.

Some authors reported similar 'CLAN-like' structures in human TM cells subjected to mechanical stretch in vitro (Tumminia et al., 1998). These structures similar to CLANs were geodesic actin arrangements with hubs and vertices of F-actin radiating away from the hub points. These authors found that after only 1 hour of stretch many polygonal triangular arrangements were expressed in human TM cells; but by 24 hours of stretch the normal stress fibres arrangement was evident with limited geodesic 'CLAN-like' structures, demonstrating that these are readily reversible. However their type of stretch was different to what was employed herein. Tumminia et al used a 'homemade' silicone moulded boat that was, like all silicone, hydrophobic and had to be coated with an extracellular matrix compound, and in this study in comparison to ours they used laminin as their extracellular matrix substrate (Tumminia et al., 1998). In our studies laminin was found not to support the attachment or growth of our cells in culture demonstrated by long elongated processes and dead floating cells. This study also made no attempt to quantify these CLAN-like geodesic structures in their human TM cells, thereby giving no indication of total or relative numbers say compared for example to non-stretched TM cells. The present investigation provides the first quantitative data on CLAN-induction by stretch.

Also in the Tummina investigation the stretch was, unlike in our study, continuous and not cyclic with alternation between stretch and relaxation of the underling silicone membrane. This type of stretch may not be physiologically relevant as it is unlikely that the TM tissue is held tight as constant tension all the time (Grierson et al., 1978, Wiederholt et al., 2000). This model of cellular deformation is more

physiological and hence more relevant. The multi-axial device is a vacuum operated system which produces bi-axial radial tensile strain with very little compression on the circular shaped silicone membranes held within the plate and hold. The airflow through the stretch plates is unrestricted, which diminishes the potential for internal pressure gradient in the cell culture plate. So the rate of deformation of the membrane is a true reflection of and the result of the pressure change due to the vacuum applied by the system (Gilbert et al., 1994). Also the direction of the strain in the Tummina system was uniaxial (along one plane) and whilst they stated that the strain was 10% quite how this was calculated is unknown. Compared to our apparatus which produces multidirectional strain resulting in a radial stretch and the percentage strain was calculated on the basis of physiological levels (Coleman and Trokel, 1969, Johnstone, 2004) that the outflow pathway is probably exposed to in vivo, their system is likely not physiologically relevant. It is interesting to note in our system when compared to a silicone membrane alone, stretch increased CLAN incidence. However, when we compared non-stretched controls to tissue culture plastics (see results section 3.7.1) the CLAN incidence was much higher after the same time period in culture. This increase is suggestive of either substrate (fibronectin) induction of CLANs or the substrate topographic cues increases CLAN incidence. While mechanical stretch has been used in various studies of TM cells (WuDunn, 2009, Bradley et al., 2001) they have principally focussed on the matrix metalloproteases and their possible signalling pathways in regulating matrix deposition (Bradley et al., 2003). Therefore this is the first cyclic radial mechanical stretch study in TM cells that describes the upregulation of CLANs. However it has recently been shown that the actin cytoskeleton arrangement has a direct effect on matrix metalloprotease-2 expression and activation (Sanka et al., 2007).

Next TGF-β2 was examined in the conditioned medium from the stretch and non-stretched cultures was increased in the conditioned media collected after cyclic mechanical stretch. There was a large upregulation in TGF-β2 secretion in response to stretch compared to control unstretched cultures (see results section 3.7.2 figure 24). However, incubation alone with DEX and non-stretched also led to an increase which was similar in magnitude to stretched cells, suggesting that DEX itself leads to an upregulation of TGF-β2 expression. Preincubation of BTM cells with DEX and subsequent exposure to stretch did not lead to an increase in TGF-β2 above either alone. Clearly there was no additive effect. This part of the study demonstrated that TGF-β2 leads to CLANs so this may represent a paracrine effect induced by mechanical stretch. Liton et al have previously shown that 5% elongation at the same frequency that was used in this study led to a significant increased secretion of TGF-β1, that was associated with activation of the TGF-β1 promoter (Liton et al., 2005a) in primary human TM cell cultures. They subsequently showed that after cyclic mechanical stress there is cross-talk between TGF-β1 and IL-6 suggesting a possible autocrine loop (Liton et al., 2009). In the present study it was demonstrated that after exposure to 10% cyclic mechanical stretch BTM cells upregulated IL-6 levels. In basal conditions no IL-6 is present but is rapidly produced and upregulated after only 12 hours of mechanical stretch. Interestingly there is also an increase in IL-6 that is higher than stretch after 14 days exposure to the CLAN inducing agent DEX. IL-6 has been found to alter cytoskeleton organisation in aortic endothelial cells in vitro (Zhongbiao and Walter, 2003). Further, IL-6 has been determined to induce F-actin alterations after IL-6 addition to macrophages and monocytes (Clahsen and Schaper, 2008). It could be suggested that BTM cells respond to cyclic mechanical stretch and therefore to normal IOP fluctuations by secreting factors such as IL-6 to modulate

permeability of Schlemm's canal, thus momentarily increasing Schlemm's canal permeability and appropriate IOP is restored. It is well known that permeability of Schlemm's canal mediates outflow facility (Alvarado et al., 2005) and has an embryonic vascular origin (Hamanaka et al., 1992).

IL-1β levels were also quantified after cyclic mechanical stretch exposure. IL-1β levels were increase compared to control non-stretched BTM cells. Interestingly, DEX treatment without mechanical stretch led to an increase in IL-1β. Moreover pre-incubation with DEX and subsequent exposure to cyclic mechanical stretch led to an increase of over 780% of control non-stretch. It appears that DEX potentiates the effect of cyclic mechanical stretch-induced IL-1β secretion. IL-1β is a pleotropic cytokine historically involved in the primary immune response. This cytokine has been shown to modulate outflow facility and also to increase secretion and activation of matrix metalloprotease-3 in TM cells (Hosseini et al., 2006, Shifera et al., 2010). Activation of this protease will mediate the quantity and distribution of extracellular matrix in the outflow pathway. It may be postulated that DEX/stretch induced secretion and upregulation of IL-1β mediates CLANs alone or in combination with IL-6. Indeed IL-1 injected into rat eyes modulates outflow facility, whether this is a specific or non-specific response is not clear however (Kee and Seo, 1997).

Hsp70 is a highly evolutionary conserved gene and protein that is induced by a variety of cellular insults, including metabolic stress, traumatic injury and mechanical stress. Previously it was shown that after cyclic mechanical stretch of both human and porcine TM cells (15% 1Hz) there was a 590 fold increase in Hsp 70 gene expression using microarray technology (Luna et al., 2009). However changes in gene expression do not necessarily reflect protein levels. Therefore intracytoplasmic levels of Hsp70 after induction of cyclic mechanical stretch were

determined. These data show that BTM cells do indeed express basal levels of Hsp70 and enormously upregulate their Hsp70 protein levels after mechanical stretch (section 3.7.5). There is also massive upregulation of Hsp70 after DEX treatment and more still after DEX and subsequent mechanical stretch and possible potentiation.

This is the first demonstration of Hsp70 protein levels in the TM of any species to date. Previous studies have demonstrated α-B-crystallin, another member of the small heat shock protein family, is initially downregulated after mechanical stretch in human TM cells (Mitton et al., 1997).

This downregulation of α-B-crystallin occurs within an hour of commencement of stretch, however returns back to basal levels (Mitton et al., 1997). α-B-crystallin is an important chaperone protein for actin and helps stabilise F-actin filaments. It could be that the BTM cells sense the nascent cytoskeletal rearrangement of actin into geodesic domes into CLANs as a misfolded protein response and thus increase their synthesis for proteasomal degradation. Thus the CLANs presence is a 'stress' related response. Alternatively, CLANs whilst not directly responsible for cellular apoptosis *per se* could, lead the TM cell to being more vulnerable to an extrinsic apoptotic stimuli leading to cell death. In other words a CLAN-containing cell is more sensitive to an apoptotic stimulus and thus the cell responds by increasing synthesis of cytoprotective Hsp70 a highly conserved response to cellular threats (Mailhos et al., 1993). DEX treatment in rat intestinal epithelial cells results in an induction of Hsp70 resulting in protection from cell damage and death (Urayama et al., 1998). Both in vitro and in vivo, indeed suppression of Hsp70 gene and protein expression by transfection with siRNA results in the attenuation of DEX-induced Hsp70 conferred protection from oxidative stress (Urayama et al., 1998). Hsp70 is in its normal state is a molecular chaperone protein whose function is to assist in

transporting client proteins intracellularly and regulating protein degradation within the proteasomal pathway (Smith et al., 1998). A common feature is upon various types of stress cells upregulate their Hsp70 levels to protect the cell from sub-lethal damage. Although Hsps have not been characterised in the TM tissue, they have been shown to be expressed in retinal ganglion cells, which are the true endpoint target cells in glaucoma (Park et al., 2001). Loss of these cells is the ultimate consequence in the pathological sequence of event that ultimately leads to vision loss in POAG (Kerrigan et al., 1997).

Indeed induction of Hsp70 in a standard animal model of glaucoma led to a reduction in apoptosis of retinal ganglion cells (Park et al., 2001). This was mediated through Hsp70 induction as the pretreatment with quercetin, an Hsp inhibitor, led to supression of retinal ganglion cell death. Furthermore it was shown that pharmacological induction of Hsp70 by the specific Hsp70 inducer geranylgeranylacetone leads to much less retinal ganglion cell apoptosis in an animal model of glaucoma (Ishii et al., 2003). Cytoprotective effects of Hsp70-mediated geranylgeranylacetone have been noted in retinal pigment epithelial cells (Tanito et al., 2005). Therefore CLANs could lead to Hsp70 expression in BTM cells that is mediating a cytoprotective response to perceived cellular 'stress' mediated by the actin rearrangement to maintain cellular homeostasis. If this Hsp70 response is attenuated (as clearly occurs with ageing) the cells become more vulnerable to apoptosis. An attenuated CLAN-mediated Hsp70 response may occur in glaucoma.

To determine which pathway is activated after mechanical stretch the canonical Nf-kb pathway was examined using a p65 subunit antibody. This demonstrated activation of the central pathway evidenced by increased Nf-κB phosphorylation and hence activation after mechanical stretch. Nf-κB was also increased in DEX treated

samples alone, which correlates with the increased IL-6 and IL-1β expression. An authoritative *Nature Medicine* paper demonstrated that a specific stress response defines the glaucoma phenotype (Wang et al., 2001). The study showed that all TM tissues studied from confirmed populations of glaucoma donors was positive for ELAM-1 and ELAM-1 was not present in normal healthy controls. ELAM-1 is a cell adhesion glycoprotein expressed only on endothelial cells activated by cytokines such as IL-1 (Bevilacqua et al., 1989). The group showed that glaucomatous tissue ELAM-1 expression is not due to inflammation as most expression is and is upregulated by IL-1 expression at both the mRNA and protein level and could be blocked by addition of IL-1 Receptor antagonist (IL-1ra). Interestingly they used cell culture studies to show that in glaucomatous-derived TM cells Nf-κB was constitutively active and increased in response to exogenous IL-1 and could be supressed by addition of IL-1ra to the medium and that glaucomatous constitutive activation of Nf-kb results in a resistance to oxidant-induced apoptosis. Addition of IL-1ra supressed this resistance and inhibition of Nf-κB through the Nf-κB antagonist SN50, led to reduced resistance to apoptosis (Wang et al., 2001). Their work has demonstrated similar activation of Nf-κB, increased expression of cytokines IL-1-β and IL-6; that could work in a feedback autocrine loop on Nf-κB pathway activation, thus amplifying and propagating the transcriptional signal.

Thus the conclusion could be drawn that the CLANs may result in an increased anti-apoptotic pathways through Nf-κB activation and subsequent Nf-κB-mediated gene expression. Testing this hypothesis was outside the scope of the present research but would be an important future investigation. Activation of Nf-κB, depending on cellular context, has been shown to be anti-apoptotic in a variety of cell types (Chen

and Greene, 2004, De Smaele et al., 2001, Rae et al., 2007) although the exact mechanisms are still elusive to date.

In recent times research, including the work conducted in this present thesis, has shown that CLAN induction in TM cells is not the exclusive property of corticosteroids. Indeed DEX, the most effective steroidal agent for CLAN production and our "gold standard", is no longer top of our league table of induction agents see table 4.1. It is now of importance to identify cell, molecular and pathway actions that are common to the various agents and may be associated with CLAN development. We were aware that at least some of the CLAN inducers such as DEX (Clark et al., 1994), aqueous humour (Fautsch et al., 2005) and TGF-β are known to influence cell shape.

Table 4.1 Inducers of CLANs in BTM cells in this study

CLAN Inducer	CLAN incidence % of CLAN containing cells after various periods of exposure
Decorin	69
TGF-β2	68.2
DEX	49.1
Aqueous humour	41
Cyclic mechanical stretch	20*

* After 12 hours of radial cyclic mechanical stretch 1Hz 10% elongation.

Cell Shape and Movement

As a result experiments were performed to see if any differences in morphology were discernable in our test BTM cells. Although BTM cells at confluence have been described as being 'endothelial-like' it became apparent that interesting differences in cell appearance and movement particularly during the pre-confluent period from routine phase contrast examination and from time-lapse video observation were clear. It has been demonstrated that DEX causes shape changes in human endometrial cells (Koukouritaki et al., 1997) and increases TM cell size (Wilson et al., 1993). TM cells are also known to get more enlarged and rounded in aqueous humour and TGF-β family members also have shape-altering properties promoted by their cytoskeletal modifying effects (Nakamura et al., 2002).

Whether the various cell appearances represented subsets of different cells within the primary cultures or (what turned out to be the case from time lapse evidence) whether seeing interchangeable phenotypes was a valid question posed. What precisely triggers the move to and from a spindle-shaped polarised elongated form to a more circular epitheliod shape and back again is not at all clear. It is not merely locomotion because although many of the epitheliod cells did not move much, others did and moved quite rapidly with fillapodial motion, as seen by time-lapse phase microscopy, while still retaining an essentially rounded shape. In addition the spindle or epithelial cells were predominantly mobile in pre-confluent culture moving by a polarised extension of cytoplasm and then posterior release with a rapid elastic-like retraction so creating forward motion. On the other hand some cells were virtually static in culture.

Stress fibres were present in all the three shapes of cell seen in BTM cultures i.e. spindle, epitheliod and kite shaped. They were most prominent in the spindle cells but were just as pronounced in stationary spindle cells as they were in the mobile

form(s). How exactly the stress fibres function in actively moving and stationary phenotypes of cultured cells in general is a matter of considerable current research (Worthylake and Burridge, 2003). Without doubt stress fibres are ATP-dependent contractile structures irrespective of whether they are present in active or stationary cells (Pellegrin and Mellor, 2007). At the outset of this study one had not predicted that there would be any specific association of CLANs with a particular TM cell appearance. Initially did not expect to find an association of CLANs with a particular cellular shape or pattern. Indeed casual, non-systematic examination of BTM cultures had been unhelpful in this respect so we were quite surprised that analysis showed the association with the epitheliod form was so strong. On the other hand, that cells with CLANs tended to be stationary or at least fairly immobile was predicted. It was also not unexpected that CLAN-containing cells exhibited, on time lapse examination, a lack of flexibility when compared with the cells that did not express CLANs. Certainly when TM cells are exposed to the CLAN forming stimuli we can predict that a rounded, epitheliod stationary cell phenotype has a high probability of having one of these cytoskeletal structures within the cytoplasm. We now have a shape predictor for the presence of a CLAN, which although not perfect is none the less useful. What is not clear is whether CLANs themselves promote the morphological shape change or whether the shape change precedes CLAN formation? Future work should be carried out to address this question.

Currently it is not known if PAAs are functionally, structurally and phenotypically the same as CLANs. CLANs were initially defined as DEX-induced polygonal arrangements found in confluent cultures in vitro (Clark et al., 1994). However, we now know that they are present in basal cultures and this work has demonstrated multiple inducers of CLANs. It has been suggested that CLAN formation is

modulated by Syndecan-4 activation (Filla et al., 2006). However, the authors in this paper used recently plated out non-confluent cultures. Specifically they used TM cells that were trypsinised and then replated with or without a variety of extracellular matrix molecules that included fibronectin and then stained for F-actin (Filla et al., 2006). Filla and co-workers found structures that were 'CLAN-like' however because their cultures and experiments were so short term and CLANs generally take a long time to become established (up to 14 days) they may well be looking at structures more akin to PAAs than true CLANs (see figures showing characteristics of the two structures). In the 'spreading' assay carried out in this thesis it was demonstrated that cells contained spectacular polygonal arrangements of actin especially around the periphery of the cell but that over time in culture this then disappeared and formed the more regular stress fibre arrangement of actin. In other words after plating the BTM cells there is an initially polygonal arrangement of actin that then subsides as the cells form interactions through focal adhesions to the underlying substrate and then on subsequent exposure to an appropriate stimuli the cells increase their incidence of CLANs. Hence the work of others and the definition of CLANs that they used in their work need to be clarified as these structures may appear similar however are not the same thing (Lazarides, 1975).

However, the structures others have described as CLANs may indeed be the same thing as they have endured an acute 'mechanical stress' after trypsinisation and the same acute mechanical stress was applied in this study with cyclic mechanical stress. It would be interesting to perform microarrays to identify common or differentially expressed genes between TM cells that have been exposed to DEX and TM cells that have been exposed to mechanical stress (trypsinisation and cyclic stretch). We had performed a PCR array for genes involved in the TGF-β pathway between TM cells

that had been exposed to either DEX or TGF-β2 to identify common genes, only one gene was increased with the two treatments: IL-6. IL-6 may play a role in the formation of CLANs however, this was a preliminary study with a rather small sample. The increase in CLANs on fibronectin coated cover slips was interesting, a similar effect was found the same increase in silicone stretch membranes that were coated with fibronectin, the control non-stretched cultures compared to standard tissue culture plastics showed an increase in CLAN containing BTM cells. Fibronectin may induce CLANs through ligation with integrins (Filla et al., 2006). A very recent paper by Filla et al has demonstrated that DEX leads to upregulation of αvβ3 integrin expression and the use of activating antibodies against these integrins upregulated CLAN in TM cells. Perhaps more importantly they report that this enhanced integrin expression and activation by DEX was in confluent cultures of TM cells, in contrast to their previous studies which were all in fresh plated cells (Filla et al.). The weakness in this paper is that the authors did not used matched isotype controls for their activating antibodies and therefore cannot rule out the possibility that other non-integrin pathways were activated by the antibodies. I propose a working model in that DEX leads to CLAN formation via an increased secretion of TGF-β2 and therefore an increased secretion of the ECM protein fibronectin (Fuchshofer et al., 2007) with a concurrent increased expression of αvβ3 integrins (Filla et al.) which binds the fibronectin leading CLAN formation via Rac1. Silencing of Rac1, an important cytoskeleton regulator, in TM cells exposed to CLAN inducers will help elucidate its role. Rac1 may play a critical role.

Table 4.2 Different features between CLANs and PAAs

CLANs	*PAAs*
Geodesic structures found in confluent cultures of cells	*Transient geodesic structures that are precursors to stress fibres*
Can extend the whole area of the occupying cell	*Spectacular and found only in the periphery of the cell*
Can be induced by a variety of stimuli	*Non-inducible; found only on replating*
Can be inhibited by blocking of TGF-β2 receptors or downstream signalling	*Cannot be inhibited*

In conclusion I have demonstrated that CLANs result in a functional alteration of BTM cell contractility which could lead to a defect in regulation of outflow facility with a subsequent raised IOP. CLANs do not appear to be associated with apoptosis. This work has also discovered multiple CLAN inducers and that, at least in the case of TGF-β2-induced CLANs, are coupled to the canonical Smad pathway, as Smad-3 inhibition attenuates the TGF-β2-induced increase in CLAN incidence. However CLANs can be formed independent of the TGF-β signalling pathway upstream of Smad-3. Moreover CLANs are associated with a specific cell phenotype. This will help identify CLAN containing cells in the future; this will be invaluable for future studies. I also demonstrated that cyclic mechanical stretch, similar to physiological levels, results in CLAN formation. Such CLAN formation in response to biomechanical stimuli may represent a homeostatic mechanism to alter the contraction of the TM cells and therefore outflow resistance. Elucidation of TGF-β2 signalling in the formation of CLANs suggests that aberrant signalling, perhaps via genetic mutation, would lead to elevated CLANs. If CLANs are pathogenic in POAG

(or other diseases) targeting the Smad pathway may represent a new therapeutic paradigm.

Conclusions

- DEX leads to functional impairment of contraction using an accepted model of cellular contraction
- Expression of CLANs are not associated with TM cell apoptosis
- CLANs are induced by a factor(s) in serum as reduction of serum leads to suppression of CLANs
- The pleotropic cytokine TGF-β2 is a potent CLAN inducing agent and is one of the agent(s) in aqueous humour responsible for CLAN formation
- TGF-β2-induced CLANs are coupled to the Smad-3 pathway and may represent a future therapeutic target
- The ubiquitous small leucine-rich proteoglycan decorin is an exceptional CLAN inducing agent
- Cyclic mechanical stretch of a physiologically relevant level results in CLAN induction
- Such mechanical stimulated CLANs appear in a short time suggesting early transcriptional responses
- Hsp 70 is expressed in TM cells and is rapidly produced and upregulated in response to biomechanical stretch and may represent an adaptive response
- TGF-β2 is upregulated and secreted in response to stretch as are IL-6 and IL-1β which could regulate vascular permeability
- The canonical Nf-kb pathway is activated after mechanical stretch and likely activates directed gene transcription for the acute response cytokines

- CLAN containing cells are associated with a circular cell phenotype giving rise to an identification system based on morphology
- BTM cells containing CLANs are less motile and malleable
- PAAs and CLANs may be different distinct entities

4.1 Future work

Future work should centre on finding further inhibitors of CLANs as more tools to inhibit would be beneficial for investigating their effect(s). It is likely that the different CLAN inducers are generated through distinct pathways, that in many cases will 'cross talk' with each other adding another layer of complexity to CLAN biology. It is probable that factors secreted by TM cells induce CLANs in other cells and the only other cell we have found CLANs present in is the lamina cribrosa cells from the optic nerve so performing microarrays for common genes that are differentially expressed would be a valid future experiment. It is noteworthy that the only other cell type found to express CLANs to date is the cell that ultimately perishes in POAG (Job et al., 2010). The proposed model that DEX leads to CLANs via integrin activation by binding to ECM components should be tested by neutralisation of fibronectin (ligand for integrins) and siRNA should be employed to knockdown Rac1 to determine its role in CLAN biogenesis. The *raison d'etre* of CLANs is unknown but may represent an adaptive response to perceived stimuli, that initially may be beneficial but in the longer term may be deleterious to cells. An analogy can be drawn with chronic inflammatory disease where the initial inflammatory response is beneficial (CLANs being anti-apoptotic), however longer term non-resolution of the inflammatory response and chronic long term cytokine expression leads to damage (CLANs inhibiting contraction and phagocytosis leading to increased free radical generation and oxidation of lipids and proteins and

inhibition of proteasomal pathways). Inhibition of Nf-κB activation should be further examined to determine if transcriptional activation is necessary for CLAN induction by the various gene products. The ciliary muscle should be analysed for CLANs. This would be important as this tissue is fundamental to outflow resistance.

5 References

ABERCROMBIE, M., HEAYSMAN, J. E. & PEGRUM, S. M. 1970. The locomotion of fibroblasts in culture. I. Movements of the leading edge. *Exp. Cell Res.*, 59, 393-8.

ADLBRECHT, C., HOETZENECKER, K., POSCH, M., STEINER, S., KOPP, C., HACKER, S., AUER, J., HORVATH, R., MOSER, B., ROTH, G., WOLNER, E., LANG, I. M. & ANKERSMIT, H. J. 2007. Elevated levels of interleukin-1β-converting enzyme and caspase-cleaved cytokeratin-18 in acute myocardial infarction. *Eur. J. Clin. Invest.*, 37, 372-380.

AGARWAL, R., TALATI, M., LAMBERT, W., CLARK, A. F., WILSON, S. E., AGARWAL, N. & WORDINGER, R. J. 1999a. Fas-activated apoptosis and apoptosis mediators in human trabecular meshwork cells. *Exp. Eye Res.*, 68, 583-90.

AGARWAL, R., TALATI, M., LAMBERT, W., CLARK, A. F., WILSON, S. E., AGARWAL, N. & WORDINGER, R. J. 1999b. Fas-Activated Apoptosis and Apoptosis Mediators in Human Trabecular Meshwork Cells. *Exp. Eye Res.*, 68, 583-590.

AIKO, I., YASUYUKI, S., MAKOTO, A., TETSUYA, Y., HARUKI, A., SHIROAKI, S., YASUAKI, K., HIROMU, K. M., HIROYUKI, S., GOJI, T., YOICHI, I. & YOSHIAKI, K. 2004. The prevalence of primary open-angle glaucoma in Japanese: The Tajimi Study. *Ophthalmology,* 111, 1641-1648.

ALEXANDER, J. P., SAMPLES, J. R. & ACOTT, T. S. 1998. Growth factor and cytokine modulation of trabecular meshwork matrix metalloproteinase and TIMP expression. *Curr. Eye Res.*, 17, 276-285.

ALVARADO, J., MURPHY, C. & JUSTER, R. 1984. Trabecular meshwork cellularity in primary open-angle glaucoma and nonglaucomatous normals. *Ophthalmology,* 91, 564-79.

ALVARADO, J. A., ALVARADO, R. G., YEH, R. F., FRANSE-CARMAN, L., MARCELLINO, G. R. & BROWNSTEIN, M. J. 2005. A new insight into the cellular regulation of aqueous outflow: how trabecular meshwork endothelial cells drive a mechanism that regulates the permeability of Schlemm's canal endothelial cells. *Br. J. Ophthalmol.*, 89, 1500-1505.

ANDERSON, D. R., DRANCE, S. M. & SCHULZER, M. 2001. Natural history of normal-tension glaucoma. *Ophthalmology,* 108, 247-53.

ARMALY, M. F. 1966. The heritable nature of dexamethasone-induced ocular hypertension. *Arch. Ophthalmol.*, 75, 32-5.

ASHTON, N., BRINI, A. & SMITH, R. 1956. ANATOMICAL STUDIES OF THE TRABECULAR MESHWORK OF THE NORMAL HUMAN EYE. *Br. J. Ophthalmol.*, 40, 257-282.

ASKARI, J. A., BUCKLEY, P. A., MOULD, A. P. & HUMPHRIES, M. J. 2009. Linking integrin conformation to function. *J. Cell Sci.*, 122, 165-170.

BALERIOLA, J., GARCIA-FEIJOO, J., MARTINEZ-DE-LA-CASA, J. M., FERNANDEZ-CRUZ, A., DE LA ROSA, E. J. & FERNANDEZ-DURANGO, R. 2008. Apoptosis in the trabecular meshwork of glaucomatous patients. *Mol. Vis.*, 14, 1513-6.

BARANY, E. H. & SCOTCHBROOK, S. 1954. Influence of testicular hyaluronidase on the resistance to flow through the angle of the anterior chamber. *Acta Physiol. Scand.*, 30, 240-8.

BARCELLOS-HOFF, M. & DIX, T. 1996. Redox-mediated activation of latent transforming growth factor-beta 1. *Mol. Endocrinol.*, 10, 1077-1083.

BECK, K. & BRODSKY, B. 1998. Supercoiled Protein Motifs: The Collagen Triple-Helix and the [alpha]-Helical Coiled Coil. *J. Struct. Biol.*, 122, 17-29.

BELL, E., IVARSSON, B. & MERRILL, C. 1979. Production of a tissue-like structure by contraction of collagen lattices by human fibroblasts of different proliferative potential in vitro. *Proc. Natl. Acad. Sci. U. S. A.*, 76, 1274-8.

BEVILACQUA, M. P., STENGELIN, S., GIMBRONE, M. A., JR. & SEED, B. 1989. Endothelial leukocyte adhesion molecule 1: an inducible receptor for neutrophils related to complement regulatory proteins and lectins. *Science,* 243, 1160-5.

BILL, A. & PHILLIPS, C. I. 1971. Uveoscleral drainage of aqueous humour in human eyes. *Exp. Eye Res.*, 12, 275-81.

BOLAND, S., BOISVIEUX-ULRICH, E., HOUCINE, O., BAEZA-SQUIBAN, A., POUCHELET, M., SCHOEVAERT, D. & MARANO, F. 1996. TGF beta 1 promotes actin cytoskeleton reorganization and migratory phenotype in epithelial tracheal cells in primary culture. *J. Cell Sci.*, 109, 2207-2219.

BRADLEY, J. M. B., KELLEY, M. J., ROSE, A. & ACOTT, T. S. 2003. Signaling Pathways Used in Trabecular Matrix Metalloproteinase Response to Mechanical Stretch. *Invest. Ophthalmol. Vis. Sci.*, 44, 5174-5181.

BRADLEY, J. M. B., KELLEY, M. J., ZHU, X., ANDERSSOHN, A. M., ALEXANDER, J. P. & ACOTT, T. S. 2001. Effects of Mechanical Stretching on Trabecular Matrix Metalloproteinases. *Invest. Ophthalmol. Vis. Sci.*, 42, 1505-1513.

BUTKEVICH, E., HÜLSMANN, S., WENZEL, D., SHIRAO, T., DUDEN, R. & MAJOUL, I. 2004. Drebrin Is a Novel Connexin-43 Binding Partner that Links Gap Junctions to the Submembrane Cytoskeleton. *Current biology : CB,* 14, 650-658.

CAI, S., LIU, X., GLASSER, A., VOLBERG, T., FILLA, M., GEIGER, B., POLANSKY, J. R. & KAUFMAN, P. L. 2000. Effect of latrunculin-A on morphology and actin-associated adhesions of cultured human trabecular meshwork cells. *Mol. Vis.*, 6, 132-43.

CAROL, B. T., MICHAEL, E. Y., YUN-LIANG, W. & CARL, B. C. 1999. Aqueous humor dynamics in the aging human eye. *Am. J. Ophthalmol.*, 127, 407-412.

CAWSTON, T. E. 1995. Proteinases and inhibitors. *Br. Med. Bull.*, 51, 385-401.

CAWSTON, T. E. 1996. Metalloproteinase inhibitors and the prevention of connective tissue breakdown. *Pharmacol. Ther.*, 70, 163-182.

CHAI, F., LUO, R., LI, Y., BAI, Y., HE, Y., WEI, Y., YAN, Z., GE, J. & ZHUO, Y. 2010. Down-regulation of GRP78 in human glaucomatous trabecular meshwork cells. *Mol. Vis.*, 16, 1122-31.

CHATZIKYRIAKIDOU, A., GEORGIOU, I., VOULGARI, P. V., GEORGIADIS, A. N., ARGYRIOU, E. S. & DROSOS, A. A. 2009. Glucocorticoid receptor variants may predispose to rheumatoid arthritis susceptibility. *Scand. J. Rheumatol.*, 38, 1-5.

CHEN, L. F. & GREENE, W. C. 2004. Shaping the nuclear action of NF-kappaB. *Nat Rev Mol Cell Biol,* 5, 392-401.

CHORITZ, L., ROSENTHAL, R., FROMM, M., FOERSTER, M. H. & THIEME, H. 2005. Pharmacological and functional characterization of endothelin receptors in bovine trabecular meshwork and ciliary muscle. *Ophthalmic Res.*, 37, 179-87.

CLAHSEN, T. & SCHAPER, F. 2008. Interleukin-6 acts in the fashion of a classical chemokine on monocytic cells by inducing integrin activation, cell adhesion, actin polymerization, chemotaxis, and transmigration. *J. Leukoc. Biol.,* 84, 1521-1529.

CLARK, A., LANE, D., WILSON, K., MIGGANS, S. & MCCARTNEY, M. 1996. Inhibition of dexamethasone-induced cytoskeletal changes in cultured human trabecular meshwork cells by tetrahydrocortisol. *Invest. Ophthalmol. Vis. Sci.,* 37, 805-813.

CLARK, A., WILSON, K., MCCARTNEY, M., MIGGANS, S., KUNKLE, M. & HOWE, W. 1994. Glucocorticoid-induced formation of cross-linked actin networks in cultured human trabecular meshwork cells. *Invest. Ophthalmol. Vis. Sci.,* 35, 281-294.

CLARK, A. F., BROTCHIE, D., READ, A. T., HELLBERG, P., ENGLISH-WRIGHT, S., PANG, I. H., ETHIER, C. R. & GRIERSON, I. 2005. Dexamethasone alters F-actin architecture and promotes cross-linked actin network formation in human trabecular meshwork tissue. *Cell Motil. Cytoskeleton,* 60, 83-95.

CLARK, A. F., MIGGANS, S. T., WILSON, K., BROWDER, S. & MCCARTNEY, M. D. 1995. Cytoskeletal changes in cultured human glaucoma trabecular meshwork cells. *J. Glaucoma,* 4, 183-8.

CLARK, A. F., STEELY, H. T., DICKERSON, J. E., ENGLISH-WRIGHT, S., STROPKI, K., MCCARTNEY, M. D., JACOBSON, N., SHEPARD, A. R., CLARK, J. I., MATSUSHIMA, H., PESKIND, E. R., LEVERENZ, J. B., WILKINSON, C. W., SWIDERSKI, R. E., FINGERT, J. H., SHEFFIELD, V. C. & STONE, E. M. 2001. Glucocorticoid Induction of the Glaucoma Gene MYOC in Human and Monkey Trabecular Meshwork Cells and Tissues. *Invest. Ophthalmol. Vis. Sci.,* 42, 1769-1780.

COLEMAN, D. J. & TROKEL, S. 1969. Direct-Recorded Intraocular Pressure Variations in a Human Subject. *Arch. Ophthalmol.,* 82, 637-640.

COLEMAN, M. L., SAHAI, E. A., YEO, M., BOSCH, M., DEWAR, A. & OLSON, M. F. 2001. Membrane blebbing during apoptosis results from caspase-mediated activation of ROCK I. *Nat Cell Biol,* 3, 339-345.

COULOMB, B., DUBERTRET, L., BELL, E. & TOURAINE, R. 1984. The contractility of fibroblasts in a collagen lattice is reduced by corticosteroids. *J. Invest. Dermatol.,* 82, 341-4.

CRAMER, L. P., SIEBERT, M. & MITCHISON, T. J. 1997. Identification of Novel Graded Polarity Actin Filament Bundles in Locomoting Heart Fibroblasts: Implications for the Generation of Motile Force. *The Journal of Cell Biology,* 136, 1287-1305.

DAN, J., BELYEA, D., GERTNER, G., LESHEM, I., LUSKY, M. & MISKIN, R. 2005. Plasminogen Activator Inhibitor-1 in the Aqueous Humor of Patients With and Without Glaucoma. *Arch. Ophthalmol.,* 123, 220-224.

DAY, J., GRIERSON, I., UNGER, W. G. & ROBINS, E. 1986. Some effects of phagocytosis on bovine meshwork cells in culture. *Exp. Eye Res.,* 43, 1077-1087.

DE BERARDINIS, E., TIERI, O., POLZELLA, A. & IUGLIO, N. 1965. The chemical composition of the human aqueous humour in normal and pathological conditions. *Exp. Eye Res.,* 4, 179-186.

DE SMAELE, E., ZAZZERONI, F., PAPA, S., NGUYEN, D. U., JIN, R., JONES, J., CONG, R. & FRANZOSO, G. 2001. Induction of gadd45[beta] by NF-[kappa]B downregulates pro-apoptotic JNK signalling. *Nature,* 414, 308-313.

DERIJK, R. H., SCHAAF, M. J., TURNER, G., DATSON, N. A., VREUGDENHIL, E., CIDLOWSKI, J., DE KLOET, E. R., EMERY, P., STERNBERG, E. M. & DETERA-WADLEIGH, S. D. 2001. A human glucocorticoid receptor gene variant that increases the stability of the glucocorticoid receptor beta-isoform mRNA is associated with rheumatoid arthritis. *J. Rheumatol.,* 28, 2383-8.

DERYNCK, R. & AKHURST, R. J. 2007. Differentiation plasticity regulated by TGF-[beta] family proteins in development and disease. *Nat Cell Biol,* 9, 1000-1004.

DIELEMANS, I., VINGERLING, J. R., WOLFS, R. C., HOFMAN, A., GROBBEE, D. E. & DE JONG, P. T. 1994. The prevalence of primary open-angle glaucoma in a population-based study in The Netherlands. The Rotterdam Study. *Ophthalmology,* 101, 1851-5.

DRANCE, S., ANDERSON, D. R. & SCHULZER, M. 2001. Risk factors for progression of visual field abnormalities in normal-tension glaucoma. *Am. J. Ophthalmol.,* 131, 699-708.

EDLUND, S., LANDSTROM, M., HELDIN, C.-H. & ASPENSTROM, P. 2002. Transforming Growth Factor-beta -induced Mobilization of Actin Cytoskeleton Requires Signaling by Small GTPases Cdc42 and RhoA. *Mol. Biol. Cell,* 13, 902-914.

EHRLICH, H. P., BUTTLE, D. J. & BERNANKE, D. H. 1989. Physiological variables affecting collagen lattice contraction by human dermal fibroblasts. *Exp. Mol. Pathol.,* 50, 220-229.

ETHIER, C. R., READ, A. T. & CHAN, D. W.-H. 2006. Effects of Latrunculin-B on Outflow Facility and Trabecular Meshwork Structure in Human Eyes. *Invest. Ophthalmol. Vis. Sci.,* 47, 1991-1998.

FADOK, V., VOELKER, D., CAMPBELL, P., COHEN, J., BRATTON, D. & HENSON, P. 1992. Exposure of phosphatidylserine on the surface of apoptotic lymphocytes triggers specific recognition and removal by macrophages. *J. Immunol.,* 148, 2207-2216.

FAUTSCH, M. P., HOWELL, K. G., VRABEL, A. M., CHARLESWORTH, M. C., MUDDIMAN, D. C. & JOHNSON, D. H. 2005. Primary Trabecular Meshwork Cells Incubated in Human Aqueous Humor Differ from Cells Incubated in Serum Supplements. *Invest. Ophthalmol. Vis. Sci.,* 46, 2848-2856.

FIGGE, R. M., DIVAKARUNI, A. V. & GOBER, J. W. 2004. MreB, the cell shape-determining bacterial actin homologue, co-ordinates cell wall morphogenesis in Caulobacter crescentus. *Mol. Microbiol.,* 51, 1321-32.

FILLA , M. S., SCHWINN , M. K., NOSIE , A. K., CLARK , R. W. & PETERS, D. M. Dexamethasone-associated cross-linked actin network (CLAN) formation in human trabecular meshwork (HTM) cells involves β3 integrin signaling. *Invest. Ophthalmol. Vis. Sci.*

FILLA, M. S., SCHWINN, M. K., SHEIBANI, N., KAUFMAN, P. L. & PETERS, D. M. 2009. Regulation of Cross-linked Actin Network (CLAN) Formation in Human Trabecular Meshwork (HTM) Cells by Convergence of Distinct {beta}1 and {beta}3 Integrin Pathways. *Invest. Ophthalmol. Vis. Sci.,* 50, 5723-5731.

FILLA, M. S., WOODS, A., KAUFMAN, P. L. & PETERS, D. M. 2006. {beta}1 and {beta}3 Integrins Cooperate to Induce Syndecan-4-Containing Cross-linked Actin Networks in Human Trabecular Meshwork Cells. *Invest. Ophthalmol. Vis. Sci.,* 47, 1956-1967.

FLEENOR, D. L., SHEPARD, A. R., HELLBERG, P. E., JACOBSON, N., PANG, I.-H. & CLARK, A. F. 2006. TGFβ2-Induced Changes in Human Trabecular Meshwork: Implications for Intraocular Pressure. *Invest. Ophthalmol. Vis. Sci.,* 47, 226-234.

FLÜGEL-KOCH, C., OHLMANN, A., FUCHSHOFER, R., WELGE-LÜSSEN, U. & TAMM, E. R. 2004. Thrombospondin-1 in the trabecular meshwork: localization in normal and glaucomatous eyes, and induction by TGF-[beta]1 and dexamethasone in vitro. *Exp. Eye Res.,* 79, 649-663.

FLÜGEL, C., TAMM, E. & LÜTJEN-DRECOLL, E. 1991. Different cell populations in bovine trabecular meshwork: An ultrastructural and immunocytochemical study. *Exp. Eye Res.,* 52, 681-690.

FREDDO, T., BARTELS, S., BARSOTTI, M. & KAMM, R. 1990. The source of proteins in the aqueous humor of the normal rabbit. *Invest. Ophthalmol. Vis. Sci.,* 31, 125-137.

FREDDO, T., PATTERSON, M., SCOTT, D. & EPSTEIN, D. 1984. Influence of mercurial sulfhydryl agents on aqueous outflow pathways in enucleated eyes. *Invest. Ophthalmol. Vis. Sci.,* 25, 278-285.

FREEDMAN, S., ANDERSON, P. & EPSTEIN, D. 1985. Superoxide dismutase and catalase of calf trabecular meshwork. *Invest. Ophthalmol. Vis. Sci.,* 26, 1330-1335.

FUCHSHOFER, R., STEPHAN, D. A., RUSSELL, P. & TAMM, E. R. 2009. Gene expression profiling of TGF[beta]2- and/or BMP7-treated trabecular meshwork cells: Identification of Smad7 as a critical inhibitor of TGF-[beta]2 signaling. *Exp. Eye Res.,* 88, 1020-1032.

FUCHSHOFER, R., WELGE-LUSSEN, U. & LÜTJEN-DRECOLL, E. 2003. The effect of TGF-[beta]2 on human trabecular meshwork extracellular proteolytic system. *Exp. Eye Res.,* 77, 757-765.

FUCHSHOFER, R., YU, A. H. L., WELGE-LÜSSEN, U. & TAMM, E. R. 2007. Bone Morphogenetic Protein-7 Is an Antagonist of Transforming Growth Factor-β2 in Human Trabecular Meshwork Cells. *Invest. Ophthalmol. Vis. Sci.,* 48, 715-726.

GAGELIN, C., PIERRE, M., GAVARET, J.-M. & TORU-DELBAUFFE, D. 1995. Rapid TGFβ1 effects on actin cytoskeleton of astrocytes: Comparison with other factors and implications for cell motility. *Glia,* 13, 283-293.

GEROMETTA, R., PODOS, S. M., CANDIA, O. A., WU, B., MALGOR, L. A., MITTAG, T. & DANIAS, J. 2004. Steroid-induced ocular hypertension in normal cattle. *Arch. Ophthalmol.,* 122, 1492-7.

GIEPMANS, B. N. G., VERLAAN, I., HENGEVELD, T., JANSSEN, H., CALAFAT, J., FALK, M. M. & MOOLENAAR, W. H. 2001. Gap junction protein connexin-43 interacts directly with microtubules. *Current biology : CB,* 11, 1364-1368.

GILBERT, J. A., WEINHOLD, P. S., BANES, A. J., LINK, G. W. & JONES, G. L. 1994. Strain profiles for circular cell culture plates containing flexible surfaces employed to mechanically deform cells in vitro. *J. Biomech.,* 27, 1169-77.

GIRY, M., POPOFF, M., VON EICHEL-STREIBER, C. & BOQUET, P. 1995. Transient expression of RhoA, -B, and -C GTPases in HeLa cells potentiates resistance to Clostridium difficile toxins A and B but not to Clostridium sordellii lethal toxin. *Infect. Immun.*, 63, 4063-4071.

GONG, H. Y., TRINKAUS-RANDALL, V. & FREDDO, T. F. 1989. Ultrastructural immunocytochemical localization of elastin in normal human trabecular meshwork. *Curr. Eye Res.*, 8, 1071-82.

GOTTANKA, J., CHAN, D., EICHHORN, M., LUTJEN-DRECOLL, E. & ETHIER, C. R. 2004. Effects of TGF-{beta}2 in Perfused Human Eyes. *Invest. Ophthalmol. Vis. Sci.*, 45, 153-158.

GRANT, W. M. 1963. Experimental aqueous perfusion in enucleated human eyes. *Arch. Ophthalmol.*, 69, 783-801.

GRIERSON, I. & HOWES, R. C. 1987. Age-related depletion of the cell population in the human trabecular meshwork. *Eye (Lond)*, 1 (Pt 2), 204-10.

GRIERSON, I., KISSUN, R., AYAD, S., PHYLACTOS, A., AHMED, S., UNGER, W. G. & DAY, J. E. 1985a. The morphological features of bovine meshwork cells in vitro and their synthetic activities. *Graefes Arch. Clin. Exp. Ophthalmol.*, 223, 225-36.

GRIERSON, I. & LEE, W. R. 1973. Erythrocyte phagocytosis in the human trabecular meshwork. *Br. J. Ophthalmol.*, 57, 400-415.

GRIERSON, I. & LEE, W. R. 1975. The fine structure of the trabecular meshwork at graded levels of intraocular pressure: (1) Pressure effects within the near-physiological range (8-30 mmHg). *Exp. Eye Res.*, 20, 505-521.

GRIERSON, I., LEE, W. R. & ABRAHAM, S. 1978. Effects of pilocarpine on the morphology of the human outflow apparatus. *Br. J. Ophthalmol.*, 62, 302-313.

GRIERSON, I., MARSHALL, J. & ROBINS, E. 1983. Human trabecular meshwork in primary culture: A morphological and autoradiographic study. *Exp. Eye Res.*, 37, 349-365.

GRIERSON, I., MILLAR, L., DE YONG, J., DAY, J., MCKECHNIE, N., HITCHINS, C. & BOULTON, M. 1986. Investigations of cytoskeletal elements in cultured bovine meshwork cells. *Invest. Ophthalmol. Vis. Sci.*, 27, 1318-1330.

GRIERSON, I., ROBINS, E., UNGER, W., MILLAR, L. & AHMED, A. 1985b. The cells of the bovine outflow system in tissue culture. *Exp. Eye Res.*, 40, 35-46.

GRISANTI, S., SZURMAN, P., WARGA, M., KACZMAREK, R., ZIEMSSEN, F., TATAR, O. & BARTZ-SCHMIDT, K. U. 2005. Decorin modulates wound healing in experimental glaucoma filtration surgery: a pilot study. *Invest. Ophthalmol. Vis. Sci.*, 46, 191-6.

HAMANAKA, T., BILL, A., ICHINOHASAMA, R. & ISHIDA, T. 1992. Aspects of the development of Schlemm's canal. *Exp. Eye Res.*, 55, 479-488.

HAYASAKA, K., OIKAWA, S., HASHIZUME, E., KOTAKE, H., MIDORIKAWA, H., SEKIKAWA, A., HOSHI, K., HARA, S., ISHIGAKI, Y. & TOYOTA, T. 1998. Anti-angiogenic effect of TGFbeta in aqueous humor. *Life Sci.*, 63, 1089-96.

HE, M., FOSTER, P. J., JOHNSON, G. J. & KHAW, P. T. 2005. Angle-closure glaucoma in East Asian and European people. Different diseases? *Eye*, 20, 3-12.

HEIJL, A., LESKE, M. C., BENGTSSON, B., HYMAN, L., BENGTSSON, B., HUSSEIN, M. & FOR THE EARLY MANIFEST GLAUCOMA TRIAL

GROUP 2002. Reduction of Intraocular Pressure and Glaucoma Progression: Results From the Early Manifest Glaucoma Trial. *Arch. Ophthalmol.,* 120, 1268-1279.

HERNANDEZ, M. R., WENK, E. J., WEINSTEIN, B. I., ABUMOHOR, P., PODOS, S. M., DUNN, M. W. & SOUTHREN, A. L. 1983. Glucocorticoid target cells in human outflow pathway: autopsy and surgical specimens. *Invest. Ophthalmol. Vis. Sci.,* 24, 1612-6.

HOARE, M.-J., GRIERSON, I., BROTCHIE, D., POLLOCK, N., CRACKNELL, K. & CLARK, A. F. 2009. Cross-Linked Actin Networks (CLANs) in the Trabecular Meshwork of the Normal and Glaucomatous Human Eye In Situ. *Invest. Ophthalmol. Vis. Sci.,* 50, 1255-1263.

HOGG, P., CALTHORPE, M., WARD, S. & GRIERSON, I. 1995a. Migration of cultured bovine trabecular meshwork cells to aqueous humor and constituents. *Invest. Ophthalmol. Vis. Sci.,* 36, 2449-60.

HOGG, P., CALTHORPE, M., WARD, S. & GRIERSON, I. 1995b. Migration of cultured bovine trabecular meshwork cells to aqueous humor and constituents. *Invest. Ophthalmol. Vis. Sci.,* 36, 2449-2460.

HOLLOWS, F. C. & GRAHAM, P. A. 1966. Intra-ocular pressure, glaucoma, and glaucoma suspects in a defined population. *Br. J. Ophthalmol.,* 50, 570-586.

HOSSEINI, M., ROSE, A. Y., SONG, K., BOHAN, C., ALEXANDER, J. P., KELLEY, M. J. & ACOTT, T. S. 2006. IL-1 and TNF Induction of Matrix Metalloproteinase-3 by c-Jun N-Terminal Kinase in Trabecular Meshwork. *Invest. Ophthalmol. Vis. Sci.,* 47, 1469-1476.

HOWELL, K. G., VRABEL, A. M., CHOWDHURY, U. R., STAMER, W. D. & FAUTSCH, M. P. 2010. Myocilin Levels in Primary Open-angle Glaucoma and Pseudoexfoliation Glaucoma Human Aqueous Humor. *J. Glaucoma,* 19, 569-575 10.1097/IJG.0b013e3181d13020.

HU, D.-N. & RITCH, R. 2001. Hepatocyte Growth Factor is Increased in the Aqueous Humor of Glaucomatous Eyes. *J. Glaucoma,* 10, 152-157.

HU, D.-N., RITCH, R., LIEBMANN, J., LIU, Y., CHENG, B. & HU, M. S. 2002. Vascular Endothelial Growth Factor is Increased in Aqueous Humor of Glaucomatous Eyes. *J. Glaucoma,* 11, 406-410.

HUTTENLOCHER, A., WERB, Z., TREMBLE, P., HUHTALA, P., ROSENBERG, L. & DAMSKY, C. H. 1996. Decorin regulates collagenase gene expression in fibroblasts adhering to vitronectin. *Matrix Biol.,* 15, 239-250.

INGBER, D. E. 2006. Cellular mechanotransduction: putting all the pieces together again. *The FASEB Journal,* 20, 811-827.

IRELAND, G. & VOON, F. 1981. Polygonal networks in living chick embryonic cells. *J. Cell Sci.,* 52, 55-69.

ISHIBASHI, T., TAKAGI, Y., MORI, K., NARUSE, S., NISHINO, H., YUE, B. Y. J. T. & KINOSHITA, S. 2002. cDNA Microarray Analysis of Gene Expression Changes Induced by Dexamethasone in Cultured Human Trabecular Meshwork Cells. *Invest. Ophthalmol. Vis. Sci.,* 43, 3691-3697.

ISHII, Y., KWONG, J. M. & CAPRIOLI, J. 2003. Retinal ganglion cell protection with geranylgeranylacetone, a heat shock protein inducer, in a rat glaucoma model. *Invest. Ophthalmol. Vis. Sci.,* 44, 1982-92.

JACOBSON, N., ANDREWS, M., SHEPARD, A. R., NISHIMURA, D., SEARBY, C., FINGERT, J. H., HAGEMAN, G., MULLINS, R., DAVIDSON, B. L., KWON, Y. H., ALWARD, W. L. M., STONE, E. M., CLARK, A. F. & SHEFFIELD, V. C. 2001. Non-secretion of mutant proteins of the glaucoma

gene myocilin in cultured trabecular meshwork cells and in aqueous humor. *Hum. Mol. Genet.*, 10, 117-125.

JAMPEL, H. D., ROCHE, N., STARK, W. J. & ROBERTS, A. B. 1990. Transforming growth factor-beta in human aqueous humor. *Curr. Eye Res.*, 9, 963-9.

JINNIN, M., IHN, H. & TAMAKI, K. 2006. Characterization of SIS3, a Novel Specific Inhibitor of Smad3, and Its Effect on Transforming Growth Factor-β1-Induced Extracellular Matrix Expression. *Mol. Pharmacol.*, 69, 597-607.

JOB, R., RAJA, V., GRIERSON, I., CURRIE, L., O'REILLY, S., POLLOCK, N., KNIGHT, E. & CLARK, A. F. 2010. Cross-linked actin networks (CLANs) are present in lamina cribrosa cells. *Br. J. Ophthalmol.*, 94, 1388-92.

JOBLING, M. F., MOTT, J. D., FINNEGAN, M. T., JURUKOVSKI, V., ERICKSON, A. C., WALIAN, P. J., TAYLOR, S. E., LEDBETTER, S., LAWRENCE, C. M., RIFKIN, D. B. & BARCELLOS-HOFF, M. H. 2006. Isoform-Specific Activation of Latent Transforming Growth Factor β (LTGF-β) by Reactive Oxygen Species. *Radiat. Res.*, 166, 839-848.

JOE, M. K. & TOMAREV, S. I. 2010. Expression of Myocilin Mutants Sensitizes Cells to Oxidative Stress-Induced Apoptosis: Implication for Glaucoma Pathogenesis. *The American Journal of Pathology,* 176, 2880-2890.

JOHNSON, D. 1997. The effect of cytochalasin D on outflow facility and the trabecular meshwork of the human eye in perfusion organ culture. *Invest. Ophthalmol. Vis. Sci.*, 38, 2790-2799.

JOHNSON, D. H. & TSCHUMPER, R. C. 1993. Ethacrynic acid: outflow effects and toxicity in human trabecular meshwork in perfusion organ culture. *Curr. Eye Res.*, 12, 385-396.

JOHNSTONE, M. A. 2004. The Aqueous Outflow System as a Mechanical Pump: Evidence from Examination of Tissue and Aqueous Movement in Human and Non-Human Primates. *J. Glaucoma,* 13, 421-438.

JONES, R. F. & MAURICE, D. M. 1966. New methods of measuring the rate of aqueous flow in man with fluorescein. *Exp. Eye Res.*, 5, 208-220.

KASS, M. A., HEUER, D. K., HIGGINBOTHAM, E. J., JOHNSON, C. A., KELTNER, J. L., MILLER, J. P., PARRISH II, R. K., WILSON, M. R., GORDON, M. O. & FOR THE OCULAR HYPERTENSION TREATMENT STUDY GROUP 2002. The Ocular Hypertension Treatment Study: A Randomized Trial Determines That Topical Ocular Hypotensive Medication Delays or Prevents the Onset of Primary Open-Angle Glaucoma. *Arch. Ophthalmol.*, 120, 701-713.

KATOH, M. & KATOH, M. 2007. WNT Signaling Pathway and Stem Cell Signaling Network. *Clin. Cancer Res.*, 13, 4042-4045.

KAWA, J. E., HIGGINBOTHAM, E. J., CHANG, I. L. & YUE, B. Y. J. T. 1993. Effects of Antiglaucoma Medications on Bovine Trabecular Meshwork Cells In Vitro. *Exp. Eye Res.*, 57, 557-565.

KAYALAR, C., ORD, T., TESTA, M. P., ZHONG, L. T. & BREDESEN, D. E. 1996. Cleavage of actin by interleukin 1 beta-converting enzyme to reverse DNase I inhibition. *Proc. Natl. Acad. Sci. U. S. A.*, 93, 2234-2238.

KEE, C. & SEO, K. 1997. The effect of interleukin-1alpha on outflow facility in rat eyes. *J. Glaucoma,* 6, 246-9.

KELLEY, M. J., ROSE, A. Y., SONG, K., CHEN, Y., BRADLEY, J. M., ROOKHUIZEN, D. & ACOTT, T. S. 2007. Synergism of TNF and IL-1 in

the Induction of Matrix Metalloproteinase-3 in Trabecular Meshwork. *Invest. Ophthalmol. Vis. Sci.,* 48, 2634-2643.

KERRIGAN, L. A., ZACK, D. J., QUIGLEY, H. A., SMITH, S. D. & PEASE, M. E. 1997. TUNEL-positive ganglion cells in human primary open-angle glaucoma. *Arch. Ophthalmol.,* 115, 1031-5.

KIM, M., CARMAN, C. V. & SPRINGER, T. A. 2003. Bidirectional Transmembrane Signaling by Cytoplasmic Domain Separation in Integrins. *Science,* 301, 1720-1725.

KIMURA, K., ITO, M., AMANO, M., CHIHARA, K., FUKATA, Y., NAKAFUKU, M., YAMAMORI, B., FENG, J., NAKANO, T., OKAWA, K., IWAMATSU, A. & KAIBUCHI, K. 1996. Regulation of Myosin Phosphatase by Rho and Rho-Associated Kinase (Rho-Kinase). *Science,* 273, 245-248.

KIMURA, S., SUZUKI, K., SAGARA, T., NISHIDA, T., YAMAMOTO, T. & KITAZAWA, Y. 2000. Regulation of Connexin Phosphorylation and Cell–Cell Coupling in Trabecular Meshwork Cells. *Invest. Ophthalmol. Vis. Sci.,* 41, 2222-2228.

KLEIN, B. E., KLEIN, R., SPONSEL, W. E., FRANKE, T., CANTOR, L. B., MARTONE, J. & MENAGE, M. J. 1992. Prevalence of glaucoma. The Beaver Dam Eye Study. *Ophthalmology,* 99, 1499-504.

KLENKLER, B. & SHEARDOWN, H. 2004. Growth factors in the anterior segment: role in tissue maintenance, wound healing and ocular pathology. *Exp. Eye Res.,* 79, 677-688.

KOGA, T., KOGA, T., AWAI, M., TSUTSUI, J.-I., YUE, B. Y. J. T. & TANIHARA, H. 2006. Rho-associated protein kinase inhibitor, Y-27632, induces alterations in adhesion, contraction and motility in cultured human trabecular meshwork cells. *Exp. Eye Res.,* 82, 362-370.

KOKAWA, N., SOTOZONO, C., NISHIDA, K. & KINOSHITA, S. 1996. High total TGF-beta 2 levels in normal human tears. *Curr. Eye Res.,* 15, 341-3.

KOUKOURITAKI, S. B., MARGIORIS, A. N., GRAVANIS, A., HARTIG, R. & STOURNARAS, C. 1997. Dexamethasone induces rapid actin assembly in human endometrial cells without affecting its synthesis. *J. Cell. Biochem.,* 65, 492-500.

KREIS, T. E. & BIRCHMEIER, W. 1980. Stress fiber sarcomeres of fibroblasts are contractile. *Cell,* 22, 555-61.

KULKARNI, A. B., HUH, C. G., BECKER, D., GEISER, A., LYGHT, M., FLANDERS, K. C., ROBERTS, A. B., SPORN, M. B., WARD, J. M. & KARLSSON, S. 1993. Transforming growth factor beta 1 null mutation in mice causes excessive inflammatory response and early death. *Proc. Natl. Acad. Sci. U. S. A.,* 90, 770-774.

KUMAR, N. M. & GILULA, N. B. 1996. The Gap Junction Communication Channel. *Cell,* 84, 381-388.

KUMAR, S., MAXWELL, I. Z., HEISTERKAMP, A., POLTE, T. R., LELE, T. P., SALANGA, M., MAZUR, E. & INGBER, D. E. 2006. Viscoelastic retraction of single living stress fibers and its impact on cell shape, cytoskeletal organization, and extracellular matrix mechanics. *Biophys. J.,* 90, 3762-73.

KWON, H.-S., LEE, H.-S., JI, Y., RUBIN, J. S. & TOMAREV, S. I. 2009. Myocilin Is a Modulator of Wnt Signaling. *Mol. Cell. Biol.,* 29, 2139-2154.

LAEMMLI, U. K. 1970. Cleavage of structural proteins during the assembly of the head of bacteriophage T4. *Nature,* 227, 680-5.

LAST, J. A., PAN, T., DING, Y., REILLY, C. M., KELLER, K., ACOTT, T. S., FAUTSCH, M. P., MURPHY, C. J. & RUSSELL, P. 2011. Elastic Modulus Determination of Normal and Glaucomatous Human Trabecular Meshwork. *Invest. Ophthalmol. Vis. Sci.,* 52, 2147-2152.

LAZARIDES, E. 1975. Immunofluorescence studies on the structure of actin filaments in tissue culture cells. *J. Histochem. Cytochem.,* 23, 507-528.

LAZARIDES, E. 1976. Actin, alpha-actinin, and tropomyosin interaction in the structural organization of actin filaments in nonmuscle cells. *The Journal of Cell Biology,* 68, 202-219.

LAZARIDES, E. & BURRIDGE, K. 1975. Alpha-actinin: immunofluorescent localization of a muscle structural protein in nonmuscle cells. *Cell,* 6, 289-98.

LEE, H., O'MEARA, S. J., O'BRIEN, C. & KANE, R. 2007. The Role of Gremlin, a BMP Antagonist, and Epithelial-to-Mesenchymal Transition in Proliferative Vitreoretinopathy. *Invest. Ophthalmol. Vis. Sci.,* 48, 4291-4299.

LEE, K. M., PARK, J., KIM, J. H., YIE, S. W., CHUN, G.-T., KIM, P.-H. & CHOI, E. Y. 1999. REORGANIZATION OF MYOSIN AND FOCAL ADHESION PROTEINS IN SWISS 3T3 FIBROBLASTS INDUCED BY TRANSFORMING GROWTH FACTOR BETA. *Cell Biol. Int.,* 23, 507-517.

LEPPLE-WIENHUES, A., STAHL, F. & WIEDERHOLT, M. 1991. Differential smooth muscle-like contractile properties of trabecular meshwork and ciliary muscle. *Exp. Eye Res.,* 53, 33-38.

LESKE, M. C., BARBARA, N., QIMEI, H., SUH-YUH, W., JAMES FIELDING, H. & ANSELM, H. 2001. Patterns of open-angle glaucoma in the Barbados Family Study. *Ophthalmology,* 108, 1015-1022.

LESKE, M. C., CONNELL, A. M. S., SCHACHAT, A. P., HYMAN, L. & BARBADOS EYE STUDY GROUP 1994. The Barbados Eye Study: Prevalence of Open Angle Glaucoma. *Arch. Ophthalmol.,* 112, 821-829.

LI, J., TRIPATHI, B. J. & TRIPATHI, R. C. 2000. Modulation of Pre-mRNA Splicing and Protein Production of Fibronectin by TGF-β2 in Porcine Trabecular Cells. *Invest. Ophthalmol. Vis. Sci.,* 41, 3437-3443.

LIN, Z. X., HOLTZER, S., SCHULTHEISS, T., MURRAY, J., MASAKI, T., FISCHMAN, D. A. & HOLTZER, H. 1989. Polygons and adhesion plaques and the disassembly and assembly of myofibrils in cardiac myocytes. *The Journal of Cell Biology,* 108, 2355-2367.

LINDSEY, J. D., KASHIWAGI, K., KASHIWAGI, F. & WEINREB, R. N. 1997. Prostaglandins alter extracellular matrix adjacent to human ciliary muscle cells in vitro. *Invest. Ophthalmol. Vis. Sci.,* 38, 2214-23.

LITON, P., LIU, X., CHALLA, P., EPSTEIN, D. & GONZALEZ, P. 2005a. Induction of TGF-β1 in the trabecular meshwork under cyclic mechanical stress. *J. Cell. Physiol.,* 205, 364-371.

LITON, P. B., LI, G., LUNA, C., GONZALEZ, P. & EPSTEIN, D. L. 2009. Cross-talk between TGF-beta1 and IL-6 in human trabecular meshwork cells. *Mol. Vis.,* 15, 326-34.

LITON, P. B., LUNA, C., BODMAN, M., HONG, A., EPSTEIN, D. L. & GONZALEZ, P. 2005b. Induction of IL-6 expression by mechanical stress in the trabecular meshwork. *Biochem. Biophys. Res. Commun.,* 337, 1229-1236.

LO, W. R., ROWLETTE, L. L., CABALLERO, M., YANG, P., HERNANDEZ, M. R. & BORRAS, T. 2003. Tissue Differential Microarray Analysis of Dexamethasone Induction Reveals Potential Mechanisms of Steroid Glaucoma. *Invest. Ophthalmol. Vis. Sci.,* 44, 473-485.

LU, Z., OVERBY, D. R., SCOTT, P. A., FREDDO, T. F. & GONG, H. 2008. The mechanism of increasing outflow facility by rho-kinase inhibition with Y-27632 in bovine eyes. *Exp. Eye Res.*, 86, 271-81.

LUNA, C., LI, G., LITON, P. B., EPSTEIN, D. L. & GONZALEZ, P. 2009. Alterations in gene expression induced by cyclic mechanical stress in trabecular meshwork cells. *Mol. Vis.*, 15, 534-44.

LUTJEN-DRECOLL, E., FUTA, R. & ROHEN, J. W. 1981. Ultrahistochemical studies on tangential sections of the trabecular meshwork in normal and glaucomatous eyes. *Invest. Ophthalmol. Vis. Sci.*, 21, 563-73.

LUTJEN-DRECOLL, E., SHIMIZU, T., ROHRBACH, M. & ROHEN, J. W. 1986. Quantitative analysis of 'plaque material' in the inner- and outer wall of Schlemm's canal in normal- and glaucomatous eyes. *Exp. Eye Res.*, 42, 443-55.

MACHESKY, L. M. & HALL, A. 1997. Role of actin polymerization and adhesion to extracellular matrix in Rac- and Rho-induced cytoskeletal reorganization. *J. Cell Biol.*, 138, 913-26.

MAIER, P., BROSZINSKI, A., HEIZMANN, U., BOEHRINGER, D. & REINHARD, T. 2006. Determination of active TGF-beta2 in aqueous humor prior to and following cryopreservation. *Mol. Vis.*, 12, 1477-82.

MAILHOS, C., HOWARD, M. K. & LATCHMAN, D. S. 1993. Heat shock protects neuronal cells from programmed cell death by apoptosis. *Neuroscience*, 55, 621-627.

MANSER, E., LEUNG, T., SALIHUDDIN, H., ZHAO, Z.-S. & LIM, L. 1994. A brain serine/threonine protein kinase activated by Cdc42 and Rac1. *Nature*, 367, 40-46.

MASSAGUÉ, J. & GOMIS, R. R. 2006. The logic of TGF[beta] signaling. *FEBS Lett.*, 580, 2811-2820.

MCCARTNEY, M. D., CANTU-CROUCH, D. & CLARK, A. F. 2006. Freeze-fracture examination of cultured human trabecular meshwork cells: Effect of dexamethasone. *Exp. Eye Res.*, 82, 994-1001.

MELLER, K. & THEISS, C. 2006. Atomic force microscopy and confocal laser scanning microscopy on the cytoskeleton of permeabilised and embedded cells. *Ultramicroscopy*, 106, 320-325.

MIN, S. H., LEE, T.-I., CHUNG, Y. S. & KIM, H. K. 2006. Transforming Growth Factor-β Levels in Human Aqueous Humor of Glaucomatous, Diabetic and Uveitic Eyes. *Korean J. Ophthalmol.*, 20, 162-165.

MITCHELL, P., SMITH, W., ATTEBO, K. & HEALEY, P. R. 1996. Prevalence of open-angle glaucoma in Australia. The Blue Mountains Eye Study. *Ophthalmology*, 103, 1661-9.

MITTON, K. P., TUMMINIA, S. J., ARORA, J., ZELENKA, P., EPSTEIN, D. L. & RUSSELL, P. 1997. Transient Loss of [alpha]B-Crystallin: An Early Cellular Response to Mechanical Stretch. *Biochem. Biophys. Res. Commun.*, 235, 69-73.

MOCHIZUKI, Y., FURUKAWA, K., MITAKA, T., YOKOI, T. & KODAMA, T. 1988. Polygonal networks, "geodomes", of adult rat hepatocytes in primary culture. *Cell Biol. Int. Rep.*, 12, 1-7.

MOHAN, R. R., GUPTA, R., MEHAN, M. K., COWDEN, J. W. & SINHA, S. 2010. Decorin transfection suppresses profibrogenic genes and myofibroblast formation in human corneal fibroblasts. *Exp. Eye Res.*, 91, 238-245.

MOON, R. T., KOHN, A. D., FERRARI, G. V. D. & KAYKAS, A. 2004. WNT and [beta]-catenin signalling: diseases and therapies. *Nat Rev Genet,* 5, 691-701.

MORGAN, M. R., HUMPHRIES, M. J. & BASS, M. D. 2007. Synergistic control of cell adhesion by integrins and syndecans. *Nat Rev Mol Cell Biol,* 8, 957-969.

MORRIS, D. G., HUANG, X., KAMINSKI, N., WANG, Y., SHAPIRO, S. D., DOLGANOV, G., GLICK, A. & SHEPPARD, D. 2003. Loss of integrin [alpha]v[beta]6-mediated TGF-[beta] activation causes Mmp12-dependent emphysema. *Nature,* 422, 169-173.

MUNGER, J. S., HUANG, X., KAWAKATSU, H., GRIFFITHS, M. J. D., DALTON, S. L., WU, J., PITTET, J.-F., KAMINSKI, N., GARAT, C., MATTHAY, M. A., RIFKIN, D. B. & SHEPPARD, D. 1999. A Mechanism for Regulating Pulmonary Inflammation and Fibrosis: The Integrin ±v²6 Binds and Activates Latent TGF ²1. *Cell,* 96, 319-328.

MYLLARNIEMI, M., LINDHOLM, P., RYYNANEN, M. J., KLIMENT, C. R., SALMENKIVI, K., KESKI-OJA, J., KINNULA, V. L., OURY, T. D. & KOLI, K. 2008. Gremlin-mediated Decrease in Bone Morphogenetic Protein Signaling Promotes Pulmonary Fibrosis. *Am. J. Respir. Crit. Care Med.,* 177, 321-329.

NAGAI, Y., LAPIERE, C. M. & GROSS, J. 1966. Tadpole Collagenase. Preparation and Purification*. *Biochemistry (Mosc).* 5, 3123-3130.

NAKAMURA, Y., HIRANO, S., SUZUKI, K., SEKI, K., SAGARA, T. & NISHIDA, T. 2002. Signaling Mechanism of TGF-{beta}1-Induced Collagen Contraction Mediated by Bovine Trabecular Meshwork Cells. *Invest. Ophthalmol. Vis. Sci.,* 43, 3465-3472.

NAKAMURA, Y., SAGARA, T., SEKI, K., HIRANO, S. & NISHIDA, T. 2003. Permissive Effect of Fibronectin on Collagen Gel Contraction Mediated by Bovine Trabecular Meshwork Cells. *Invest. Ophthalmol. Vis. Sci.,* 44, 4331-4336.

NOBES, C. D. & HALL, A. 1995. Rho, Rac, and Cdc42 GTPases regulate the assembly of multimolecular focal complexes associated with actin stress fibers, lamellipodia, and filopodia. *Cell,* 81, 53-62.

PANCHINA, Y., KELMANSON, I., MATZ, M., LUKYANOV, K., USMAN, N. & LUKYANOV, S. 2000. A ubiquitous family of putative gap junction molecules. *Curr. Biol.,* 10, R473-R474.

PARK, K. H., COZIER, F., ONG, O. C. & CAPRIOLI, J. 2001. Induction of heat shock protein 72 protects retinal ganglion cells in a rat glaucoma model. *Invest. Ophthalmol. Vis. Sci.,* 42, 1522-30.

PELLEGRIN, S. & MELLOR, H. 2007. Actin stress fibres. *J. Cell Sci.,* 120, 3491-3499.

PIEK, E., HELDIN, C. H. & TEN DIJKE, P. 1999. Specificity, diversity, and regulation in TGF-beta superfamily signaling. *FASEB J.,* 13, 2105-24.

POCIASK, D. A., SIME, P. J. & BRODY, A. R. 2004. Asbestos-derived reactive oxygen species activate TGF-[beta]1. *Lab. Invest.,* 84, 1013-1023.

POLANSKY, J., WEINREB, R., BAXTER, J. & ALVARADO, J. 1979a. Human trabecular cells. I. Establishment in tissue culture and growth characteristics. *Invest. Ophthalmol. Vis. Sci.,* 18, 1043-1049.

POLANSKY, J. R., WEINREB, R. & ALVARADO, J. A. 1981. Studies on human trabecular cells propagated in vitro. *Vision Res.,* 21, 155-60.

POLANSKY, J. R., WEINREB, R. N., BAXTER, J. D. & ALVARADO, J. 1979b. Human trabecular cells. I. Establishment in tissue culture and growth characteristics. *Invest. Ophthalmol. Vis. Sci.,* 18, 1043-9.

QUIGLEY, H. A. 1996. Number of people with glaucoma worldwide. *Br. J. Ophthalmol.,* 80, 389-393.

QUIGLEY, H. A. & BROMAN, A. T. 2006. The number of people with glaucoma worldwide in 2010 and 2020. *Br. J. Ophthalmol.,* 90, 262-267.

QUIGLEY, H. A., NICKELLS, R. W., KERRIGAN, L. A., PEASE, M. E., THIBAULT, D. J. & ZACK, D. J. 1995. Retinal ganglion cell death in experimental glaucoma and after axotomy occurs by apoptosis. *Invest. Ophthalmol. Vis. Sci.,* 36, 774-86.

RAE, C., LANGA, S., TUCKER, S. J. & MACEWAN, D. J. 2007. Elevated NF-κB responses and FLIP levels in leukemic but not normal lymphocytes: reduction by salicylate allows TNF-induced apoptosis. *Proceedings of the National Academy of Sciences,* 104, 12790-12795.

RAO, P. V., DENG, P.-F., KUMAR, J. & EPSTEIN, D. L. 2001. Modulation of Aqueous Humor Outflow Facility by the Rho Kinase–Specific Inhibitor Y-27632. *Invest. Ophthalmol. Vis. Sci.,* 42, 1029-1037.

RAVIOLA, G. & RAVIOLA, E. 1981. Paracellular route of aqueous outflow in the trabecular meshwork and canal of Schlemm. A freeze-fracture study of the endothelial junctions in the sclerocorneal angel of the macaque monkey eye. *Invest. Ophthalmol. Vis. Sci.,* 21, 52-72.

READ, A. T., CHAN, D. W. H. & ETHIER, C. R. 2007. Actin structure in the outflow tract of normal and glaucomatous eyes. *Exp. Eye Res.,* 84, 214-226.

REDDY, V. N., GIBLIN, F. J., LIN, L. R. & CHAKRAPANI, B. 1998. The effect of aqueous humor ascorbate on ultraviolet-B-induced DNA damage in lens epithelium. *Invest. Ophthalmol. Vis. Sci.,* 39, 344-50.

REHNBERG, M., AMMITZBÖLL, T. & TENGROTH, B. 1987. Collagen distribution in the lamina cribrosa and the trabecular meshwork of the human eye. *Br. J. Ophthalmol.,* 71, 886-892.

REISS, G. R., WERNESS, P. G., ZOLLMAN, P. E. & BRUBAKER, R. F. 1986. Ascorbic Acid Levels in the Aqueous Humor of Nocturnal and Diurnal Mammals. *Arch. Ophthalmol.,* 104, 753-755.

RIBEIRO, S. M. F., POCZATEK, M., SCHULTZ-CHERRY, S., VILLAIN, M. & MURPHY-ULLRICH, J. E. 1999. The Activation Sequence of Thrombospondin-1 Interacts with the Latency-associated Peptide to Regulate Activation of Latent Transforming Growth Factor-β. *J. Biol. Chem.,* 274, 13586-13593.

RICH, T., WATSON, C. J. & WYLLIE, A. 1999. Apoptosis: the germs of death. *Nat Cell Biol,* 1, E69-E71.

RIDLEY, A. J. 2001. Rho family proteins: coordinating cell responses. *Trends Cell Biol.,* 11, 471-7.

RIDLEY, A. J. & HALL, A. 1992. The small GTP-binding protein rho regulates the assembly of focal adhesions and actin stress fibers in response to growth factors. *Cell,* 70, 389-99.

RIENTO, K. & RIDLEY, A. J. 2003. ROCKs: multifunctional kinases in cell behaviour. *Nat Rev Mol Cell Biol,* 4, 446-456.

RIORDAN-EVA, P., WHITCHER, J., VAUGHAN, D. & ASBURY, T. 2008. *Vaughan & Asbury's general ophthalmology,* New York, Lange medical books/McGraw-Hill Medical Pub. Division.

ROHEN, J., FUTA, R. & LUTJEN-DRECOLL, E. 1981. The fine structure of the cribriform meshwork in normal and glaucomatous eyes as seen in tangential sections. *Invest. Ophthalmol. Vis. Sci.,* 21, 574-585.

ROMERO, I. A., RADEWICZ, K., JUBIN, E., MICHEL, C. C., GREENWOOD, J., COURAUD, P.-O. & ADAMSON, P. 2003. Changes in cytoskeletal and tight junctional proteins correlate with decreased permeability induced by dexamethasone in cultured rat brain endothelial cells. *Neurosci. Lett.,* 344, 112-116.

ROSENTHAL, R., CHORITZ, L., SCHLOTT, S., BECHRAKIS, N. E., JAROSZEWSKI, J., WIEDERHOLT, M. & THIEME, H. 2005a. Effects of ML-7 and Y-27632 on carbachol- and endothelin-1-induced contraction of bovine trabecular meshwork. *Exp. Eye Res.,* 80, 837-845.

ROSENTHAL, R., CHORITZ, L., SCHLOTT, S., BECHRAKIS, N. E., JAROSZEWSKI, J., WIEDERHOLT, M. & THIEME, H. 2005b. Effects of ML-7 and Y-27632 on carbachol- and endothelin-1-induced contraction of bovine trabecular meshwork. *Exp. Eye Res.,* 80, 837-45.

ROSENTHAL, R. & FROMM, M. 2011. Endothelin antagonism as an active principle for glaucoma therapy. *Br. J. Pharmacol.,* 162, 806-816.

SAGARA, T., GATON, D. D., LINDSEY, J. D., GABELT, B. T., KAUFMAN, P. L. & WEINREB, R. N. 1999. Topical prostaglandin F2alpha treatment reduces collagen types I, III, and IV in the monkey uveoscleral outflow pathway. *Arch. Ophthalmol.,* 117, 794-801.

SAIKA, S., IKEDA, K., YAMANAKA, O., MIYAMOTO, T., OHNISHI, Y., SATO, M., MURAGAKI, Y., OOSHIMA, A., NAKAJIMA, Y., KAO, W. W., FLANDERS, K. C. & ROBERTS, A. B. 2005. Expression of Smad7 in mouse eyes accelerates healing of corneal tissue after exposure to alkali. *Am. J. Pathol.,* 166, 1405-18.

SANFORD, L. P., ORMSBY, I., GITTENBERGER-DE GROOT, A. C., SARIOLA, H., FRIEDMAN, R., BOIVIN, G. P., CARDELL, E. L. & DOETSCHMAN, T. 1997. TGFbeta2 knockout mice have multiple developmental defects that are non-overlapping with other TGFbeta knockout phenotypes. *Development,* 124, 2659-2670.

SANKA, K., MADDALA, R., EPSTEIN, D. L. & RAO, P. V. 2007. Influence of Actin Cytoskeletal Integrity on Matrix Metalloproteinase-2 Activation in Cultured Human Trabecular Meshwork Cells. *Invest. Ophthalmol. Vis. Sci.,* 48, 2105-2114.

SATO, Y. & RIFKIN, D. B. 1989. Inhibition of endothelial cell movement by pericytes and smooth muscle cells: activation of a latent transforming growth factor-beta 1-like molecule by plasmin during co-culture. *The Journal of Cell Biology,* 109, 309-315.

SCHLÖTZER-SCHREHARDT, U., LOMMATZSCH, J., KÜCHLE, M., KONSTAS, A. G. P. & NAUMANN, G. O. H. 2003. Matrix Metalloproteinases and Their Inhibitors in Aqueous Humor of Patients with Pseudoexfoliation Syndrome/Glaucoma and Primary Open-Angle Glaucoma. *Invest. Ophthalmol. Vis. Sci.,* 44, 1117-1125.

SCHULTZ-CHERRY, S. & MURPHY-ULLRICH, J. 1993. Thrombospondin causes activation of latent transforming growth factor-beta secreted by endothelial cells by a novel mechanism. *The Journal of Cell Biology,* 122, 923-932.

SCOTT, D. R., KARAGEUZIAN, L. N., ANDERSON, P. J. & EPSTEIN, D. L. 1984. Glutathione peroxidase of calf trabecular meshwork. *Invest. Ophthalmol. Vis. Sci.,* 25, 599-602.

SHEPARD, A. R., JACOBSON, N., FINGERT, J. H., STONE, E. M., SHEFFIELD, V. C. & CLARK, A. F. 2001. Delayed Secondary Glucocorticoid Responsiveness of MYOC in Human Trabecular Meshwork Cells. *Invest. Ophthalmol. Vis. Sci.,* 42, 3173-3181.

SHIFERA, A. S., TRIVEDI, S., CHAU, P., BONNEMAISON, L. H., IGUCHI, R. & ALVARADO, J. A. 2010. Constitutive secretion of chemokines by cultured human trabecular meshwork cells. *Exp. Eye Res.,* 91, 42-47.

SMITH, D. F., WHITESELL, L. & KATSANIS, E. 1998. Molecular Chaperones: Biology and Prospects for Pharmacological Intervention. *Pharmacol. Rev.,* 50, 493-514.

SNYDER, R. W., STAMER, W. D., KRAMER, T. R. & SEFTOR, R. E. B. 1993. Corticosteroid Treatment and Trabecular Meshwork Proteases in Cell and Organ Culture Supernatants. *Exp. Eye Res.,* 57, 449-460.

SOMMER, A., TIELSCH, J. M., KATZ, J., QUIGLEY, H. A., GOTTSCH, J. D., JAVITT, J., SINGH, K. & BALTIMORE EYE SURVEY RESEARCH GROUP 1991. Relationship Between Intraocular Pressure and Primary Open Angle Glaucoma Among White and Black Americans: The Baltimore Eye Survey. *Arch. Ophthalmol.,* 109, 1090-1095.

STANDLEY, P. R., CAMARATTA, A., NOLAN, B. P., PURGASON, C. T. & STANLEY, M. A. 2002. Cyclic stretch induces vascular smooth muscle cell alignment via NO signaling. *American Journal of Physiology - Heart and Circulatory Physiology,* 283, H1907-H1914.

STEELY, H., BROWDER, S., JULIAN, M., MIGGANS, S., WILSON, K. & CLARK, A. 1992. The effects of dexamethasone on fibronectin expression in cultured human trabecular meshwork cells. *Invest. Ophthalmol. Vis. Sci.,* 33, 2242-2250.

STEINHAUSEN, K., STUMPFF, F., STRAUSS, O., THIEME, H. & WIEDERHOLT, M. 2000. Influence of muscarinic agonists and tyrosine kinase inhibitors on L-type Ca(2+)Channels in human and bovine trabecular meshwork cells. *Exp. Eye Res.,* 70, 285-93.

STONE, E. M., FINGERT, J. H., ALWARD, W. L. M., NGUYEN, T. D., POLANSKY, J. R., SUNDEN, S. L. F., NISHIMURA, D., CLARK, A. F., NYSTUEN, A., NICHOLS, B. E., MACKEY, D. A., RITCH, R., KALENAK, J. W., CRAVEN, E. R. & SHEFFIELD, V. C. 1997. Identification of a Gene That Causes Primary Open Angle Glaucoma. *Science,* 275, 668-670.

SUGURO, K., TORIS, C. & PEDERSON, J. 1985. Uveoscleral outflow following cyclodialysis in the monkey eye using a fluorescent tracer. *Invest. Ophthalmol. Vis. Sci.,* 26, 810-813.

SUMIOKA, T., IKEDA, K., OKADA, Y., YAMANAKA, O., KITANO, A. & SAIKA, S. 2008. Inhibitory effect of blocking TGF-beta/Smad signal on injury-induced fibrosis of corneal endothelium. *Mol. Vis.,* 14, 2272-81.

TADOKORO, S., SHATTIL, S. J., ETO, K., TAI, V., LIDDINGTON, R. C., DE PEREDA, J. M., GINSBERG, M. H. & CALDERWOOD, D. A. 2003. Talin Binding to Integrin {beta} Tails: A Final Common Step in Integrin Activation. *Science,* 302, 103-106.

TAMM, E., LUTJEN-DRECOLL, E. & ROHEN, J. W. 1990. Age-related changes of the ciliary muscle in comparison with changes induced by treatment with prostaglandin F2 alpha. An ultrastructural study in rhesus and cynomolgus monkeys. *Mech. Ageing Dev.,* 51, 101-20.

TAMM, E. R. 2009. The trabecular meshwork outflow pathways: Structural and functional aspects. *Exp. Eye Res.,* 88, 648-655.

TANIHARA, H., OHIRA, A., TAKAHASHI, M., HONDA, Y. & SUZUKI, S. 1995. Localization and possible gene expression of proteoglycan decorin in the trabecular meshwork. *Curr. Eye Res.,* 14, 727-30.

TANITO, M., KWON, Y.-W., KONDO, N., BAI, J., MASUTANI, H., NAKAMURA, H., FUJII, J., OHIRA, A. & YODOI, J. 2005. Cytoprotective Effects of Geranylgeranylacetone against Retinal Photooxidative Damage. *J. Neurosci.,* 25, 2396-2404.

TATTI, O., VEHVILÄINEN, P., LEHTI, K. & KESKI-OJA, J. 2008. MT1-MMP releases latent TGF-[beta]1 from endothelial cell extracellular matrix via proteolytic processing of LTBP-1. *Exp. Cell Res.,* 314, 2501-2514.

TEKTAS, O.-Y., HAMMER, C. M., DANIAS, J., CANDIA, O., GEROMETTA, R., PODOS, S. M. & LUTJEN-DRECOLL, E. 2010. Morphologic Changes in the Outflow Pathways of Bovine Eyes Treated with Corticosteroids. *Invest. Ophthalmol. Vis. Sci.,* 51, 4060-4066.

TEKTAS, O. Y. & LUTJEN-DRECOLL, E. 2009. Structural changes of the trabecular meshwork in different kinds of glaucoma. *Exp. Eye Res.,* 88, 769-75.

THIEME, H., HILDEBRANDT, J., CHORITZ, L., STRAUSS, O. & WIEDERHOLT, M. 2001. Muscarinic receptors of the M2 subtype in human and bovine trabecular meshwork. *Graefes Arch. Clin. Exp. Ophthalmol.,* 239, 310-5.

THOMPSON, C. 1995. Apoptosis in the pathogenesis and treatment of disease. *Science,* 267, 1456-1462.

TIAN, B., KAUFMAN, P. L., VOLBERG, T., GABELT, B. A. T. & GEIGER, B. 1998. H-7 Disrupts the Actin Cytoskeleton and Increases Outflow Facility. *Arch. Ophthalmol.,* 116, 633-643.

TIELSCH, J. M., KATZ, J., SOMMER, A., QUIGLEY, H. A. & JAVITT, J. C. 1994. Family History and Risk of Primary Open Angle Glaucoma: The Baltimore Eye Survey. *Arch. Ophthalmol.,* 112, 69-73.

TIELSCH, J. M., SOMMER, A., KATZ, J., ROYALL, R. M., QUIGLEY, H. A. & JAVITT, J. 1991. Racial Variations in the Prevalence of Primary Open-angle Glaucoma: The Baltimore Eye Survey. *JAMA,* 266, 369-374.

TOMASEK, J. J., GABBIANI, G., HINZ, B., CHAPONNIER, C. & BROWN, R. A. 2002. Myofibroblasts and mechano-regulation of connective tissue remodelling. *Nat Rev Mol Cell Biol,* 3, 349-363.

TOWNSEND, D. & BRUBAKER, R. 1980. Immediate effect of epinephrine on aqueous formation in the normal human eye as measured by fluorophotometry. *Invest. Ophthalmol. Vis. Sci.,* 19, 256-266.

TRIPATHI, R. C., CHAN, W. A., LI, J. & TRIPATHI, B. J. 1994a. Trabecular Cells Express the TGF-[beta]2 Gene and Secrete the Cytokine. *Exp. Eye Res.,* 58, 523-528.

TRIPATHI, R. C., LI, J., CHAN, W. A. & TRIPATHI, B. J. 1994b. Aqueous Humor in Glaucomatous Eyes Contains an Increased Level of TGF-[beta]2. *Exp. Eye Res.,* 59, 723-728.

TRIPATHI, R. C., MILLARD, C. B. & TRIPATHI, B. J. 1989. Protein composition of human aqueous humor: SDS-PAGE analysis of surgical and post-mortem samples. *Exp. Eye Res.,* 48, 117-130.

TSAPARA, A., LUTHERT, P., GREENWOOD, J., HILL, C. S., MATTER, K. & BALDA, M. S. 2010. The RhoA Activator GEF-H1/Lfc Is a Transforming Growth Factor-{beta} Target Gene and Effector That Regulates {alpha}-Smooth Muscle Actin Expression and Cell Migration. *Mol. Biol. Cell,* 21, 860-870.

TUFVESSON, E. & WESTERGREN-THORSSON, G. 2003. Biglycan and decorin induce morphological and cytoskeletal changes involving signalling by the small GTPases RhoA and Rac1 resulting in lung fibroblast migration. *J. Cell Sci.,* 116, 4857-64.

TUMMINIA, S., MITTON, K., ARORA, J., ZELENKA, P., EPSTEIN, D. & RUSSELL, P. 1998. Mechanical stretch alters the actin cytoskeletal network and signal transduction in human trabecular meshwork cells. *Invest. Ophthalmol. Vis. Sci.,* 39, 1361-1371.

UMIHIRA, J., NAGATA, S., NOHARA, M., HANAI, T., USUDA, N. & SEGAWA, K. 1994. Localization of elastin in the normal and glaucomatous human trabecular meshwork. *Invest. Ophthalmol. Vis. Sci.,* 35, 486-494.

URAYAMA, S., MUSCH, M. W., RETSKY, J., MADONNA, M. B., STRAUS, D. & CHANG, E. B. 1998. Dexamethasone protection of rat intestinal epithelial cells against oxidant injury is mediated by induction of heat shock protein 72. *J. Clin. Invest.,* 102, 1860-5.

VANDEKERCKHOVE, J. & WEBER, K. 1978. At least six different actins are expressed in a higher mammal: An analysis based on the amino acid sequence of the amino-terminal tryptic peptide. *J. Mol. Biol.,* 126, 783-802.

VERMES, I., HAANEN, C., STEFFENS-NAKKEN, H. & REUTELINGSPERGER, C. 1995. A novel assay for apoptosis. Flow cytometric detection of phosphatidylserine expression on early apoptotic cells using fluorescein labelled Annexin V. *J. Immunol. Methods,* 184, 39-51.

VITALE, M. L., AKPOVI, C. D. & PELLETIER, R. M. 2009. Cortactin/tyrosine-phosphorylated cortactin interaction with connexin 43 in mouse seminiferous tubules. *Microsc. Res. Tech.,* 72, 856-867.

WADE, N. C., GRIERSON, I., O'REILLY, S., HOARE, M. J., CRACKNELL, K. P. B., PARAOAN, L. I., BROTCHIE, D. & CLARK, A. F. 2009. Cross-linked actin networks (CLANs) in bovine trabecular meshwork cells. *Exp. Eye Res.,* 89, 648-659.

WANG, D. Y., FAN, B. J., YAM, G. Y., LAM, D. S. & PANG, C. P. 2008a. The cytotoxic and stress responses of human trabecular meshwork cells treated with triamcinolone acetonide. *Mol. Vis.,* 14, 105-13.

WANG, N., CHINTALA, S. K., FINI, M. E. & SCHUMAN, J. S. 2001. Activation of a tissue-specific stress response in the aqueous outflow pathway of the eye defines the glaucoma disease phenotype. *Nat. Med.,* 7, 304-9.

WANG, W.-H., MCNATT, L. G., PANG, I.-H., MILLAR, J. C., HELLBERG, P. E., HELLBERG, M. H., STEELY, H. T., RUBIN, J. S., FINGERT, J. H., SHEFFIELD, V. C., STONE, E. M. & CLARK, A. F. 2008b. Increased expression of the WNT antagonist sFRP-1 in glaucoma elevates intraocular pressure. *The Journal of Clinical Investigation,* 118, 1056-1064.

WEBER, B. H. F., VOGT, G., PRUETT, R. C., STOHR, H. & FELBOR, U. 1994. Mutations in the tissue inhibitor of metalloproteinases-3 (TIMP3) in patients with Sorsby's fundus dystrophy. *Nat. Genet.*, **8**, 352-356.

WEINREB, R., RYDER, M. & POLANSKY, J. 1986. The cytoskeleton of the cynomolgus monkey trabecular cell. II. Influence of cytoskeleton-active drugs. *Invest. Ophthalmol. Vis. Sci.*, **27**, 1312-1317.

WEINREB, R. N., BLOOM, E., BAXTER, J. D., ALVARADO, J., LAN, N., O'DONNELL, J. & POLANSKY, J. R. 1981. Detection of glucocorticoid receptors in cultured human trabecular cells. *Invest. Ophthalmol. Vis. Sci.*, **21**, 403-7.

WELGE-LÜßEN, U., MAY, C. A. & LÜTJEN-DRECOLL, E. 2000. Induction of Tissue Transglutaminase in the Trabecular Meshwork by TGF-β1 and TGF-β2. *Invest. Ophthalmol. Vis. Sci.*, **41**, 2229-2238.

WIEDERHOLT, M., STURM, A. & LEPPLE-WIENHUES, A. 1994. Relaxation of trabecular meshwork and ciliary muscle by release of nitric oxide. *Invest. Ophthalmol. Vis. Sci.*, **35**, 2515-2520.

WIEDERHOLT, M., THIEME, H. & STUMPFF, F. 2000. The regulation of trabecular meshwork and ciliary muscle contractility. *Prog. Retin. Eye Res.*, **19**, 271-295.

WILBANKS, G. A., MAMMOLENTI, M. & STREILEIN, J. W. 1992. Studies on the induction of anterior chamber-associated immune deviation (ACAID) III. Induction of ACAID depends upon intraocular transforming growth factor-β. *Eur. J. Immunol.*, **22**, 165-173.

WILSON, K., MCCARTNEY, M. D., MIGGANS, S. T. & CLARK, A. F. 1993. Dexamethasone induced ultrastructural changes in cultured human trabecular meshwork cells. *Curr. Eye Res.*, **12**, 783-93.

WIRTZ, M. K., BRADLEY, J. M., XU, H., DOMREIS, J., NOBIS, C. A., TRUESDALE, A. T., SAMPLES, J. R., VAN BUSKIRK, E. M. & ACOTT, T. S. 1997. Proteoglycan expression by human trabecular meshworks. *Curr. Eye Res.*, **16**, 412-21.

WORDINGER, R., CLARK, A., AGARWAL, R., LAMBERT, W., MCNATT, L., WILSON, S., QU, Z. & FUNG, B. 1998. Cultured human trabecular meshwork cells express functional growth factor receptors. *Invest. Ophthalmol. Vis. Sci.*, **39**, 1575-1589.

WORDINGER, R. J., FLEENOR, D. L., HELLBERG, P. E., PANG, I.-H., TOVAR, T. O., ZODE, G. S., FULLER, J. A. & CLARK, A. F. 2007. Effects of TGF-{beta}2, BMP-4, and Gremlin in the Trabecular Meshwork: Implications for Glaucoma. *Invest. Ophthalmol. Vis. Sci.*, **48**, 1191-1200.

WORTHYLAKE, R. A. & BURRIDGE, K. 2003. RhoA and ROCK Promote Migration by Limiting Membrane Protrusions. *J. Biol. Chem.*, **278**, 13578-13584.

WUDUNN, D. 2009. Mechanobiology of trabecular meshwork cells. *Exp. Eye Res.*, **88**, 718-723.

YAMADA, E. 1969. Some Structural Features of the Fovea Centralis in the Human Retina. *Arch. Ophthalmol.*, **82**, 151-159.

YAMAGUCHI, Y., MANN, D. M. & RUOSLAHTI, E. 1990. Negative regulation of transforming growth factor-[beta] by the proteoglycan decorin. *Nature*, **346**, 281-284.

YING, Q.-L., NICHOLS, J., CHAMBERS, I. & SMITH, A. 2003. BMP Induction of Id Proteins Suppresses Differentiation and Sustains Embryonic Stem Cell Self-Renewal in Collaboration with STAT3. *Cell,* 115, 281-292.

ZHANG, X., CLARK, A. F. & YORIO, T. 2005. Regulation of Glucocorticoid Responsiveness in Glaucomatous Trabecular Meshwork Cells by Glucocorticoid Receptor-{beta}. *Invest. Ophthalmol. Vis. Sci.,* 46, 4607-4616.

ZHANG, X., OGNIBENE, C. M., CLARK, A. F. & YORIO, T. 2007. Dexamethasone inhibition of trabecular meshwork cell phagocytosis and its modulation by glucocorticoid receptor [beta]. *Exp. Eye Res.,* 84, 275-284.

ZHANG, Z., GARRON, T. M., LI, X. J., LIU, Y., ZHANG, X., LI, Y. Y. & XU, W. S. 2009. Recombinant human decorin inhibits TGF-beta1-induced contraction of collagen lattice by hypertrophic scar fibroblasts. *Burns,* 35, 527-37.

ZHONGBIAO, W. & WALTER, H. N. 2003. Smooth muscle cell migration stimulated by interleukin 6 is associated with cytoskeletal reorganization. *The Journal of surgical research,* 111, 261-266.

ZHOU, L., FUKUCHI, T., KAWA, J., HIGGINBOTHAM, E. & YUE, B. 1995. Loss of cell-matrix cohesiveness after phagocytosis by trabecular meshwork cells. *Invest. Ophthalmol. Vis. Sci.,* 36, 787-795.

ZHUO, Y. H., HE, Y., LEUNG, K. W., HOU, F., LI, Y. Q., CHAI, F. & GE, J. 2010. Dexamethasone disrupts intercellular junction formation and cytoskeleton organization in human trabecular meshwork cells. *Mol. Vis.,* 16, 61-71.